E-9638

NASA TECHNICAL MEMORANDUM

NASA TM-78902

NASA TM-78902

TRANSIENT RESPONSE TO THREE-PHASE FAULTS ON A WIND TURBINE GENERATOR

by Leonard J. Gilbert
Lewis Research Center
Cleveland, Ohio 44135

June 1978

A Thesis

entitled

TRANSIENT RESPONSE TO THREE-PHASE FAULTS ON A WIND TURBINE GENERATOR

by

Leonard J. Gilbert

as partial fulfillment of the requirements of
the Degree of Doctor of Philosophy

The University of Toledo
June 1978

An Abstract of

TRANSIENT RESPONSE TO THREE-PHASE FAULTS ON A WIND TURBINE GENERATOR

Leonard J. Gilbert

Submitted in partial fulfillment
of the requirements of the
Doctor of Philosophy Degree

The University of Toledo
June 1978

As a consequence of the world energy supply problems large kilowatt and megawatt capacity wind turbine generators are being designed and built to take advantage of the energy in the wind. These apparatus are equipped with synchronous alternators for direct synchronization with utility networks. Because a wind turbine generator inherently has unique power system features - such as a large moment of inertia relative to its power capacity and a continuously varying input torque - its electrical behavior must be investigated either by testing or by analysis. The transient response of the system to electrical faults is one mode of the system behavior that must be studied analytically rather than experimentally.

In order to obtain a measure of its response to short circuits a large horizontal axis wind turbine generator is modeled and its performance is simulated on a digital computer. The baseline model for the simulation is the DOE/NASA 100 kW wind turbine generator located near Sandusky, Ohio.

Simulation of short circuit faults on the synchronous alternator of a wind turbine generator, without resort to the classical assumptions generally made for that analysis, indicates that maximum clearing times for the system tied to an infinite bus are longer than the typical clearing times for equivalent capacity conventional machines. Also, maximum clearing times are independent of tower shadow and wind shear. Variation of circuit conditions produce the modifications in the transient response predicted by analysis.

The model and simulation developed for this study of transient stability are applicable for more extensive investigations of power systems involving wind turbine generators, and will continue to be useful until the extent that standard power system technology applies directly to wind turbine power systems is fully determined.

TRANSIENT RESPONSE TO THREE-PHASE FAULTS ON A WIND TURBINE GENERATOR

by

Leonard J. Gilbert

Submitted in partial fulfillment

of the requirements of the

Doctor of Philosophy Degree

University of Toledo

June 1978

Certified by: _____

Advisor and Co-Chairman of Systems Committee

Certified by: _____

Advisor and Co-Chairman of Systems Committee

Accepted by: _____

Dean, Graduate School

ABSTRACT

As a consequence of the world energy supply problems large kilowatt and megawatt capacity wind turbine generators are being designed and built to take advantage of the energy in the wind. These apparatus are equipped with synchronous alternators for direct synchronization with utility networks. Because a wind turbine generator inherently has unique power system features - such as a large moment of inertia relative to its power capacity and a continuously varying input torque - its electrical behavior must be investigated either by testing or by analysis. The transient response of the system to electrical faults is one mode of the system behavior that must be studied analytically rather than experimentally.

In order to obtain a measure of its response to short circuits a large horizontal axis wind turbine generator is modeled and its performance is simulated on a digital computer. The baseline model for the simulation is the DOE/NASA 100 kW wind turbine generator located near Sandusky, Ohio.

Simulation of short circuit faults on the synchronous alternator of a wind turbine generator, without resort to the classical assumptions generally made for that analysis, indicates that maximum clearing times for the system tied to an infinite bus are longer than the typical clearing times for equivalent capacity conventional machines. Also, maximum clearing times are independent of tower shadow and wind shear. Variation of circuit conditions produce the modifications in

E-9638

the transient response predicted by analysis.

The model and simulation developed for this study of transient stability are applicable for more extensive investigations of power systems involving wind turbine generators, and will continue to be useful until the extent that standard power system technology applies directly to wind turbine power systems is fully determined.

ACKNOWLEDGMENTS

My appreciation and gratitude are extended to Dr. Gary G. Leininger and Dr. Thomas A. Stuart, dissertation co-advisors, for the assistance and encouragement during the preparation of this thesis.

I want to recognize as well the assistance of Professor John Hansell and Dr. Ronald Little who along with Drs. Leininger and Stuart served on my Dissertation Advisory Committee

The support of the NASA Lewis Research Center Training Committee for this research is gratefully acknowledged. The personal encouragement and guidance of Miss Gertrude R. Collins of the Training Section is particularly noted.

I wish also to express my appreciation for the tolerance and forbearance of the Wind Energy Project Office of Lewis Research Center during the extended period of this research.

TABLE OF CONTENTS

LIST OF FIGURES

LIST OF TABLES

Chapter I

INTRODUCTION

As the Department of Energy (DOE) of the United States expands its efforts to make wind turbine generators a viable and appreciable part of the national power network, it becomes necessary that power engineers gain a complete understanding of the electrical behavior of wind turbine generators. The depletion of established sources of fossil fuels and the consequent price increases for those energy sources have turned attention to the energy available in sunlight and wind.

1.1 Feasibility of Large Wind Turbine Generators

There has been, geographically, a widespread effort to produce commercially economical quantities of electrical power with wind turbines. Heretofore, all such efforts have been abandoned because of the relatively high cost of producing the electrical power from wind energy.

The largest wind powered electric system that has been built to date was the Smith-Putnam machine, built in the early 1940's in Vermont. This machine produced 1.25 MW of a.c. power (1). The Danish government helped to develop and operate 200 kW experimental wind powered systems after World War II (2). The British government built a 100 kW wind turbine generator in the Orkney Islands in 1950 (3). The French built and operated several large wind powered

powered electric generators in the period from 1958 to 1966 (4). Some of the most advanced wind turbines that have yet been built were constructed and operated in Germany during the period from 1957 to 1968 (5).

In every case the cost of the wind powered electricity was considerably in excess of the cost of conventional fossil fuel electric generation. As a consequence, the projects were abandoned. Despite their rejection what these early efforts to generate electricity from the wind energy proved was the technical feasibility of producing electrical power in this manner.

1.2 U.S. Government Wind Energy Program

The Federal Government has undertaken an accelerated program with the objective of stimulating the development of wind energy conversion systems capable of producing a significant amount of U.S. energy needs by the year 2000. To accomplish this, a series of experimental wind turbines from 100 kW to several megawatts rated capacity will be developed over the next decade. It is anticipated that these developments will be supported by an extensive research and technology effort, leading eventually to the installation of 10 to 100 MW multi-unit demonstration systems.

The first large scale wind turbine generator was designed and built for the Department of Energy by the National Aeronautics and Space Administration (NASA) at the NASA/Lewis Research Facility at Plum Brook, Ohio, in 1976. One of the specific objectives of the NASA/Lewis wind energy program was to develop cost effective wind conversion systems that are compatible with user applications. The

wind power generator at Plum Brook is used as the baseline model for this research study.

1.3 Power System Stability

An important consideration of a practical power system is stability. For an alternating voltage power system stability is that property which makes it possible to maintain synchronism between all interconnected machines for both steady state and transient conditions. The most important type of power system disturbance in transient stability studies is a fault applied and subsequently cleared (6). System disturbances from faults may upset the balance between input and output power of one or more machines of a synchronous system. If the unbalance is too great or too prolonged, synchronism will be lost. The most effective method of improving stability is to reduce the duration of faults with the use of high speed relays and circuit breakers. This study of the effects of three phase short circuits on a wind powered synchronous alternator and how some of the system parameters govern these effects has been made in order to predict the requirements of fault correction relays and breakers for wind turbine power systems.

1.4 Available Literature

Although there exists an appreciable catalog of literature dealing with wind power (7, 8), there is little documentation of analytical and experimental data related to the power system stability of wind power generators which have been built and operated in the past. This sparse documented experience is the result of several conditions:

lack of funding to provide extensive analysis and data taking, private proprietary projects, lack of support for mathematical analysis, disposal of records when projects were discontinued, failure to catalog documentation. Further, the computational facilities and analytical techniques available today were not available to earlier projects. In any case, there is a scarcity of literature describing the electrical considerations and network experience of wind powered generators.

With the advent of the current national program to develop wind turbines, analysis of the electrical aspects of these systems has been undertaken. Hwang and Gilbert (9, 10) have studied synchronization of a wind turbine generator with an infinite bus. Johnson and Smith (11) have investigated the dynamics of wind powered generators on utility networks. Work has been done by the General Electric Company as part of an extensive analytical study for ERDA on wind turbine system application. Pantalone has studied effects of large interconnected wind generators on power systems (12). Hwang has also studied the use of excitation control and reactance to help stabilize wind turbine generators (13).

1.5 Distinctive Wind Turbine Generator Features

There are distinctive features of wind turbine generators that make them different enough from conventional power systems to warrant an analytical study to determine the effect of wind turbine characteristics on power system stability. Among the characteristic features of wind turbine generators the two which have the most significant effect on the power system performance are (1) high rotational inertia of the wind turbine, and (2) the variability of the turbine

excitation. The first characteristic is the product of the necessarily large area that the turbine blades must sweep in order to capture appreciable energy from the wind. The second characteristic is the result of the inherent variability of the wind as well as modifications to the wind stream that result from the large system structure.

This study of the transient response of a wind turbine generator to three phase faults considers especially these two characteristics and the concomitant features that these characteristics produce. Variations of the baseline wind turbine model have been used to examine the effects of three phase faults on the performance of the electric power system.

1.6 Summary

The chapters which follow discuss the theory applied in this analytical study. Chapter II expresses the electrical theory involved in first swing transient stability analysis of synchronous machinery. Chapter III presents the model used for studying the behavior of the wind turbine power system. Included in Chapter III is a discussion of the computer simulation. In Chapter IV the results of the analysis are presented and explained. The last section discusses the conclusions derived from the analysis and the recommendations for additional study of wind turbine power system stability.

Chapter II

ANALYSIS OF THE RESEARCH PROBLEM

The transient stability analysis of a wind turbine generator can be approached with the standard analytical tools used to investigate alternating current electric power systems. The wind turbine generator, as any other alternating current power source, consists of a prime mover, a transmission, and an alternator with an excitation control for the alternator and a prime mover control to adjust the input torque. However, significant differences exist between the wind turbine generator and its operating environment and the conventional power system and its environment.

2.1 Research Problem

The research problem is to determine the extent to which these differences affect the fault response of the wind turbine generator power system.

Two distinctive features of the wind power system are considered in this analysis:

(1) the turbine (prime mover) has much more rotary inertia than any other rotating component of the system, in fact, much more inertia than the rotating elements of conventional power systems of equivalently rated output power;

(2) wind, the source of excitation (torque input), is continually varying.

A wind turbine generator is an electromechanical system, and any system disturbance produces a transient response. If any bounded input disturbance to the system produces a bounded output, the system is stable. Power system stability is that property of a power system that enables it to remain in operating equilibrium (synchronism) during and following transient faults and circuit changes.

The power system stability problem becomes very complex when a network of machines and loads is considered. A large set of nonlinear coupled equations of the form

$$\dot{x} = f(x,u,t) \tag{2.1}$$

must be used to describe the system performance.

2.2 Problem of the Single Machine on an Infinite Bus

Before undertaking network problems, an understanding of the performance of a single machine must be developed. For this purpose one synchronous alternator tied electrically to an infinite bus is investigated. Figure 2.1 is a one-line diagram of a single alternator tied to an infinite bus through a transmission line. x_e Is the lumped reactance between the alternator voltage source and the infinite bus. Line resistance is assumed to be negligible.

2.2.1 Swing equation. - Classically the motion of the alternator is described by the "swing equation" which relates the rotary inertia torque of the rotating shaft to the net mechanical and electrical torque on the shaft.

$$I\ddot{\theta} = T \tag{2.2}$$

For convenience the angle θ is measured with respect to the synchronously rotating reference of the infinite bus.

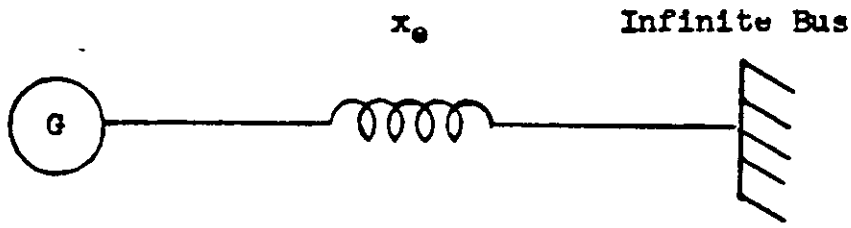

Figure 2.1-One machine tied to an infinite bus

$$\theta = \delta + \omega_o t$$

$$\ddot{\theta} = \ddot{\delta}$$

$$I\ddot{\delta} = T \qquad (2.3)$$

The variation of δ as a function of time is indicative of the transient stability of the machine represented. In practice, the first swing of this function is usually the most significant in assessing the stability of the machine. If the rotor angle increases indefinitely, the machine will pull out of synchronism and stability will be lost.

2.2.2 Classical assumptions. - The transient stability of one synchronous alternator tied to an infinite bus is a classical problem. The solution is based customarily on the following assumptions (6):

(1) The mechanical input torque remains constant during the entire duration of the swing curve.

(2) Damping or asynchronous power is negligible.

(3) Synchronous power may be calculated from a steady state solution of the network to which the machine is connected.

(4) The machine can be represented by a constant reactance (direct axis transient reactance) in series with a constant voltage source (voltage behind transient reactance).

(5) The mechanical angles of the machine rotor coincides with the electrical phase of the voltage behind transient reactance.

2.2.3 Applicability of assumptions to research problem. - For this research effort, which considers the performance of a wind turbine generator in response to an electrical fault, none of the

"classical assumptions" has been made. However, the applicability of the assumptions to the wind turbine generator problem is discussed.

Assumption 1 is usually made because the input to the alternator is controlled by a speed governor. When a fault occurs at the output of the alternator, the output is abruptly changed, but the input remains unchanged. The alternator will vary about the synchronous speed, but until synchronism is lost, the speed change is very small. Usually the input governor will not respond until there has been a one percent speed change, and even then there is usually a time lag in the response. Accordingly, in the classical problem it is reasonable to assume that the mechanical input torque is constant during the duration of the swing curve.

In the case of the wind turbine generator, however, the torque input to the alternator is not controlled by a speed governor. The torque input to the alternator is a function of the power limit of the alternator. If the wind speed is below the system rated value, the rotor blades are set at a fixed pitch angle, and the torque input remains constant during a fault. If the wind speed is above the system rated value, the input torque is limited to its rated value by a power error signal controlling the rotor blade pitch. Then the input torque response to the output change resulting from the fault is limited only by the power sensor response time.

Assumption 2 is usually an acceptable simplification in the classical model because damping or asynchronous power is small relative to the synchronous power. The electrical output of a synchronous alternator consists of a synchronous part, dependent on the angular position of the machine, and an asynchronous part depending

on the angular speed of the machine.

$$P_e = P_d(\dot{\delta}) + P(\delta) \tag{2.4}$$

Although the asynchronous power may be small, its effect on transient stability of wind power generators may not be negligible. As may be seen in plots of angle-time variation for a wind turbine generator (Chapter IV), there is considerable variation of δ. The damping of the rotor swing is the result of the interaction between the airgap flux and the rotor windings, particularly the damper winding, during slip ($(d\delta/dt) \neq 0$).

Because the oscillation period of the alternator is relatively long in comparison to time constants of the network, steady-state conditions are usually assumed (Assumption 3). In this research study two different network models are considered for comparison.

The use of a fixed voltage behind the transient reactance for the alternator model (Assumption 4) is usually acceptable when the only electrical transient which must be considered is the transient component (rather than both the transient and subtransient components) and its time constant is longer than the period of mechanical oscillation. The transient component and its time constant are not necessarily longer than the mechanical oscillation period in the wind turbine generator with its large rotor inertia. The prolongation of the first swing due to the large rotor inertia and the availability of fast response voltage regulators mean that the assumption of fixed voltage during the transient is not warranted. Further, the theoretical model of fixed voltage behind transient reactance is derived for the case of zero transient saliency or a round rotor machine. To avoid any unwarranted simplification the alternator model

for this research is the complete set of Park's equations. The use of this model makes Assumption 5 unnecessary.

The set of equations describing the model for this research was solved on a large digital computer. This facility made it unnecessary and undesirable to make any assumptions merely to simplify the mathematical solution.

Analyses of synchronous machines are simplified if the effects of saturation, hysteresis, and eddy currents in the iron are neglected. The importance of these neglected effects varies with the problem and the operating conditions. They are relatively unimportant in the calculation of initial symmetrical rms short circuit currents of fundamental frequency, especially if the fault is separate from the synchronous machine by transformers and transmission lines (14).

2.2.4 Critical clearing time. - When a three phase dead short is placed across the output terminals of an alternator, the output power is reduced to zero immediately. There is then an accelerating torque applied to the alternator rotor because the input power has not been reduced. The alternator rotor continues to accelerate as long as this unbalance remains. The displacement of the power angle with respect to the infinite bus increases and synchronism is lost.

If the short is removed before synchronism is lost, the accelerating power becomes negative with the resumption of the electrical load. If the decelerating power of the load is sufficient, the rate of change of the alternator power angle will become zero and reverse the angle change before synchronism is lost. For a given initial load, the maximum power angle at which the short circuit must be

cleared in order to prevent loss of synchronism is the critical clearing angle. Because power angle is ordinarily not known explicitly, critical clearing time, the time between application of the fault and clearing of the fault, is used in stability studies. The relays and breakers that are used to clear faults operate as timing devices rather than power angle devices.

2.3 Factors Affecting Clearing Time

2.3.1. Effect of inertia on clearing time. - Two synchronous generator design parameters which affect the critical clearing time for faults are the rotary inertia and the transient reactance. Intuitively it is rational that an increase in inertia increases the time required to reach the critical angle. Analytically, from the classical swing equation it can be shown (6) that the time required for the power angle to change from δ_1 to δ_2 as a result of an accelerating torque T is

$$t = \left(\frac{I}{2}\right)^{-1/2} \int_{\delta_1}^{\delta_2} \int_{\delta_1}^{\delta_2} (T\, d\delta)^{-1/2} \cdot d\delta \qquad (2.5)$$

Usually no literal solution for this equation exists. The equation indicates, however, the dependence of the clearing time on the square root of the inertia as well as on the accelerating torque.

2.3.2 Effect of transient reactance on clearing time. - The effect of the transient reactance, x'_d, on the clearing time can be seen from the relationship that the accelerating torque in the swing equation is the difference between the input shaft torque and the

electrical torque.

$$T = T_{sh} - T_e \tag{2.6}$$

For a synchronous machine with both a field and an amortisseur winding the fundamental frequency component of torque following a three-phase short is given by Concordia (15) as

$$T_e(\text{fund}) = v_t^2 \varepsilon^{-t/T_A}\left[\left(\frac{1}{x_d''} - \frac{1}{x_d'}\right)\varepsilon^{-t/T_d''} + \left(\frac{1}{x_d'} - \frac{1}{x_d}\right)\varepsilon^{-t/T_d'} + \frac{1}{x_d}\right]\sin t \tag{2.7}$$

where

$$T_A = \frac{2x_d''x_q''}{r_a(x_d'' + x_q'')} \tag{2.8}$$

The first term within the brackets of equation (2.7) is the sub-transient component with a very short time constant relative to the transient component, the second term within the brackets. The first term can be neglected for the comparison being made. In the second term, x_d is ordinarily four to ten times the magnitude of x_d'. Therefore, the magnitude of the torque T_e decreases with increasing x_d'. The unbalanced accelerating torque thus increases with increasing x_d'. As a consequence, the clearing time decreases with increasing reactance between the machine terminals and the short circuit. This conclusion follows from the fact that a symmetrical three phase reactance x_e between the machine terminals and the short circuit becomes part of the armature circuit and is added to x_d, x_d', x_d'', x_q, x_q', and x_q''.

2.3.3 Synchronous damping. - Two of the functions of damper windings in a synchronous alternator are (1) to suppress hunting, and (2) to damp oscillations that result from faults. Damper action

in the synchronous machine is explained with induction motor theory. In an induction machine the torque at small slips is almost directly proportional to the slip. Therefore, in calculation of synchronous damping the damping torque is assumed proportional to the slip. However, because of the difference between the direct and quadrature axes, the constant of proportionality depends upon the angular position of the rotor, the power angle (16). An equation for the damping power has been developed by Park (17) and modified by Dahl (18). The relationship is based on the following assumptions:

(1) No resistance in either the armature or field circuit.

(2) Small slip; where slip s is per unit slip.

(3) Damping caused by only one set of damper windings.

$$P_d = E^2 s\omega \left[\frac{(x'_d - x''_d)}{(x_e + x'_d)^2} T''_{do} \sin^2\delta + \frac{(x'_q - x''_q)}{(x_e + x'_q)^2} T''_{qo} \cos^2\delta \right] \quad (2.9)$$

The derivative of this damping power with respect to δ is

$$\frac{dP_d}{d\delta} = E^2 s\omega \left[\frac{(x'_d - x''_d)}{(x_e + x'_d)^2} T''_{do} - \frac{(x_q - x''_q)}{(x_e + x'_q)^2} T''_{qo} \right] \sin 2\delta \quad (2.10)$$

$$= (-4.2\text{x}10^{-3} \sin 2\delta)\dot{\delta} \qquad \text{for } x_e = 0.4 \text{ pu}$$

$$= (-5.9\text{x}10^{-3} \sin 2\delta)\dot{\delta} \qquad \text{for } x_e = 0.009 \text{ pu}$$

Equation (2.9) shows the inverse relationship between damping power and external reactance which is one of the parameters examined in this research. Equation (2.10) has been evaluated for the synchronous alternator modeled in this study. The negative coefficients for practical values of the power angle δ show that the damping power decreases with increasing load.

2.4 Wind Phenomena with Respect to Power Output

The wind, the normal driving energy source for a wind turbine system is variable in speed and direction. This variability is very much evident in the resultant drive train torque as well as the forces imposed on the structure of the wind turbine system. Thus, even when the system is operating with a fixed load, the input to the system is varying. Steady-state operation of the system is an infrequent mode and must be defined with reference to the input torque variation.

Several phenomena affect the velocity of the wind relative to the wind turbine, and, consequently, affect the torque developed in the drive train. These phenomena include wind shear, tower shadow, and blade flapping.

2.4.1 Tower shadow. - The significant wind variation in the technology of wind turbine generators is that caused by tower shadow.

Most of the large wind turbines that have been built have had the rotor downwind. The principal reasons for this configuration are that (1) the flapping blade is less likely to strike the tower on which the rotor is placed, (2) the rotor can be closer to the tower and less balancing mass is necessary to keep the center of gravity over the base of the tower, and (3) if allowed to yaw freely, the rotor will seek a downwind location as a stable position. As a consequence of the rotor being downwind of the tower on which it is mounted, the tower is between the wind and the rotor blades as they rotate. Even though the tower may be an open truss structure, it

provides considerable blockage to a free stream of air. The impedance to the wind and the resulting torque reduction in the turbine drive each time a blade passes behind the tower with respect to the wind is termed tower shadow.

The wind speed reduction and corresponding torque reduction that are the result of tower shadow can be as much as 35 percent with a truss tower (19). The torque reduction occurs n times per rotor revolution for n-bladed rotor. Thus, tower shadow produces an ever present torque pulse n times per rotor revolution.

2.4.2 Wind shear. - Wind shear is the result of ground surface friction on the wind. The wind speed normally increases with height above the ground. The speed variation is expressed by the relationship

$$V_w = V_{w_{ref}}(h/h_{ref})^k \qquad (2.11)$$

where the exponent k, is a function of the reference surface roughness.

As a result of the wind shear the torque produced by each blade varies as the turbine rotates. Because of the variation of the wind speed with height, there is a periodically varying shaft torque as the blades move through the wind field. For the wind turbine system studied a value of $k = 0.22$ is used. This is a k value representative of open country acceptable for installation of large wind turbines (20). The torque variation resulting from the wind shear is not large (21). The frequency of the variation is twice the turbine rotation frequency, however, and reinforces the tower shadow effect.

2.4.3 Blade flexibility. - The rotor blades of large wind turbines are relatively flexible structures. The response of these structures to aerodynamics and inertial loading results in blade motion, particularly flapping, which alters the torque developed. Study has indicated that these effects on rotor shaft torque are not significant (21). These effects are not considered in this study.

2.5 Coupling of Tower Shadow Excitation and Output

The tower shadow excitation has very important implications to the wind turbine generator designer and operator. The entire system structure must be strong enough to withstand the loading which results from the pulsing excitation. The frequency of the excitation must be kept sufficiently different from any structural natural frequencies to avoid resonances. For the power engineers the concern is the extent to which tower shadow excitation is coupled to the system power output.

2.5.1 Analysis of reduced model. - The existence of a twice per turbine rotor revolution torque pulse is inherent in a downwind rotor wind turbine with a two-bladed rotor. In order to reduce the coupling of that twice per revolution excitation into the alternator power output the stiffness of the transmission drive can be reduced. The variation of the mode frequencies of the transmission drive train as a function of drive train stiffnesses can be examined with the simplified model shown in figure 2.2. The figure represents the rotary inertias of the turbine rotor and the alternator coupled by a stiffness equivalent to all the drive train stiffnesses. The alter-

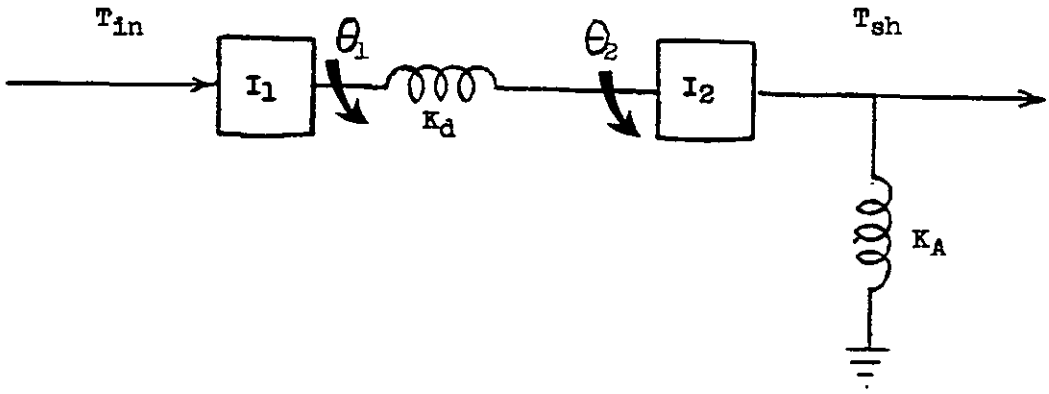

Figure 2.2-Simplified model of drive train and alternator

nator is represented by the second spring with a stiffness equal to the transient synchronous torque coefficient. The rotary motion of the transmission drive is given by equations (2.12) and (2.13).

$$I_1\ddot{\theta}_1 + K_d(\theta_1 - \theta_2) = T_{in} \tag{2.12}$$

$$I_2\ddot{\theta}_2 - K_d(\theta_1 - \theta_2) + K_A\theta_2 = +T_{sh} \tag{2.13}$$

The eigenvalue frequencies of the model are given by equation (2.14) and are plotted as a function of drive train stiffness in figure 2.3.

$$\omega^2 = \frac{K_d + K_A}{2I_2} + \frac{K_d^2}{2I_1} \pm \left[\frac{(K_d + K_A)}{4I_2^2} + \frac{K_d(K_d - K_A)}{2I_1I_2} + \frac{K_d^2}{4I_1^2}\right]^{1/2} \tag{2.14}$$

The magnitude of these frequencies are carefully considered by wind turbine structural designers in order to avoid a resonance from the tower shadow excitation of the input torque. In this study these resonant frequencies are of interest because the step action of a three-phase short circuit will excite these frequencies.

Another, and a closer, approximation of these natural frequencies of the drive train and alternator can be obtained from an eigenvalue analysis of the closed-loop system using linearized versions of the system equations. A linearized set of these equations is included in appendix D of this study.

2.5.2 Effect of tower shadow on swing curve. - The tower shadow pulses that modulate the input torque of a downwind rotor wind turbine generator can affect the clearing time for faults across the output of the alternator. Although the excitation is unidirectional and approximates a half cosine wave in its variation, the alternator responds by swinging continuously, almost sinusoidally. (This re-

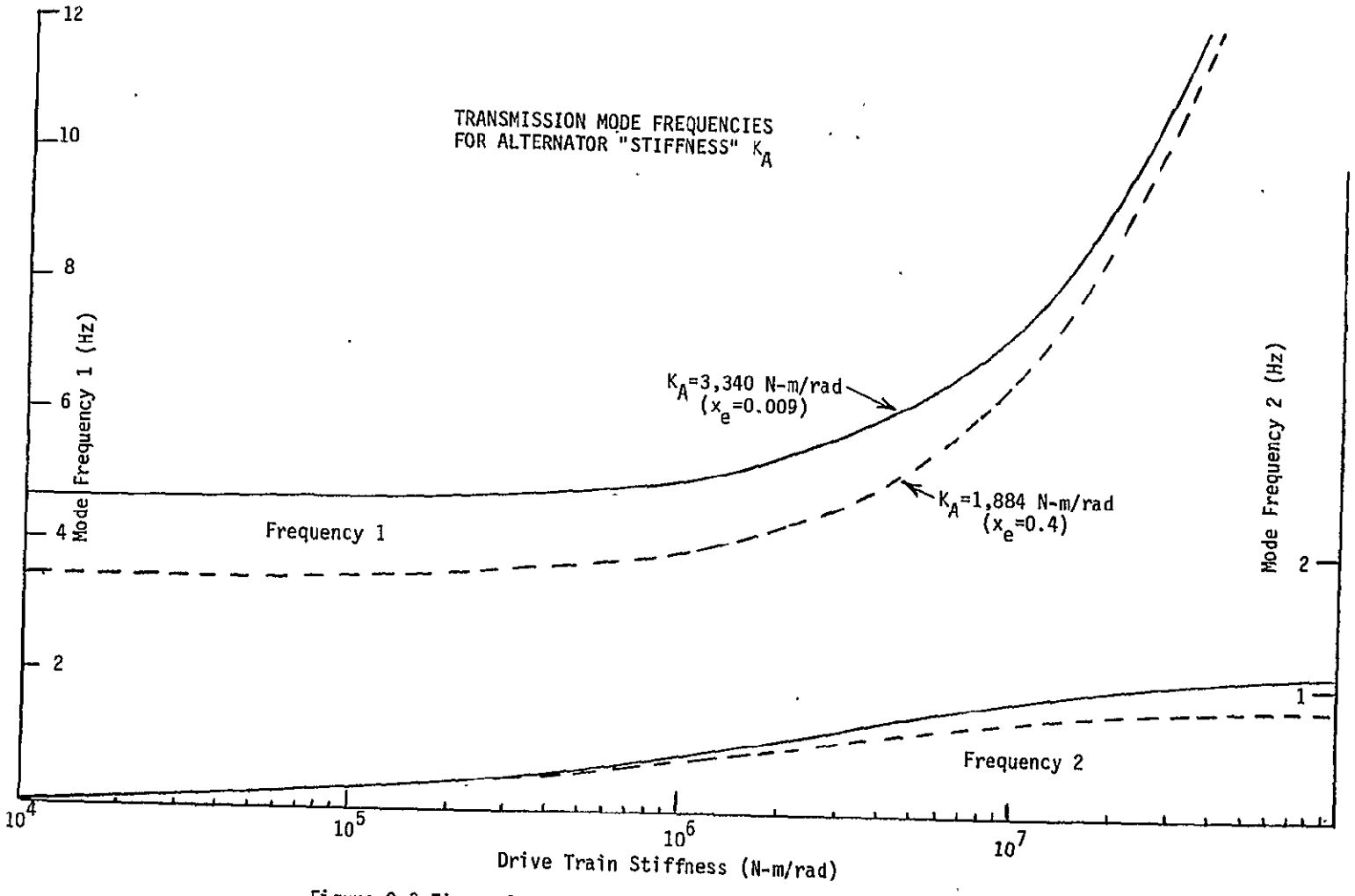

Figure 2.3-Eigenvalues of simplified drive train model

sponse is illustrated in Chapter IV where the results of the system simulation are described.) The rotor is continuously accelerating and decelerating. The clearing time for a three-phase short circuit depends upon the rotor acceleration due to the power pulsations plus the acceleration due to the unbalanced torque from the fault.

2.5.3 Effect of alternator excitation system on swing curve. - The effect of the alternator excitation system on the severity of the first swing is relatively small, except for faults with long clearing times (22). A very fast, high-response, excitation system will usually reduce the first swing by only a few degrees, or will increase the generator transient stability power limit by a few percent. The large inertia constant H of a wind turbine alternator makes for longer than usual clearing time. A representation of the alternator excitation system is warranted for this study.

2.6 Summary

The type of power system disturbance which is most important in stability studies is a fault applied and subsequently cleared (6). Faults are usually not permitted to remain on power systems any longer than is required for relays to detect their presence and open the appropriate circuit breakers.

The classical approach to the transient stability analysis of a faulted synchronous alternator tied to an infinite bus involves several simplifying assumptions. With the availability of modern digital computers for the solution of sets of nonlinear differential equations one of the reasons for making the assumptions is eliminated. At this early stage of investigations into the developing

technology of wind turbine generators, it is preferable to represent the system characteristics more closely. Concordia points out (23) that when the effect of delayed fault clearing is to be studied, a detailed alternator representation is desirable even though only the first swing transients of the alternator rotor are considered. If the simple concept of generator voltage behind transient reactance is used, the effect of clearing time is smaller than in reality. It follows that critical clearing times determined by a simplified stability survey are likely to be longer than in reality.

Chapter III

SIMULATION MODEL

The model used in this study is that of a typical large horizontal axis wind turbine generator system. The essential elements of the wind turbine system model are shown in the block diagram in figure 3.1. This is the configuration of the DOE/NASA 100 and 200 kW wind turbine generators already constructed as well as the larger 2 MW systems in development for the DOE.

A representative model consists of a large inertia turbine which converts wind energy to mechanical energy by applying torque to a low speed (20-40 r/min) shaft. A speed increaser converts the low speed, high torque energy to a high speed (1800-3600 r/min), low torque energy required to drive a conventional synchronous alternator. This transmission is illustrated in figure 3.2.

For this study the model has a rigid turbine developing torque that is transmitted by a drive shaft through a 1:45 speed changing gear box. The reduced torque is transmitted to a synchronous generator. The model is detailed in the following sections. The definitions of the terms in all equations are given in appendix A.

3.1 Turbine

The turbine model is a two-bladed propeller. The magnitudes of the useful torque developed by the turbine are calculated with a

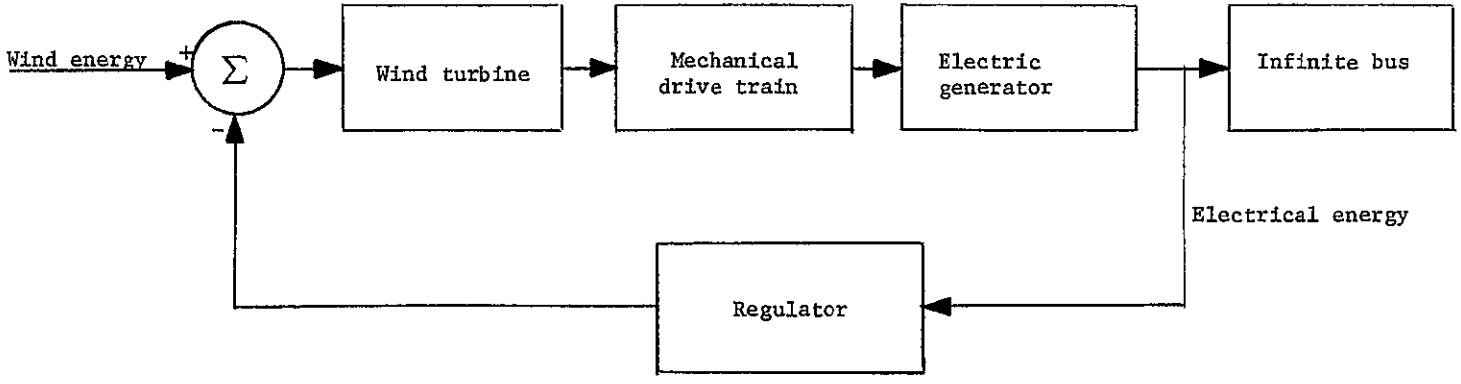

Figure 3.1. - Elements of wind turbine generator

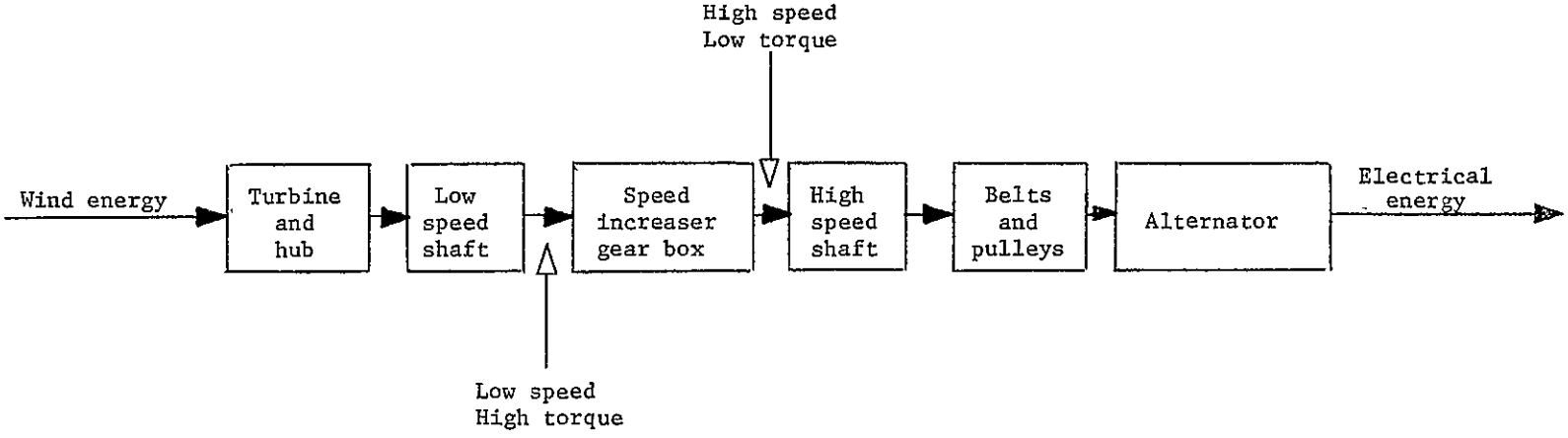

Figure 3.2. - Energy transmission through wind turbine generator.

digital computer program developed by Wilson and Lissaman (24) and modified for this research program. The turbine torque computer program uses a modified blade element theory and includes corrections for tip losses. The usable wind energy depends on wind velocity, turbine rotary speed, blade pitch angle, airfoil characteristics, and turbine geometry. The turbine geometry consists of the characteristics: blade length, number of blades, coning angle, and radial distributions of chord and twist angle. The turbine model computer program calculates shaft power, shaft torque, and thrust on the blades.

For a given blade geometry the torque was generated as a function of the wind speed perpendicular to the plane of the turbine, the turbine rotational speed, and the blade pitch angle. The relation for torque is

$$T_{in} = f(V_w, \dot{\theta}_1, \beta_1) \tag{3.1}$$

Torque-pitch angle characteristics calculated by the program for several wind speeds at 40 r/min are shown in figure 3.3.

3.2 Drive Train

The drive train elements, that is, the low speed shaft, the gear box, the high speed shaft, and the couplings, have been modeled as the pi-network indicated in figure 3.4. The rotational inertias of all elements on the low speed side of the gear box, including the gear box, have been combined into one inertia, I_1, separated from the combined inertia, I_2, of all components on the high speed side of the gear box, including the generator rotor, by the composite stiffness, K_d, of all elements between the turbine and the alternator. Transmission train lossed are accounted for by the damping factors B_1 and B_2.

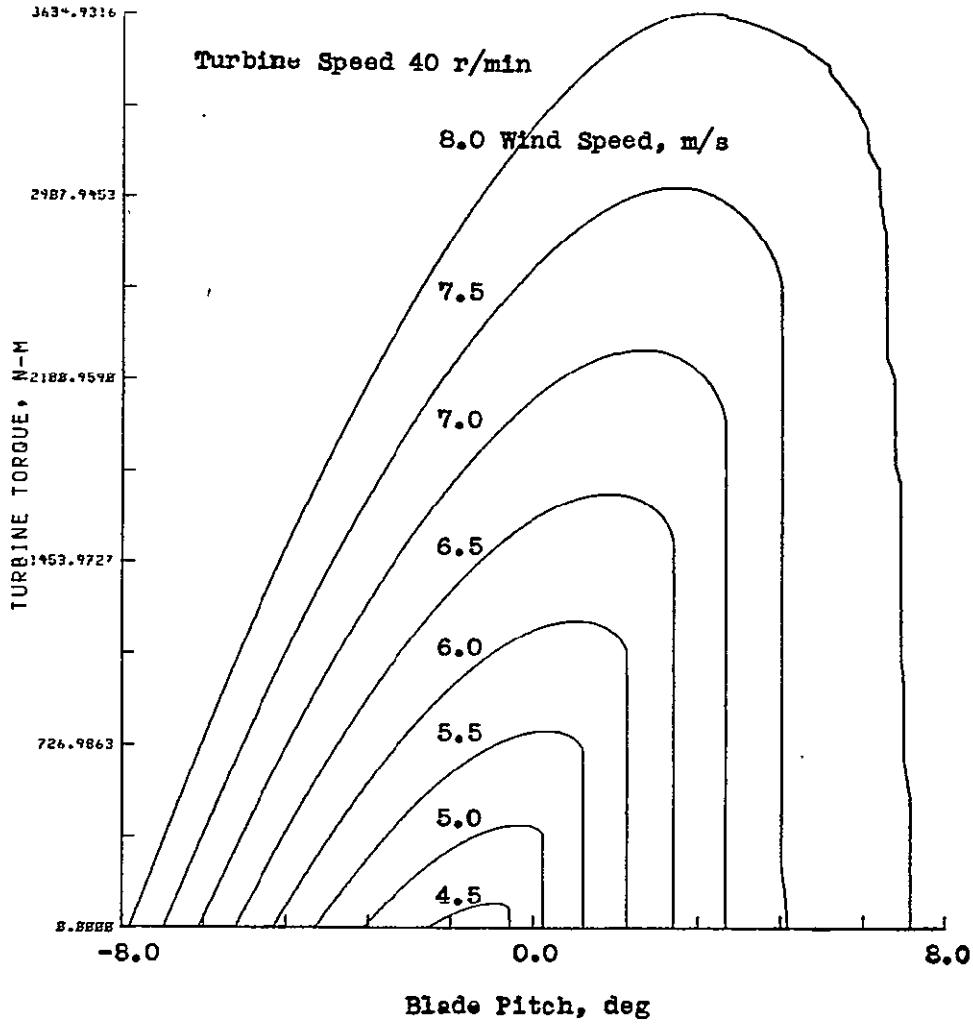

Figure 3.3-Mod-0 Wind Turbine Generator Torque-Pitch Characteristics

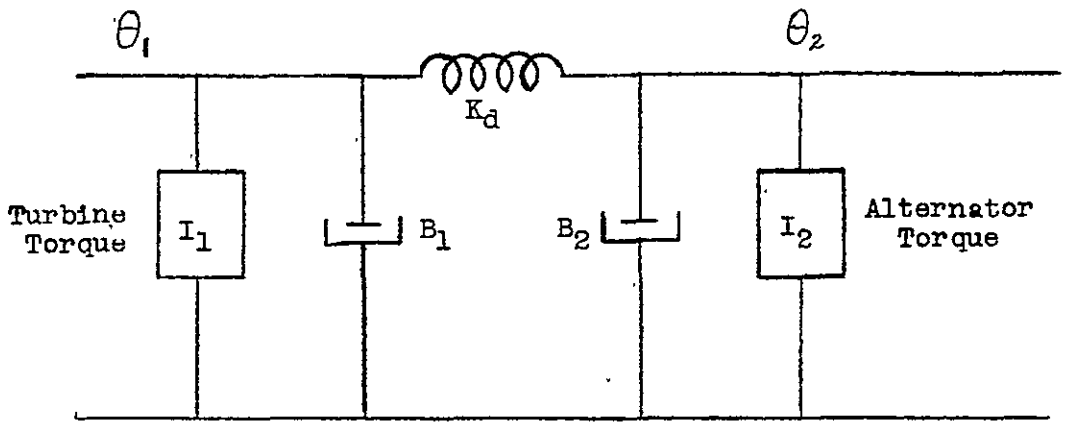

Figure 3.4-Equivalent Pi-network of Drive Train

The simplification of the drive train to a pi-network is justified on the basis that

(1) the rotational inertia of the turbine is much greater (15 times) than the combined rotational inertias of all other elements of the drive train, and therefore, it alone essentially determines I_1,

(2) the alternator rotor provides the largest rotational inertia on the high speed side of the gear box, and essentially determines I_2, and

(3) the large low speed drive shaft and the gear box are the softest springs in the drive train and essentially determine its effective stiffness.

The stiffness of the drive train determines the amount of coupling between the turbine and the alternator. The extent of this coupling becomes important to the network performance of the wind turbine generator because of the tower shadow effect on the input torque excitation (21). Composing all the drive train stiffnesses into one spring facilitates treating the coupling parametrically while permitting retention of the lowest oscillatory mode of the drive train which is in a range most likely to excite power network modes. Since the stiffnesses and inertias of elements other than the turbine, the low speed shaft, and the alternator rotor are not readily available from measurements or calculation, they are estimated. Little accuracy is lost, therefore, in resorting to an equivalent pi-network for the drive train. The numerical values of the baseline model drive train parameters are listed in Table 3.1.

Table 3.1

STIFFNESS AND MASS MOMENT OF INERTIA OF BASELINE DRIVE TRAIN COMPONENTS

	Mass moment of inertia, N-m-sec^2	Torsional stiffness, N-m/rad
Turbine	127,735	"Rigid"
Low speed shaft	835	2.26×10^7
Gear box	281	1.88×10^7
High speed shaft[a]	[b]992	11.54×10^7
Alternator rotor[a]	3,887	96.40×10^7
Pulleys and belts[a]	3,356	7.28×10^7

[a]Referred to turbine speed.
[b]Includes disk brake.

The state space model of the equations of motion of the drive train is

$$\begin{bmatrix} \dot{\theta}_1 \\ \ddot{\theta}_1 \\ \dot{\theta}_2 \\ \ddot{\theta}_2 \end{bmatrix} = \begin{bmatrix} 0 & 1 & 0 & 0 \\ -\frac{K_d}{I_1} & -\frac{B_1}{I_1} & \frac{K_d}{I_1} & 0 \\ 0 & 0 & 0 & 1 \\ \frac{K_d}{I_2} & 0 & -\frac{K_d}{I_2} & -\frac{B_2}{I_2} \end{bmatrix} \begin{bmatrix} \theta_1 \\ \dot{\theta}_1 \\ \theta_2 \\ \dot{\theta}_2 \end{bmatrix} + \begin{bmatrix} 0 & 0 \\ \frac{1}{I_1} & 0 \\ 0 & 0 \\ 0 & -\frac{1}{I_2} \end{bmatrix} \begin{bmatrix} T_{in} \\ T_{sh} \end{bmatrix} \tag{3.2}$$

$$\Omega_A = N\dot{\theta}_2 \tag{3.3}$$

$$\dot{\delta} = \left(\frac{\text{poles}}{2}\right)\Omega_A \tag{3.4}$$

3.3 Alternator

The electrical generator modeled is a synchronous alternator described the classical Park's equations (17), modified by Olive (25) to eliminate any explicit expression of inductance. The alternator

equations reflect the assumption that the synchronous generator frequency is the same as the bus frequency as long as synchronism is maintained (26). No assumptions are made with respect to the relative magnitudes of the "transformer voltages" ($d\lambda_d/dt$, $d\lambda_q/dt$) and the "speed voltages" ($\omega\lambda_d$, $\omega\lambda_q$). The following equations describe the alternator.

$$i_d = \frac{e''_q - \lambda_d}{x''_d} \tag{3.5}$$

$$i_q = \frac{e''_d + \lambda_q}{-x''_d} \tag{3.6}$$

$$\frac{d\lambda_d}{dt} = [v_d + r_a i_d - (e_d + x_q i_q)\omega]\omega_0 \tag{3.7}$$

$$\frac{d\lambda_q}{dt} = [v_q + r_a i_q + (x_d i_d - e_{q1} - e_{q2})\omega]\omega_0 \tag{3.8}$$

$$e_d = \frac{(x_q - x''_q)\lambda_q + x_q e''_d}{x''_q} \tag{3.9}$$

$$e_{q1} = \frac{(x_d - x''_d)}{(x'_d - x''_d)} e'_q - \frac{(x_d - x'_d)}{(x'_d - x''_d)} e''_q \tag{3.10}$$

$$e_{q2} = \frac{(x'_d - x''_d)\lambda_d + x''_d e'_q - x'_d e''_q}{-x''_d \frac{(x'_d - x''_d)}{(x_d - x''_d)}} \tag{3.11}$$

$$\frac{de'_q}{dt} = \frac{v_f - e_{q1}}{T'_{do}} \tag{3.12}$$

$$\frac{de''_q}{dt} = -\frac{(x'_d - x''_d)}{T''_{do}(x_d - x''_d)} e_{q2} \tag{3.13}$$

$$\frac{de''_d}{dt} = -\frac{e_d}{T''_{qo}} \tag{3.14}$$

The electromagnetic torque is

$$T_e = e''_d i_d + e''_q i_q - i_d i_q (x''_d - x''_q) \tag{3.15}$$

$$T_L = N\left(\frac{\text{poles}}{2}\right)\left(\frac{737.8 \text{ kvabase}}{\omega_o}\right) T_e \qquad \text{lb-ft} \tag{3.16}$$

$$= N\left(\frac{\text{poles}}{2}\right)\left(\frac{737.8 \text{ kvabase}}{\omega_o}\right)(0.1383) T_e \qquad \text{n-m}$$

The machine reactances appearing in the alternator equations include the output transformer and the tie line reactances. Therefore, the terms v_d and v_q in equations (3.7) and (3.8) are the infinite bus direct and quadrature axes voltage components as shown in figure 3.5 where v_t is the alternator terminal voltage.

3.4 Alternator Excitation System

The modeled excitation system tends to maintain a constant power factor load on the alternator as well as a constant output voltage (13). Shown in block diagram form in figure 3.6 the excitation system is described by the following equations:

$$\Delta v_t = V_{ref} - v_t + K_{PF}\left(\frac{p}{v_t} - PF \cdot i_a\right) \tag{3.17}$$

$$\Delta v_f = \frac{K_{VR}}{\tau_e} \Delta v_t \left(\exp - \frac{t}{\tau_e}\right) \tag{3.18}$$

$$\Delta v_f = V_{R_{nom}} + \Delta v_f \tag{3.19}$$

where, as shown in figure 3.5,

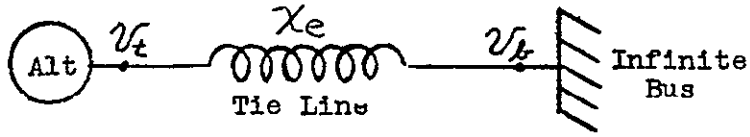

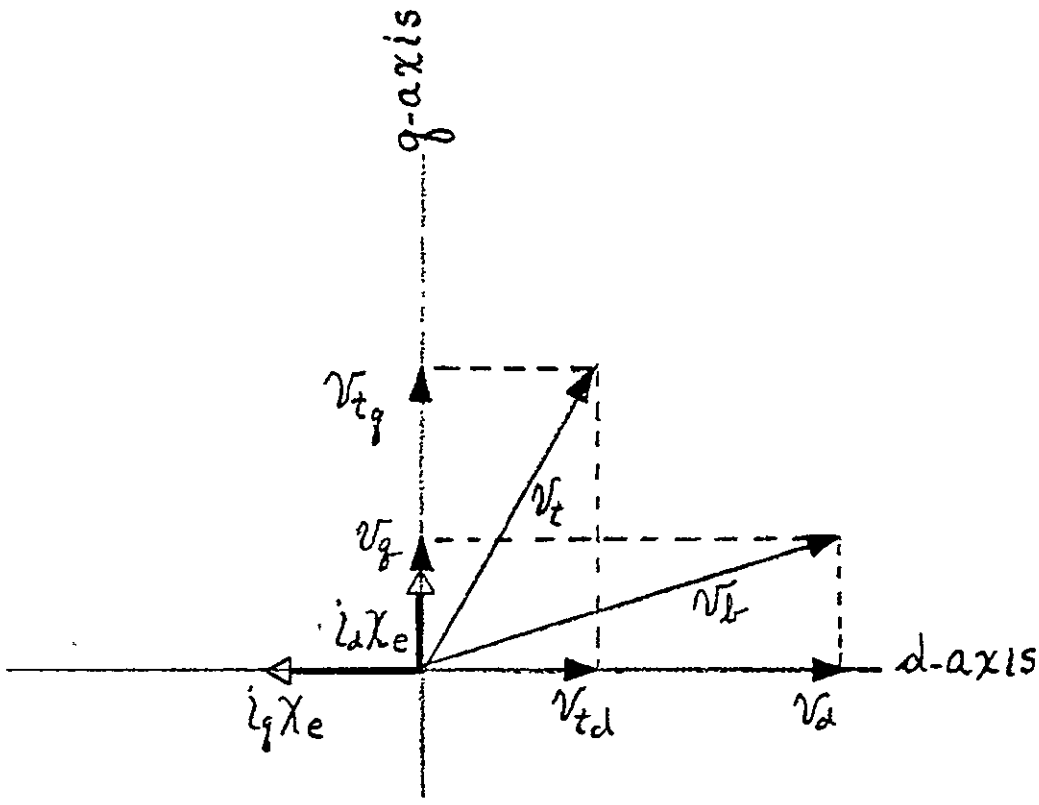

$$V_{td} = V_d - i_q X_e$$

$$V_{tq} = V_q + i_d X_e$$

$$V_t = (V_{td}^2 + V_{tq}^2)^{\frac{1}{2}}$$

Figure 3.5-Terminal Voltages

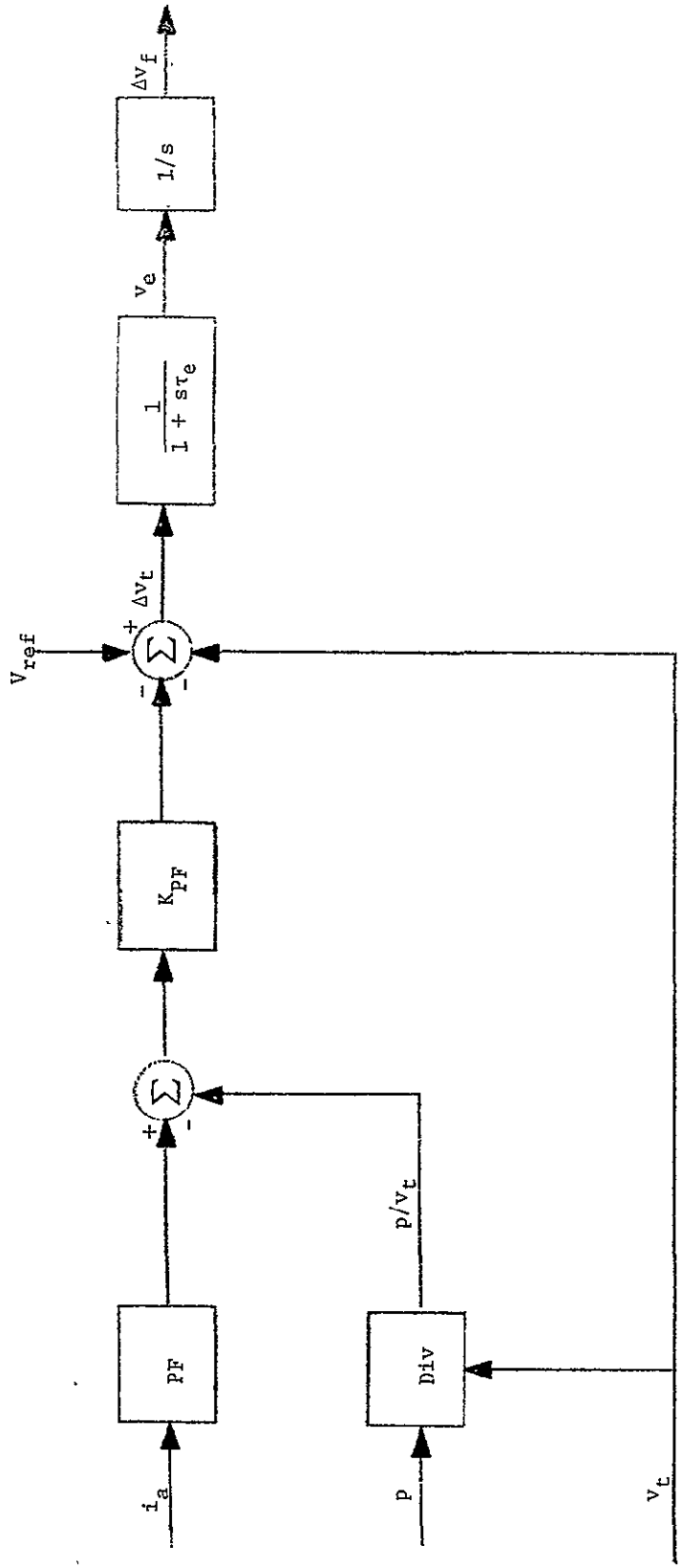

$$v_t = (V_{ref} - v_t) - K_{PF}\left(PF \cdot i_a - \frac{p}{v_t}\right)$$

Voltage deviation — Power factor deviation

Figure 3.6. - Constant power factor excitation system.

$$v_{td} = v_d - i_q x_e \tag{3.20}$$

$$v_{tq} = v_q + i_d x_e \tag{3.21}$$

$$v_t = \left(v_{td}^2 + v_{tq}^2\right)^{1/2} \tag{3.22}$$

$$v_d = \sin \delta \tag{3.23}$$

given

$$v_q = \cos \delta \tag{3.24}$$

The term $(v_{ref} - v_t)$ in equation (3.17) represents the voltage deviation; the term $((p/v_t) - PF \cdot i_a)$ represents the power factor deviation.

3.5 Turbine Blade Pitch Control

Blade pitch control is used to regulate power output of the alternator. At wind speeds below the system rated wind speed, alternator output is correspondingly below the rated alternator power. At these less than rated conditions the blades are kept at a fixed pitch - "maximum power position." When the wind speed is above the rated value (Table 3.1), the alternator is actively limited. Limitation is effected by pitching the turbine blades. Output power is measured and compared with the reference value to generate an error signal that actuates the controller and the blade pitch servomechanism (fig. 3.7). The equations describing the control action at and above rated wind conditions are listed in state space form.

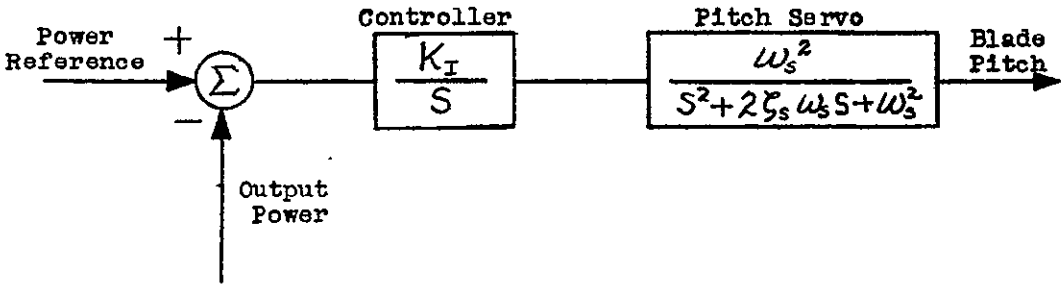

Figure 3.7-Controller and Blade Pitch Servo Models

$$\dot{\beta}_i = \begin{vmatrix} 0 & 1 & 0 \\ 0 & 0 & 1 \\ 0 & -\omega_s^2 & -2\zeta_s\omega_s \end{vmatrix} \beta_i + \begin{vmatrix} 0 \\ 0 \\ -K_I\omega_s^2 \end{vmatrix} \Delta p \qquad (3.25)$$

3.6 Computer Simulation

The wind turbine generator model described in the preceding sections provides a set of nonlinear, interrelated, differential equations. This set of equations was solved numerically with a computer code developed for this study using CSMP - Continuous System Modeling Program (27). Integration is performed using a fourth order Runge-Kutta integration method with a fixed step size of 0.002. Options are provided in the code for the inclusion of tower shadow effect, wind shear effect, and gusting of the wind.

The CSMP INITIAL segment of the code includes a set of equations that establishes the initial conditions of the system for any selected power and power factor loading of the alternator. In the CSMP DYNAMIC segment of the program a three phase short circuit can be applied at any time for any duration. Subsequent to the application of the fault the bus and alternator rotor speeds, which are identical prior to the occurrence of the fault, are computed independently.

In cases for which a constant wind speed is assumed, the output transients result from a three phase fault short circuit applied at time $t = 0$. In cases for which tower shadow effect is included, the transient resulting from the introduction of tower shadow is permitted to stabilize to a "steady state" prior to the application of the fault.

A listing of the computer program used for this study is included as Appendix F of the dissertation.

3.7 Summary

A block diagram of the complete wind turbine generator system model for this study is shown in figure 3.8. The model has been configured for simulation on a digital computer to provide a measure of the response of the alternator to three phase zero impedance short circuits.

The numerical values of the system constants used in the simulation are listed in Appendix E.

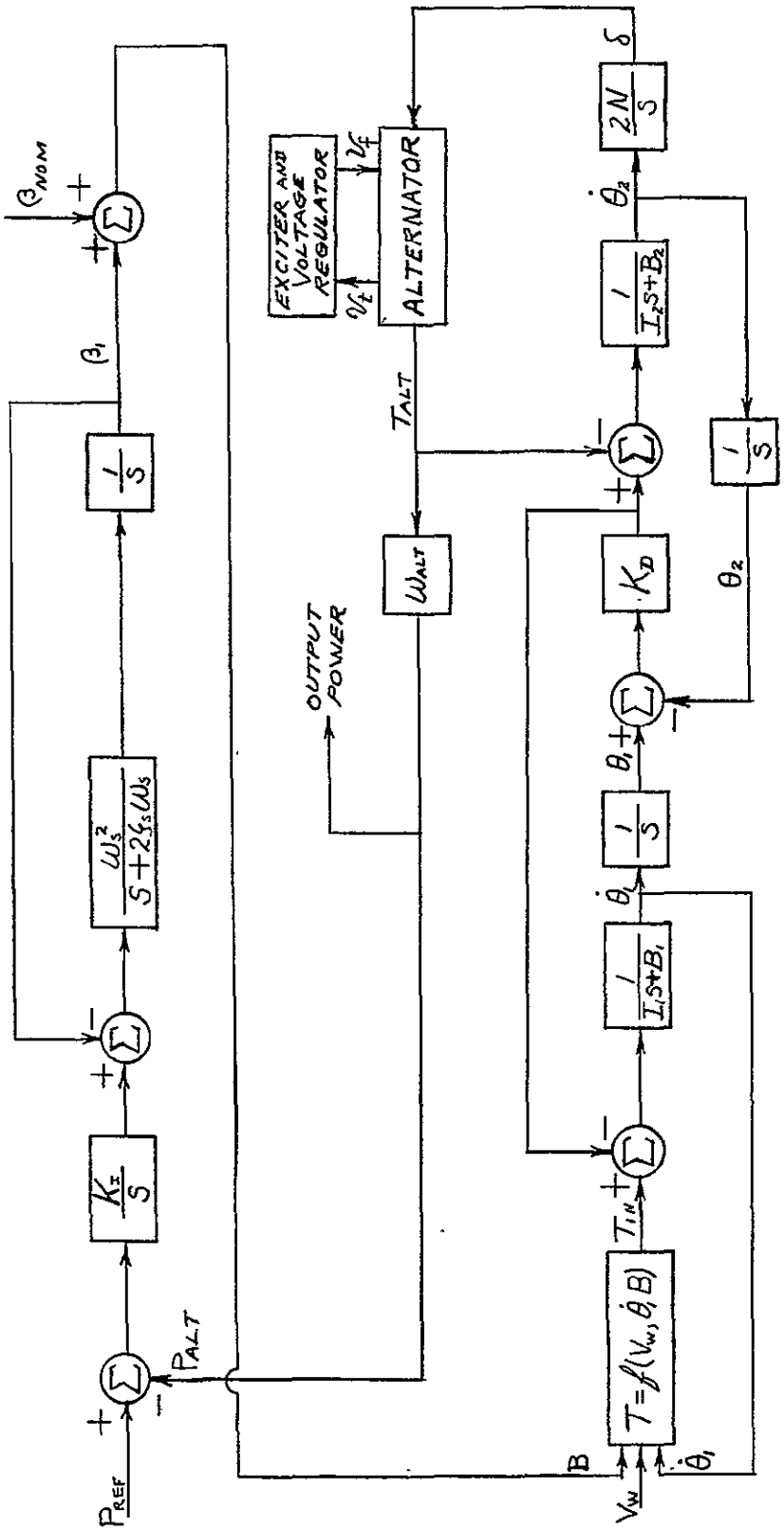

Figure 3.8-Simulation model block diagram

Chapter IV

RESULTS OF SIMULATION

The response of the synchronized wind turbine alternator to a three phase, zero impedance, short circuit was simulated to examine the nature of the swing curve and to determine maximum clearing time required to maintain synchronism. A tabulation of the numerical results of the simulation are presented in Table 4.1 for the selected parameters and operating conditions examined in the study.

4.1 Selected Operating Conditions and Parameters

4.1.1 External reactance. - Two values of external reactances were selected for comparison. The lower value, x_e = 0.009 pu, is the tie line reactance of the Mod-0 wind turbine which was used as the baseline model for the research study. The second tie line reactance, x_e = 0.4 pu was selected as representative of a high reactance so that the two reactances spanned the probable range of values to be expected realistically. In both cases the line resistance was assumed negligible.

4.1.2 System parameters. - Two parameters of the wind turbine system, the equivalent drive train stiffness and the total rotary inertia, were varied to observe the effects on first swing transients resulting from short circuit faults. Both of these parameters are structural features of concern to system designers as well as power engineers.

TABLE 4.1

MAXIMUM CLEARING TIME (WITHOUT LOSS OF SYNCHRONISM)

Tie-line reactance, pu	Drive train relative stiffness	Relative rotary inertia	Number of 60 Hz cycles in maximum short at given wind speed		
			14 mph	18 mph	30 mph (wind speed*)
0.009	0.1	1.0	25	15	15
	1.0	1.0	67	37	37
	10.0	1.0	67	38	38
	.1	.5	18	12	12
	1.0	.5	56	28	29
	10.0	.5	53	29	30
0.4	0.1	1.0	15	7	7
	1.0	1.0	45	21	21
	10.0	1.0	44	23	24
	.1	.5	11	5	5
	1.0	.5	33	15	16
	10.0	.5	32	17	18

*Wind speed	Corresponding load
14 mph = 6.2 m/s	0.4 pu, 0.8 PF
18 mph = 8.0 m/s	0.8 pu, 0.8 PF
30 mph = 13.4 m/s	0.8 pu, 0.8 PF

4.1.3 Electrical loads. - Three loading conditions were selected for examination: a 0.4 pu power load at a wind speed of 14 mph, a 0.8 pu power load at a wind speed of 18 mph, and a 0.8 pu power load at a wind speed of 30 mph. All the loads have a 0.8 lagging power factor. The 0.8 pu load at 18 mph wind speed represents the rated loading at rated wind speed for the baseline model wind turbine. The 0.4 pu load is a 50 percent rated load and occurs in the fixed blade pitch control mode of the system operation. The 0.8 pu load at 30 mph wind is the rated load in the variable pitch or power limiting control mode of the system. The rated load at rated wind speed is nominally at the interface of the two control modes.

4.2 Determination of Maximum Clearing Time

To determine the maximum clearing time for a particular set of operating conditions and system parameters a three phase short circuit, zero impedance, fault was applied to the system at the infinite bus terminals. The duration of the simulated fault, measured in terms of cycles of the 60 Hz frequency, was increased successively in integral values until a power angle swing that exceeded 180° was observed. The short circuit transient preceding the occurrence of the slipped pole determined the maximum clearing time.

4.3 Tower Shadow and Wind Shear

The ever present tower shadow phenomenon in the downwind rotor wind turbine generator and the wind shear produce a twice per turbine rotor revolution torque excitation that is coupled to the alternator through the drive train transmission. (A two-bladed turbine rotor is implied.) The effect of this excitation on the baseline system power output is shown in figures 4.1 and 4.2.

A three phase short circuit fault applied to the system at a time when the alternator rotor acceleration is at a maximum produces the transient displayed in figures 4.3 and 4.4. The figure displays the maximum clearing time for the system operating at the given power conditions and experiencing tower shadow and wind shear. A short circuit duration 1 cycle longer causes loss of synchronism, and that result is also indicated in figures 4.3 and 4.4.

A short circuit applied to the baseline model simulated without the tower shadow and wind shear effects produces the transient and maximum clearing time illustrated in figures 4.5 and 4.6. The com-

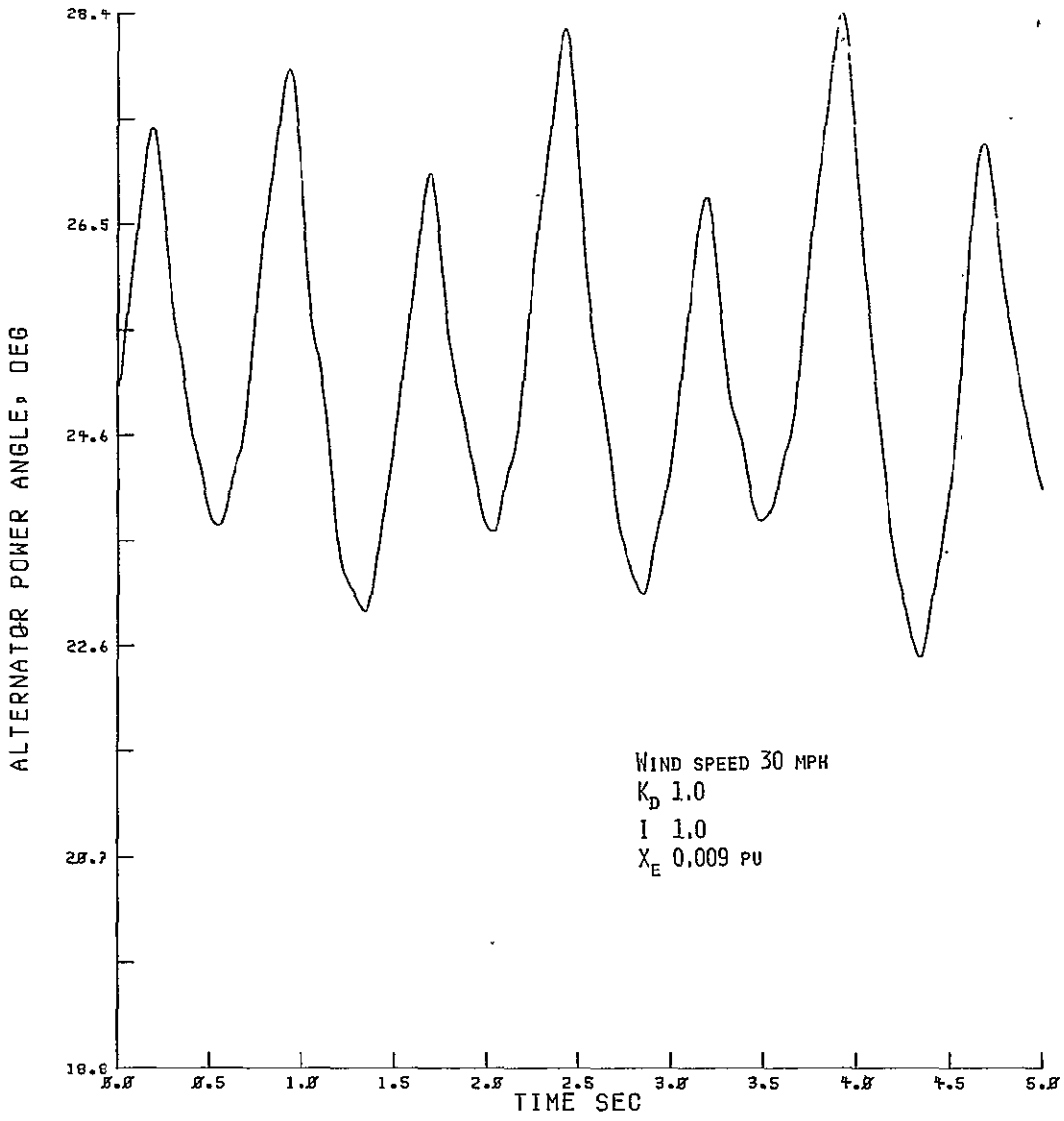

FIGURE 4.1. - BASELINE MODEL POWER ANGLE OSCILLATIONS FROM TOWER SHADOW AND WIND SHEAR.

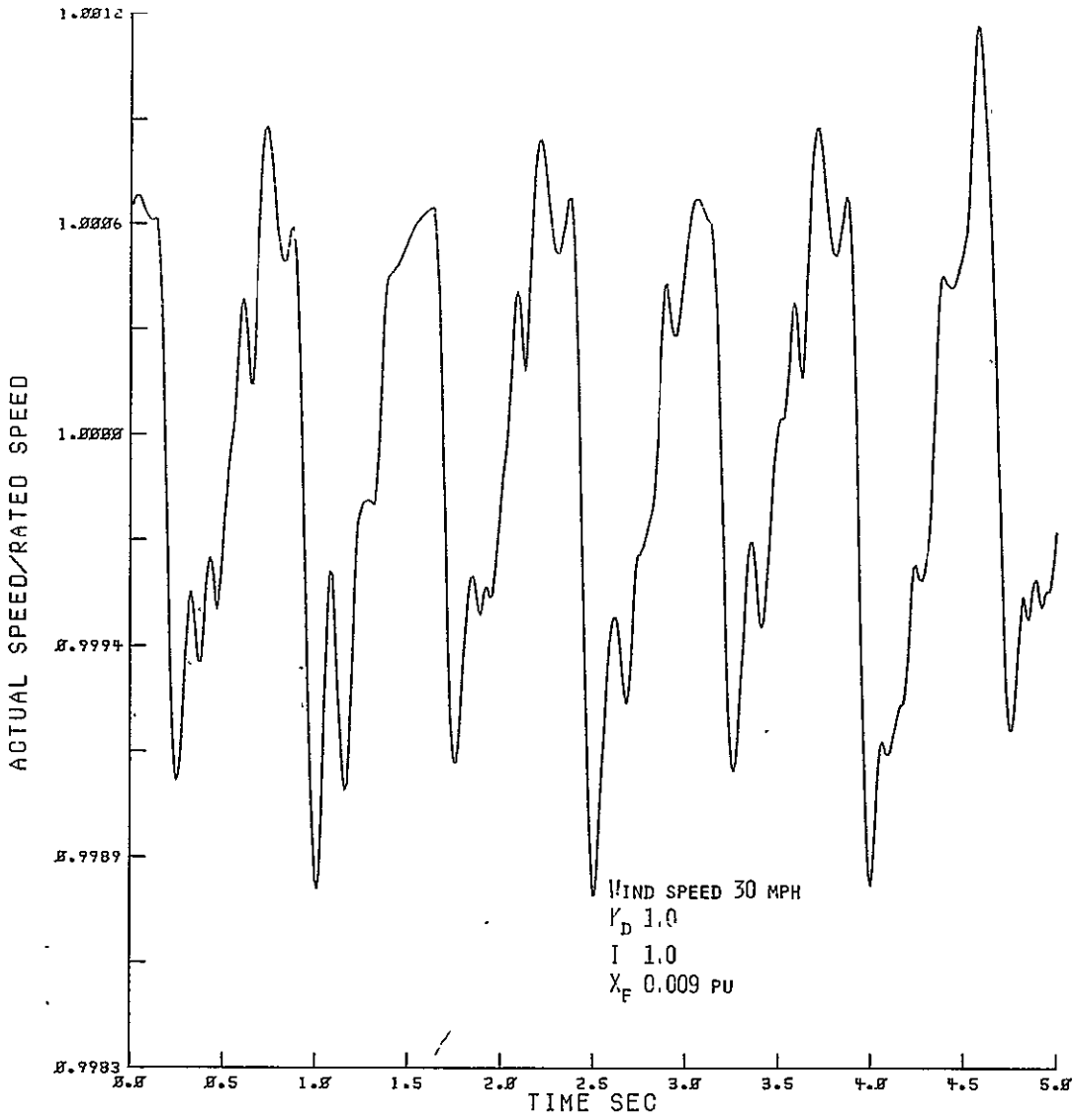

FIGURE 4.2. - BASELINE MODEL SPEED VARIATION FROM TOWER SHADOW AND WIND SHEAR.

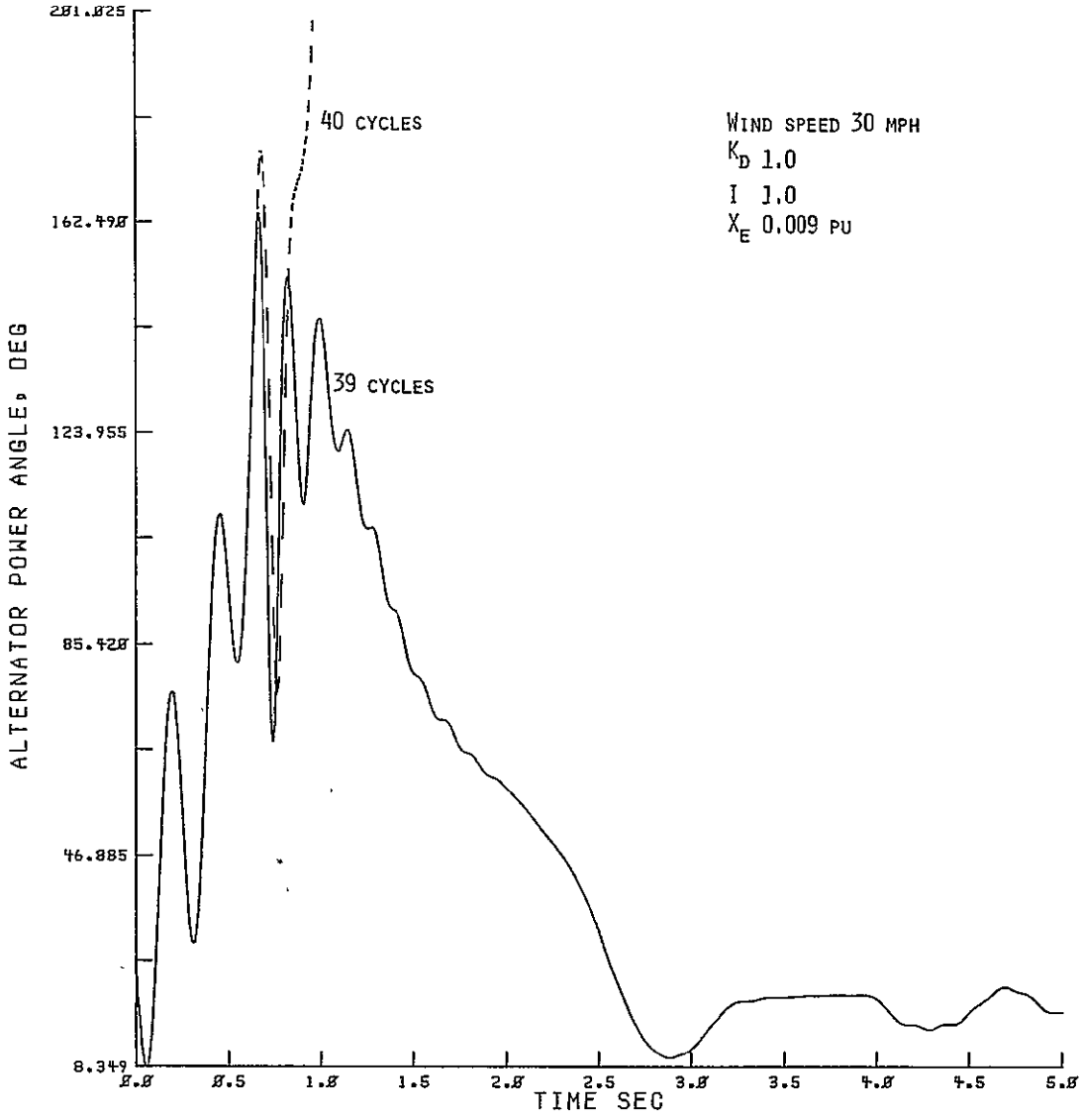

FIGURE 4.3. - SWING CURVE OF BASELINE MODEL WITH TOWER SHADOW AND WIND SHEAR.

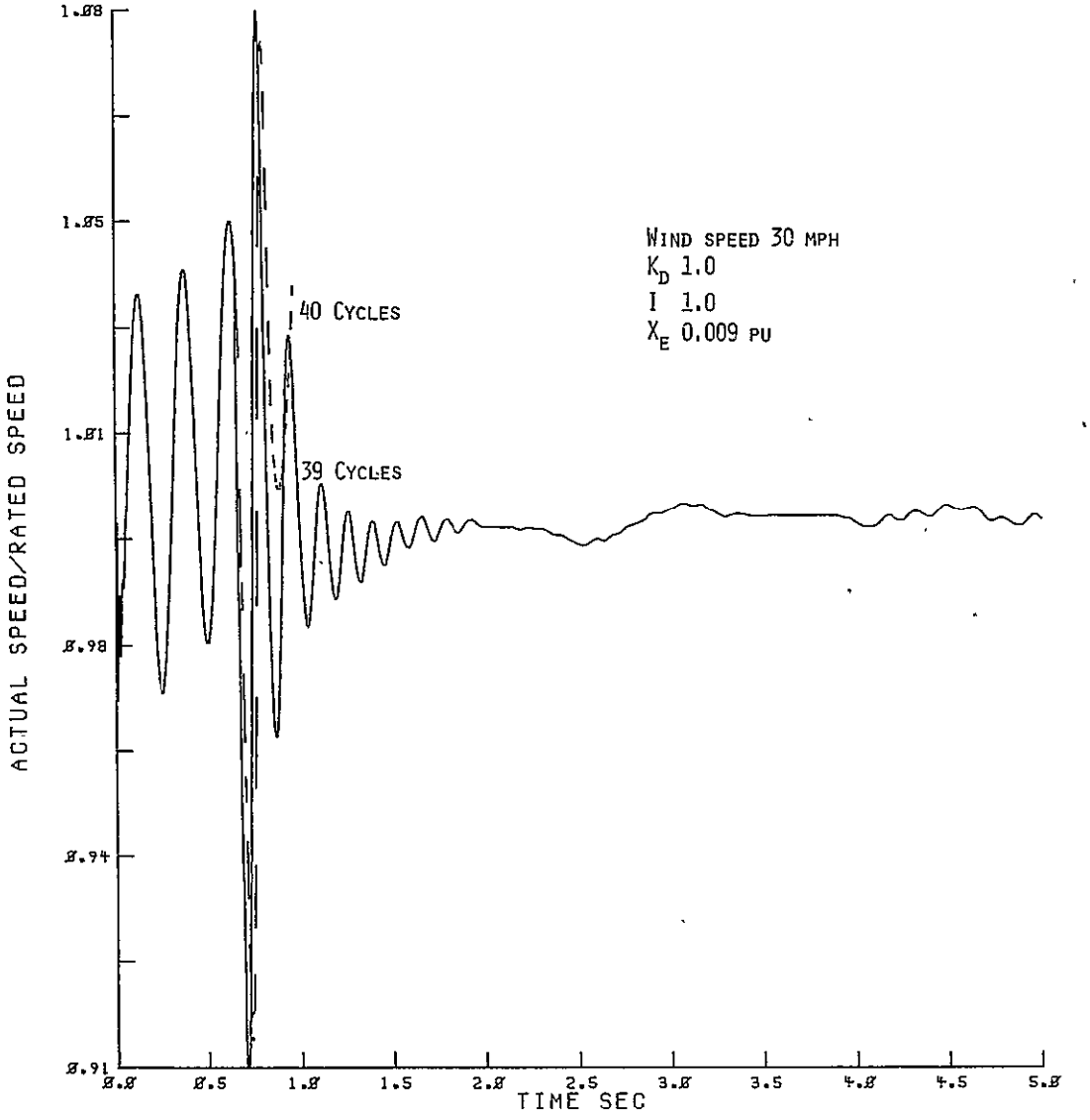

FIGURE 4.4. - ROTOR SPEED CURVES OF BASELINE MODEL WITH TOWER SHADOW AND WIND SHEAR.

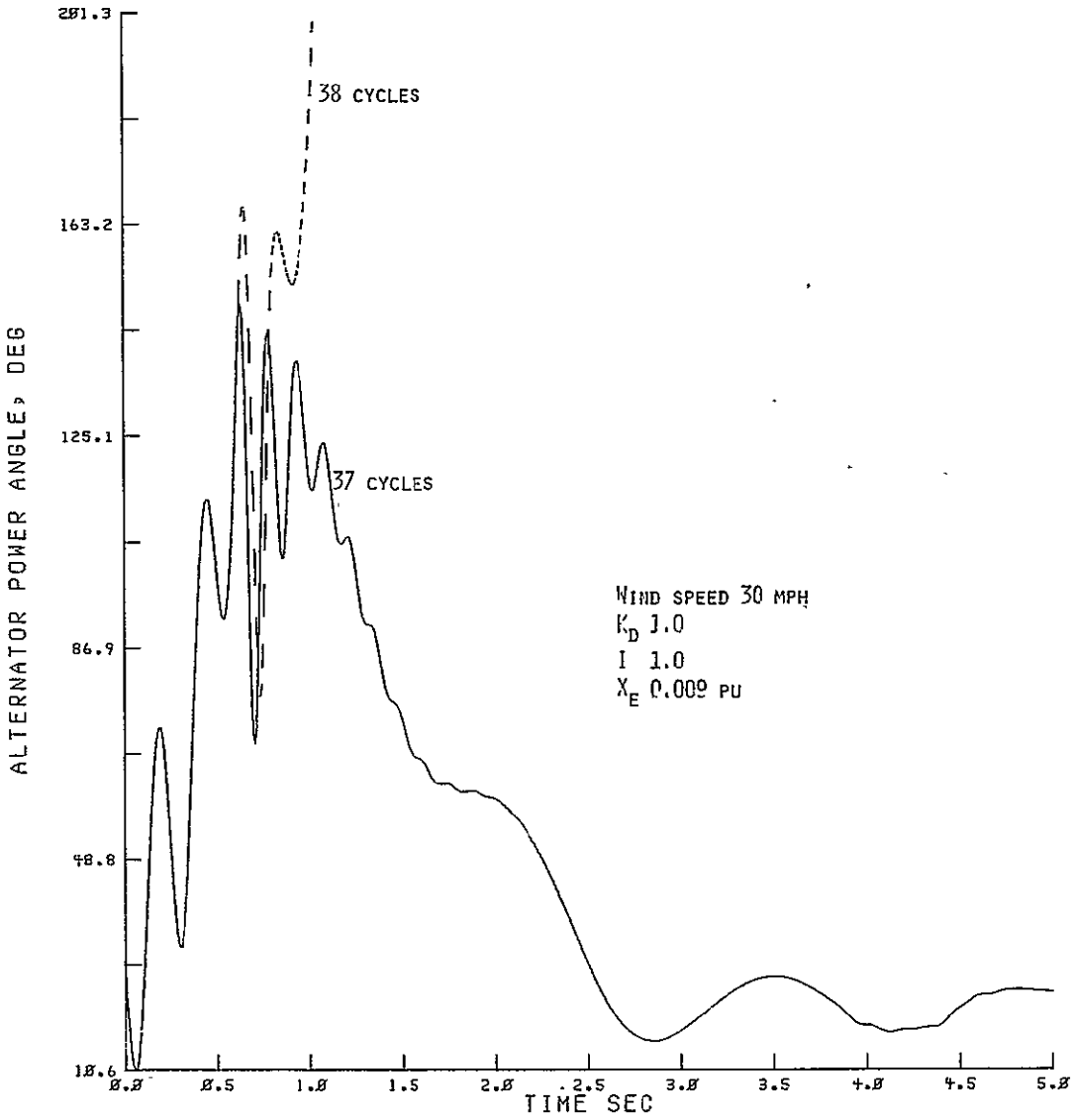

FIGURE 4.5. -"SWING" CURVE OF BASELINE MODEL WITHOUT TOWER SHADOW AND WIND SHEAR.

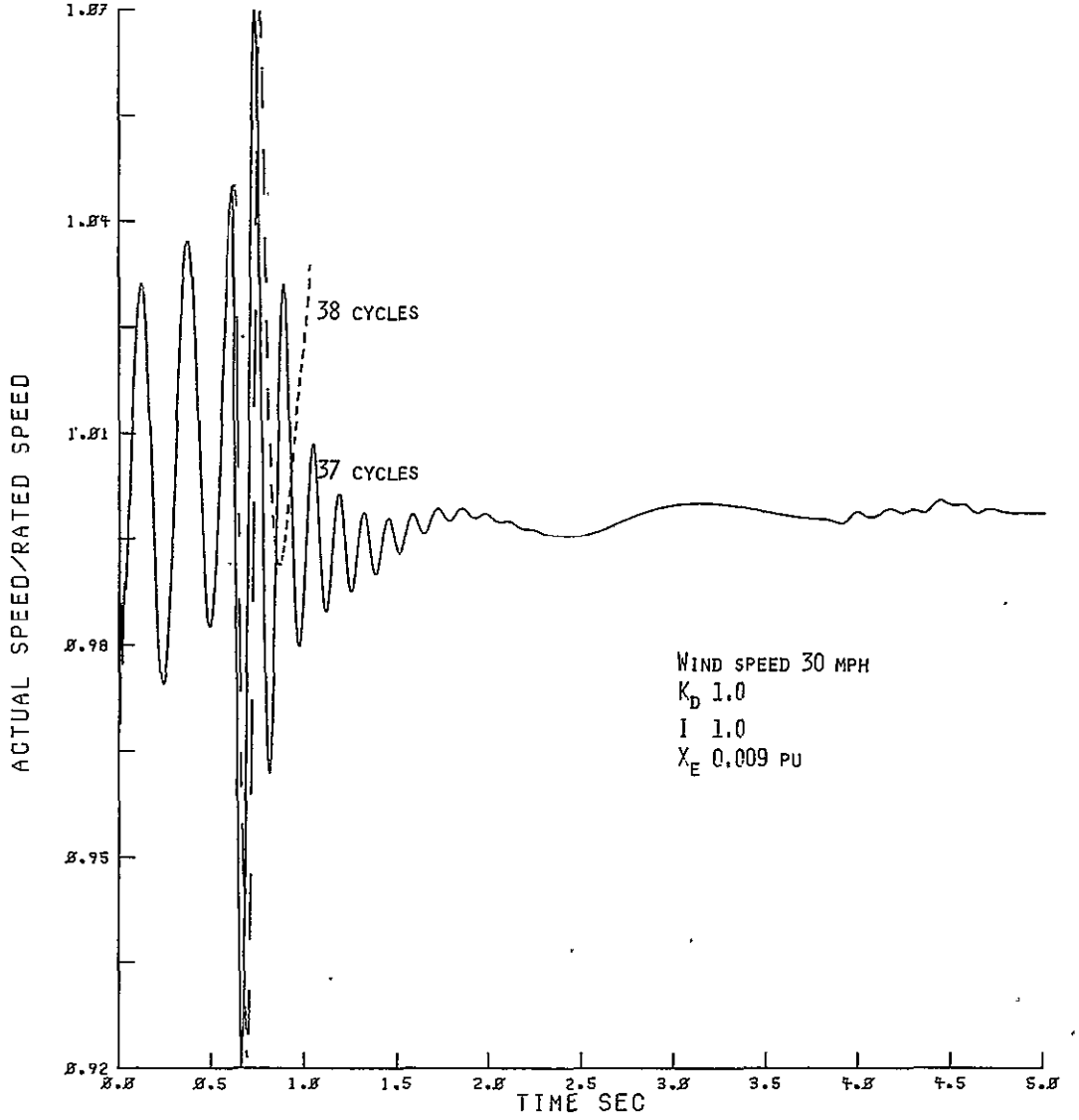

FIGURE 4.6. - ROTOR SPEED CURVES OF BASELINE MODEL WITHOUT TOWER SHADOW AND WIND SHEAR.

parison is more easily seen in figures 4.7 to 4.10 in which the transient curves of figures 4.3 to 4.6 are superimposed. The similarity of the two transients implies that for the study of the effects of this fault on the wind turbine generator tower and wind shear can be neglected. This inference is drawn because the magnitude of both tower shadow and wind shear simulated is probably as high as each would ever be in a real wind turbine generator system.

For the nominal turbine speed used for the model the twice per turbine rotation excitation produces a 1.33 Hz excitation frequency. This frequency is above any of the low frequency mode values indicated in Table 4.2 and does not excite other oscillation modes.

TABLE 4.2

COMPARISON OF SIMULATION AND EIGENANALYSIS FREQUENCIES

Alternator stiffness, K_A	2537 lb-ft/elec rad (x_e = 0.009)			1390 lb-ft/elec rad (x_e = 0.4)		
Drive train relative stiffness, K_D[a]	0.1	1.0	10.0	0.1	1.0	10.0
	Low-frequency mode					
Simulation frequency, Hz[b]	0.3	0.7	0.7	0.3	0.6	0.8
Eigenanalysis frequency, Hz	0.3	0.7	0.8	0.3	0.6	0.8
	High-frequency mode					
Simulation frequency, Hz[b]	5.1	6.4	14.0	3.9	4.8	13.3
Eigenanalysis frequency, Hz	4.8	6.0	13.5	3.6	5.2	13.1

[a]Stiffness relative to baseline model stiffness.
[b]Frequency determined from digital computer output listing.

The option to neglect the tower shadow and wind shear effects was selected for this research study. This simplification materially reduced computer time. If there is error in making this assumption,

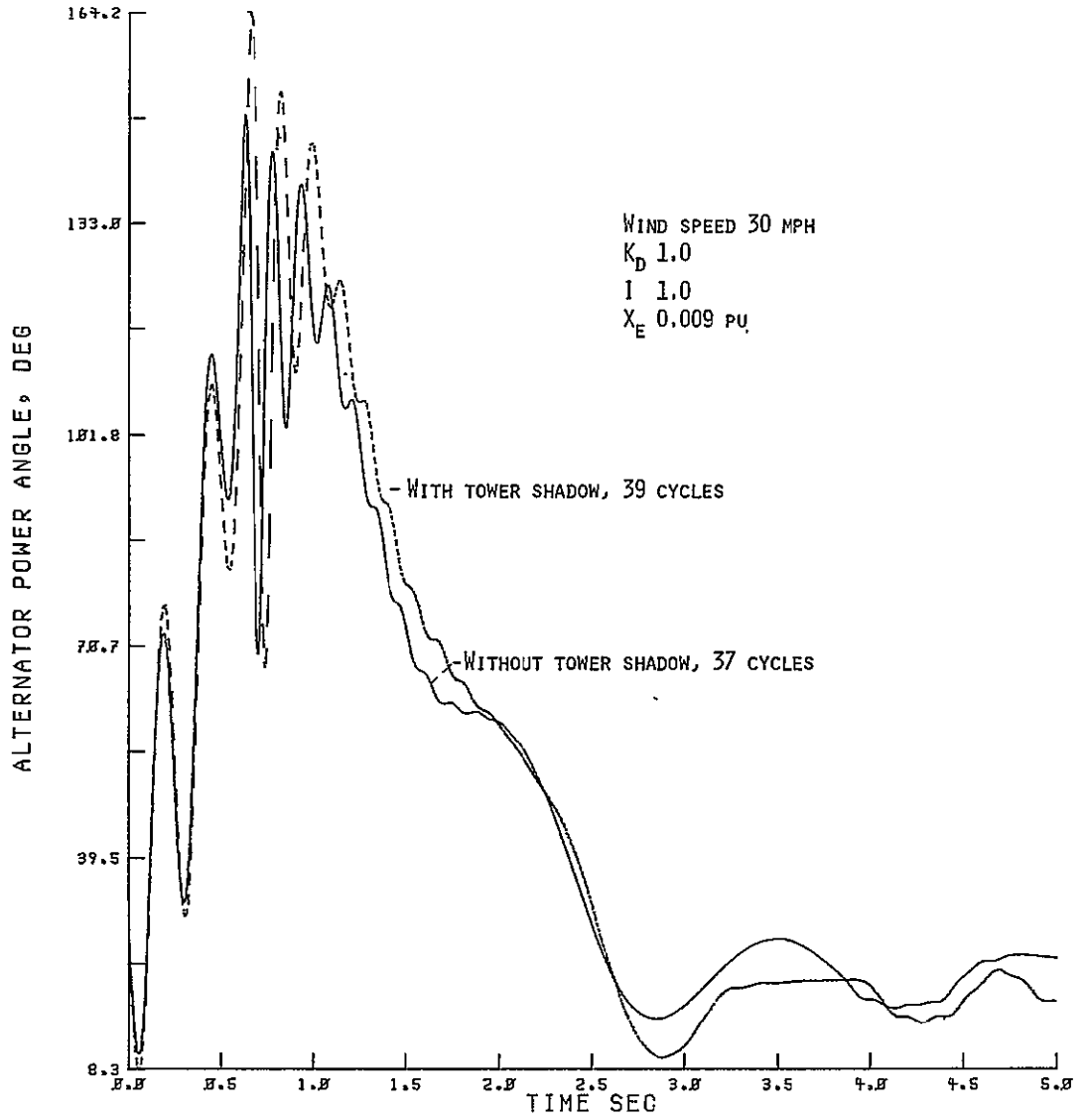

FIGURE 4.7. - COMPARISON OF SWING CURVES OF BASELINE MODEL WITH AND WITHOUT TOWER SHADOW AND WIND SHEAR.

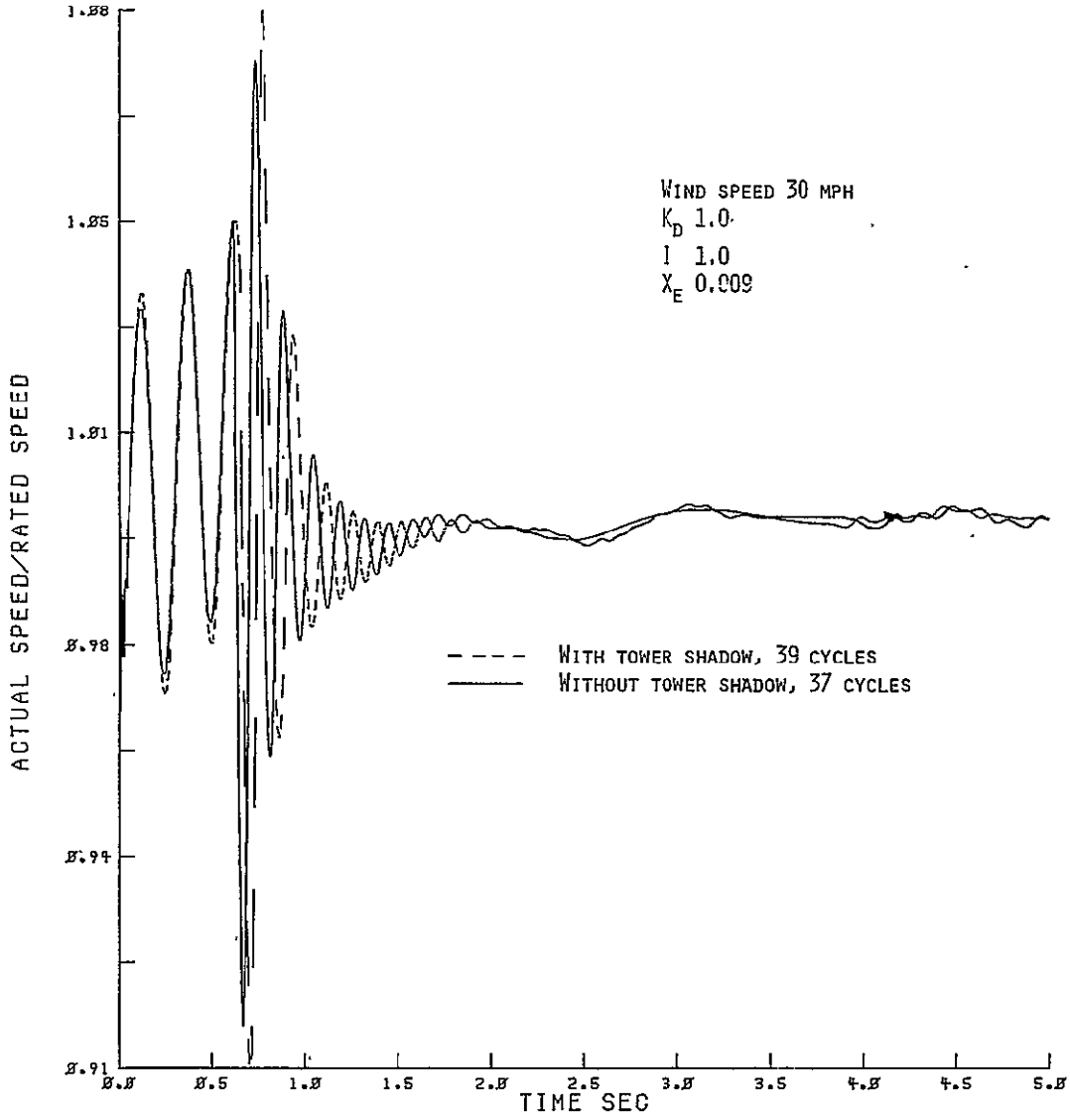

FIGURE 4.8. - COMPARISON OF ROTOR SPEED CURVES OF BASELINE MODEL WITH AND WITHOUT TOWER SHADOW AND WIND SHEAR.

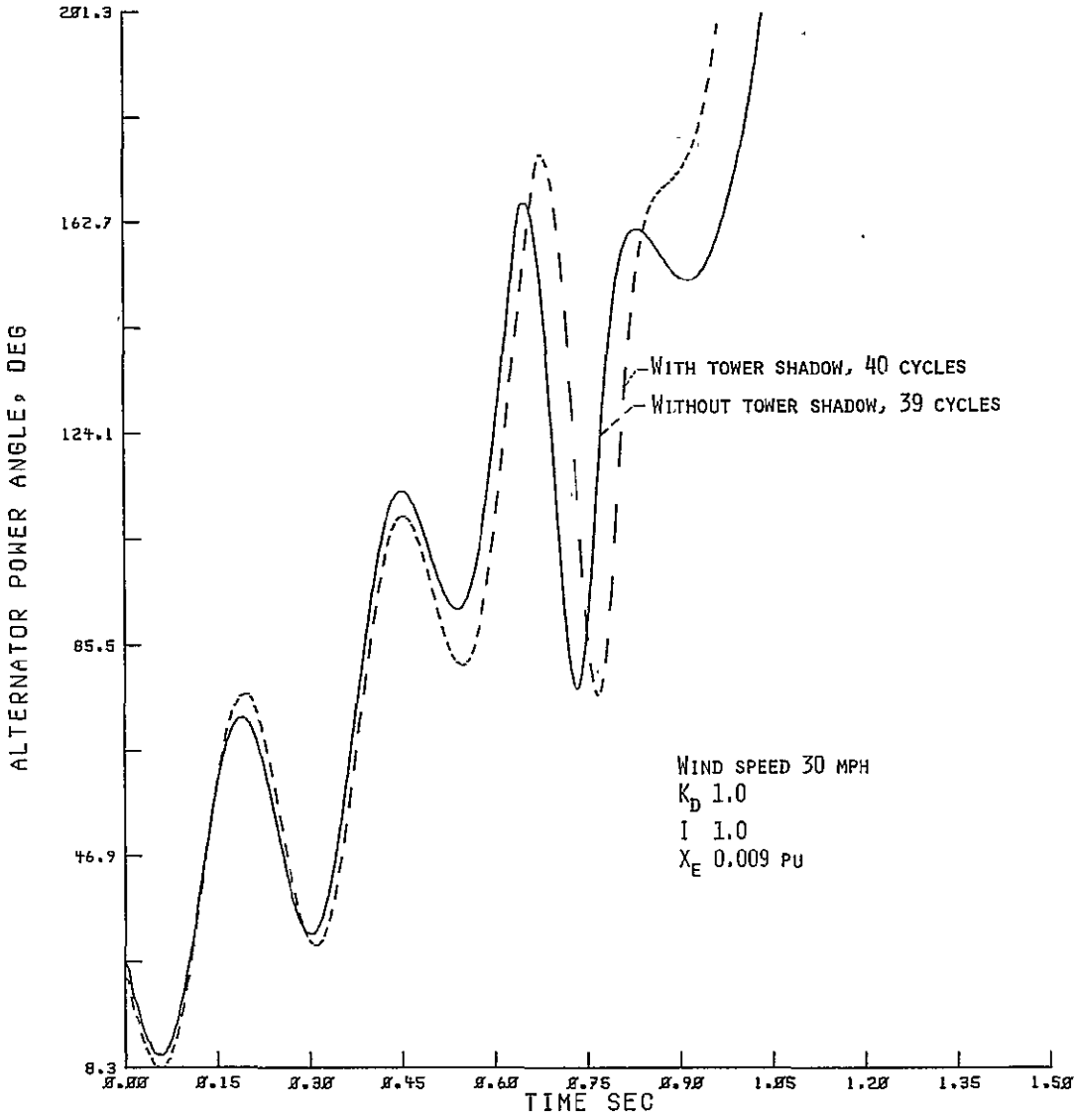

FIGURE 4.9. - COMPARISON OF SWING CURVES OF BASELINE MODEL WITH AND WITHOUT TOWER SHADOW AND WIND SHEAR SHOWING LOSS OF SYNCHRONISM.

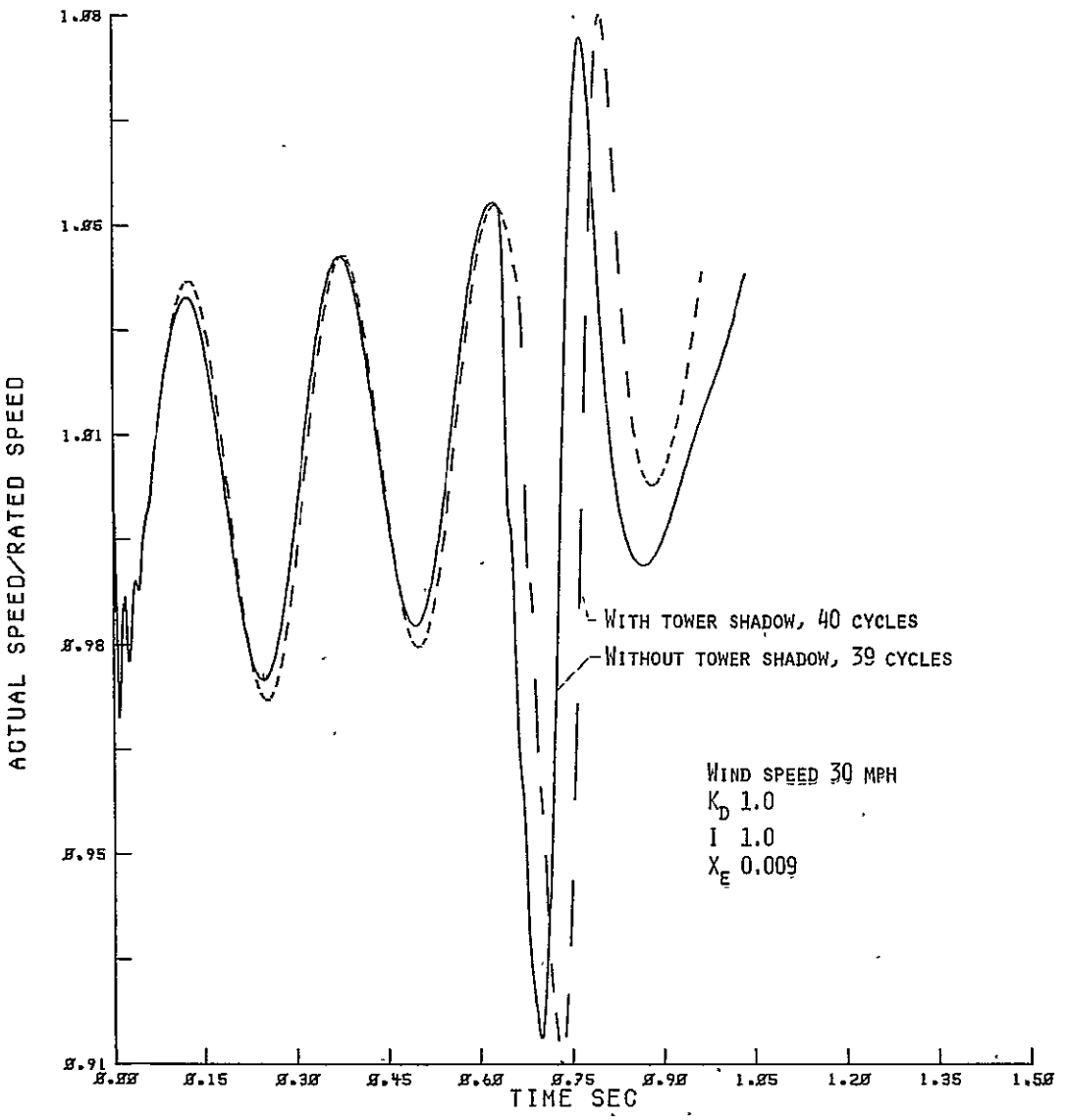

FIGURE 4.10. - COMPARISON OF ROTOR SPEED CURVES OF BASELINE MODEL WITH AND WITHOUT TOWER SHADOW AND WIND SHEAR SHOWING LOSS OF SYNCHRONISM.

it is in the direction to reduce the maximum clearing time; that is, the determination is conservative.

4.4 Typical Swing Curve

The typical result of the scheme of clearing time determination adopted for this study is illustrated in figure 4.5. In this example a 37 cycle duration short circuit produces one big swing that rapidly is damped so that the power angle returns to its steady state value. A short circuit one cycle longer produces sufficient acceleration to the rotor to cause loss of synchronism. The same alternator rotor behavior is illustrated in figure 4.6 which shows the relative speed of the rotor. Upon application of the fault at time = 0, the rotor accelerates. At time 0.617 second (37 cycles) the fault is removed and the frequency difference between the alternator voltage and the bus voltage produces the ensuing speed oscillation that rapidly is damped. Increasing the short circuit duration to time = 0.633 second (38 cycles) produces sufficient rotor acceleration to drive the alternator out of synchronism.

The configuration of the swing curve presented in figure 4.5 and the damped oscillation of the rotor speed curve of figure 4.6 are representative of the transient responses produced by the application of a three-phase short to the wind turbine generator system output for different system parameter values and/or operating conditions. In each case for which synchronism is not lost, application of the fault produces a large positive swing of the power angle curve that lasts for 1 to 3 seconds before the angle returns to a damped oscillation about the final value. The generalization is indicative of the

order of magnitude of the duration of the transient.

4.5 Oscillation Modes

Two frequencies are evident in the swing and the ensuing damped portion of the transient. The same oscillation frequencies are recognizable in the rotor speed curves. The higher frequency oscillation is rapidly damped; the lower frequency experiences less damping as the transient gradually subsides to the steady state value.

Changing system parameter values and/or operating conditions changes the frequency and amplitude of the oscillation, but does not alter the transient function radically.

The eigenvalue analysis of the simplified model depicted in figure 3.4 provides good predictions of these two modes of oscillation which occur in the more detailed, closed loop simulation output. The correspondence of the system simulation output frequencies determined from the digital computer printout and the eigenvalue analysis frequencies is shown in table 4.2.

The lower frequency mode is the effective natural frequency of the alternator. It is determined by the "spring" of the alternator synchronous torque and the rotary inertia of the rotating shaft. The higher frequency mode is produced by the spring-mass combination of the alternator rotor and the synchronous torque paralleled to the drive train spring.

4.6 Effect of Rotational Inertia

The influence of the rotary inertia on the maximum clearing time

is shown in Table 4.3. Tabulated are the ratios of maximum clearing times for system conditions matching in all respects except rotary inertia. The mean value for the 18 ratios examined is 1.3. The predicted ratio from the analysis (eq. (2.5)) is $2^{1/2}$. The result of the simulated effect of inertia on clearing times matches the expectations from earlier analysis.

4.7 Effect of Power Load

Clearing time is effectively inversely proportional to load. The dependence of the duration of maximum clearing time on alternator power level is illustrated by the ratios in Table 4.4. The ratio of clearing times for a 0.4 pu load and an 0.8 pu load for 12 otherwise matching systems is calculated. The mean value of the 12 ratios tabulated is 1.9, corresponding to the inverse of the load ratio. This result implies the generalization that, in spite of the nonlinearities present in the wind torque characteristics, in the alternator model, in the control modes, and in the parameter selections used, clearing time is effectively inversely proportional to load. The implication is further substantiated by the result that clearing times for an 0.8 pu load at 18 mph and at 30 mph wind speeds are substantially the same.

This close correspondence in clearing time ratios exists even though the values of the partial derivatives which describe the wind turbine torque characteristics differ considerably at the two wind speeds investigated. The differential torque developed by the wind turbine can be expressed by equation (4.1). (See also Appendix D.)

TABLE 4.3

EFFECT OF ROTARY INERTIA ON MAXIMUM CLEARING TIME

Tie-line reactance, pu	Drive train relative stiffness	Relative rotary inertia	Number of 60 Hz cycles in maximum short at given wind speeds			Clearing times ratio for 2:1 inertia ratio		
			14 mph	18 mph	30 mph	14 mph	18 mph	30 mph (wind speed*)
0.009	0.1	1.0	25	15	15	1.4	1.2	1.2
	.1	.5	18	12	12			
	1.0	1.0	67	37	37	1.2	1.3	1.3
	1.0	.5	56	28	29			
	10.0	1.0	67	38	38	1.3	1.3	1.3
	10.0	.5	53	29	30			
0.4	0.1	1.0	15	7	7	1.4	1.4	1.4
	.1	.5	11	5	5			
	1.0	1.0	45	21	21	1.4	1.4	1.3
	1.0	.5	33	15	16			
	10.0	1.0	44	23	24	1.4	1.4	1.3
	10.0	.5	32	17	18			

*Wind speed — Corresponding load — Mean ratio = 1.3

14 mph = 6.2 m/s — 0.4 pu, 0.8 PF
18 mph = 8.0 m/s — 0.8 pu, 0.8 PF
30 mph = 13.4 m/s — 0.8 pu, 0.8 PF

TABLE 4.4

EFFECT OF POWER LOAD ON MAXIMUM CLEARING TIME

x_e	Drive train relative stiffness	Relative rotary inertia	Number of 60 Hz cycles in maximum short at given wind speed*		Clearing times ratio for 0.4/0.8 load ratio
			14 mph	18 mph	
0.009	0.1	1.0	25	15	1.7
	1.0	1.0	67	37	1.8
	10.0	1.0	67	38	1.8
	.1	.5	18	12	1.5
	1.0	.5	56	28	2.0
	10.0	.5	53	29	1.8
0.4	0.1	1.0	15	7	2.1
	1.0	1.0	45	21	2.1
	10.0	1.0	44	23	1.9
	.1	.5	11	5	2.2
	1.0	.5	33	15	2.2
	10.1	.5	32	17	1.9
					Mean ratio = 1.9

*Wind speed — Corresponding load

14 mph = 6.2 m/s — 0.4 pu, 0.8 PF
18 mph = 8.0 m/s — 0.8 pu, 0.8 PF

$$\Delta T_{in} = \frac{\partial T_{in}}{\partial V_w} \Delta V_w + \frac{\partial T_{in}}{\partial \dot{\theta}_1} \Delta \dot{\theta}_1 + \frac{\partial T_{in}}{\partial \beta} \Delta \beta_1$$

$$= K_v \Delta V_w + K_\Omega \Delta \dot{\theta}_1 + K_\beta \Delta \beta_1 \qquad (4.1)$$

The variation of the values of the gain factors (partial derivatives) for the wind speeds 14, 18, and 30 mph are shown in Table 4.5. A plot of the wind turbine torque characteristics are shown in figure 4.11.

The relationship between alternator load and clearing time is seen in the similarity of the transient swing curves and speed curves

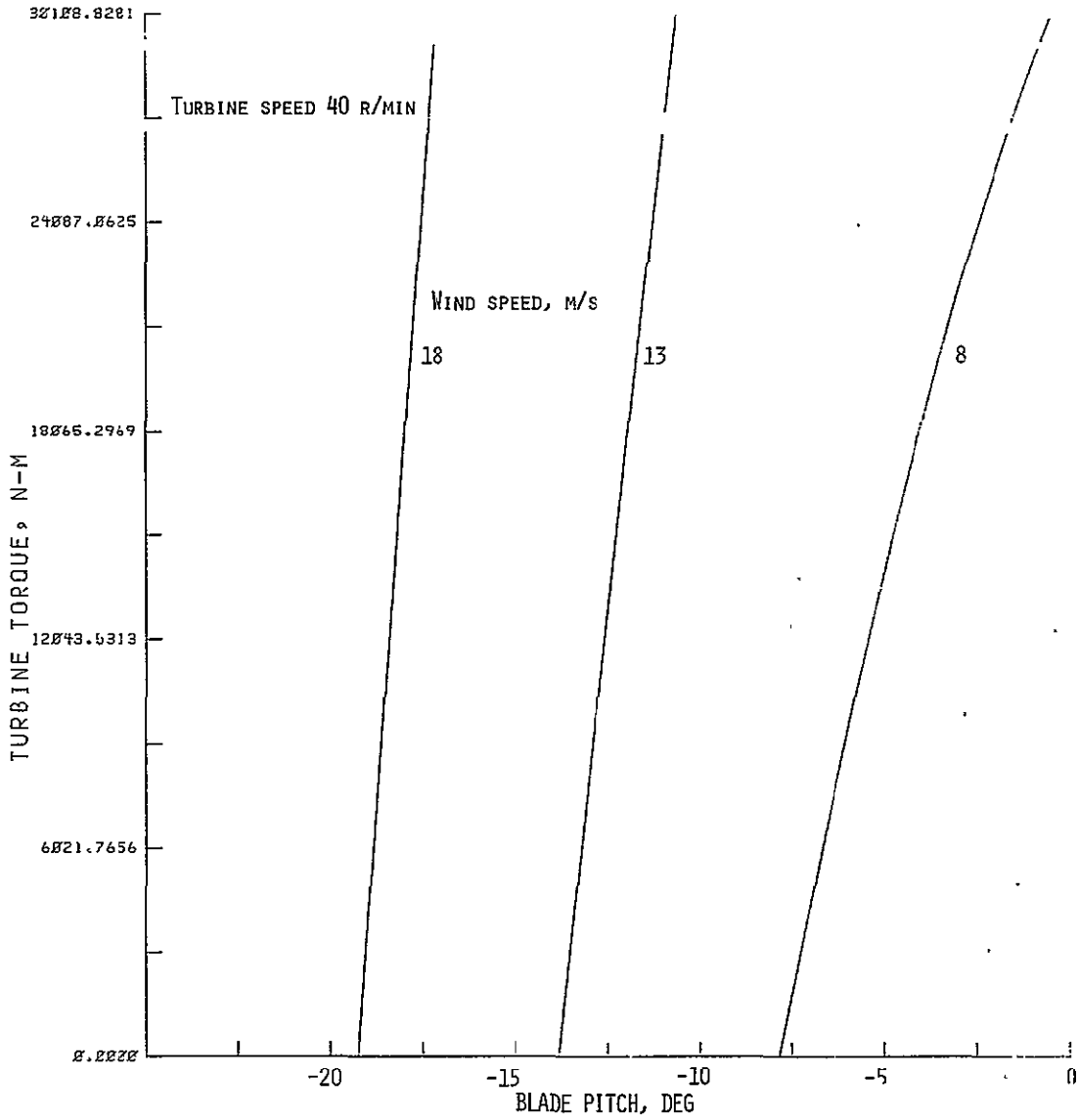

FIGURE 4.11. - MOD-0 WIND TURBINE GENERATOR TORQUE-PITCH CHARACTERISTICS FOR HIGH WIND SPEEDS.

TABLE 4.5

GAIN VALUES OF DIFFERENTIAL INPUT TORQUE
AT MODELED WIND SPEEDS

Wind speed, mph	K_V, (ft-lb/ft/sec)	K_Ω, (ft-lb/rad/sec)	K_β, (ft-lb/rad)
14	1771	-4 152	71 418
18	2441	-4 834	121 127
30	2946	-20 382	393 707

for the three sample wind speeds applied to the same system illustrated in figures 4.12 and 4.13. The clearing time for the 14 mph, 0.4 pu load is almost twice as long as the 0.8 pu loads. The same comparison is made for the three sample loading conditions in figures 4.14 and 4.15 for a tie-line reactance of 0.4 pu. For each value of x_e the reduced damping associated with the lower frequency for the 0.4 pu power trace is evident. The lower frequency is associated with the alternator. The more lightly loaded alternator is more lightly damped. This result is consistent with the theory expressed by equation (2.10).

4.8 Effect of Drive Train Stiffness

Reduced drive train stiffness has a "decoupling" effect. The effect of different drive train stiffness is illustrated in figures 4.16 and 4.17, one set of curves for x_e = 0.009 pu, and the other set for x_e = 0.4 pu. In each set of curves the transient swings for the system with the baseline value of the drive train stiffness and the system with the increased value of ten times the baseline stiffness are not very different. However, the systems with the reduced drive train stiffness show the "decoupling" effect of the softer transmission line. In the case of each external reactance

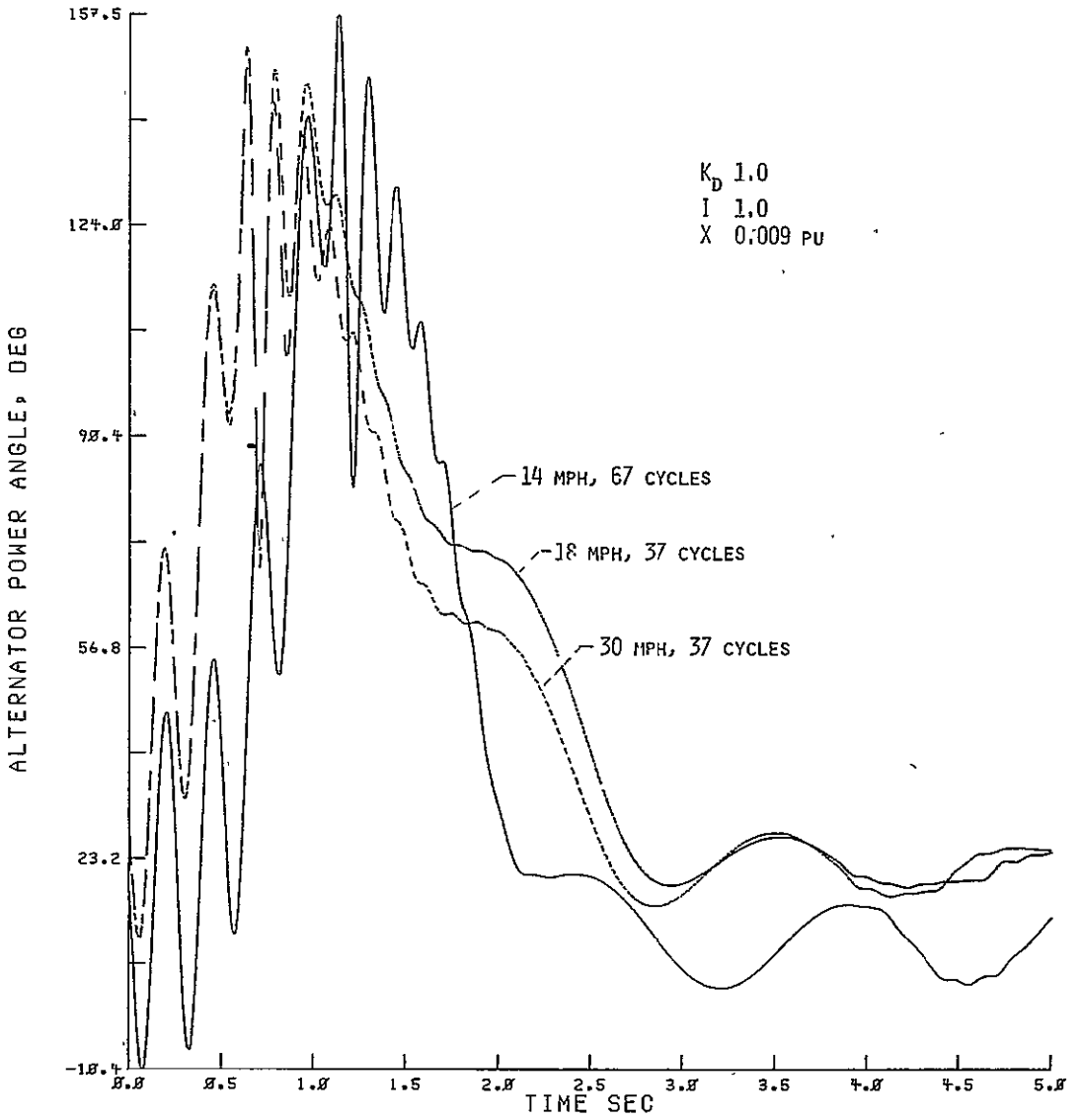

FIGURE 4.12. - SWING CURVES FOR BASELINE MODEL AT SELECTED WIND SPEEDS.

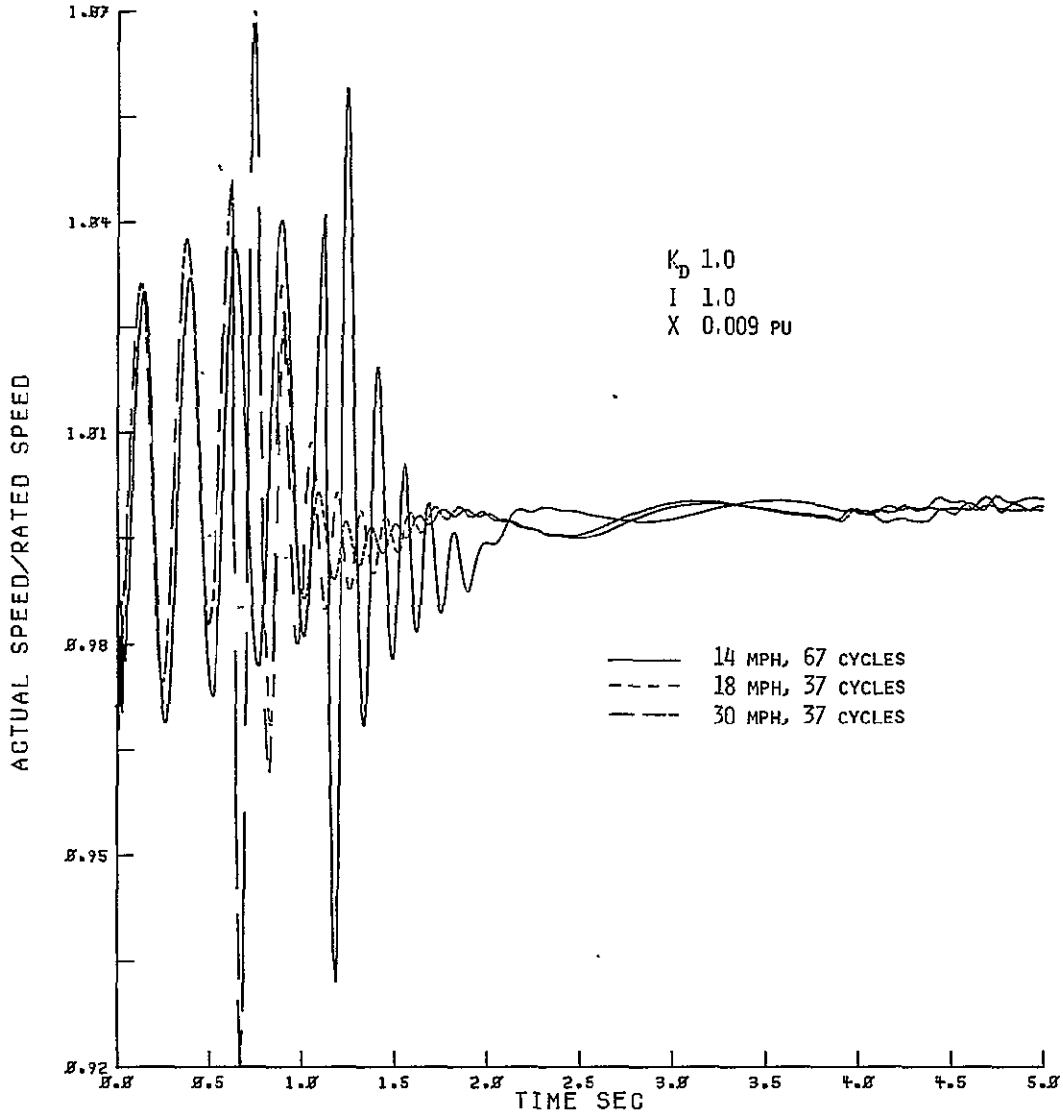

FIGURE 4.13. - ROTOR SPEED CURVES FOR BASELINE MODEL AT SELECTED WIND SPEEDS.

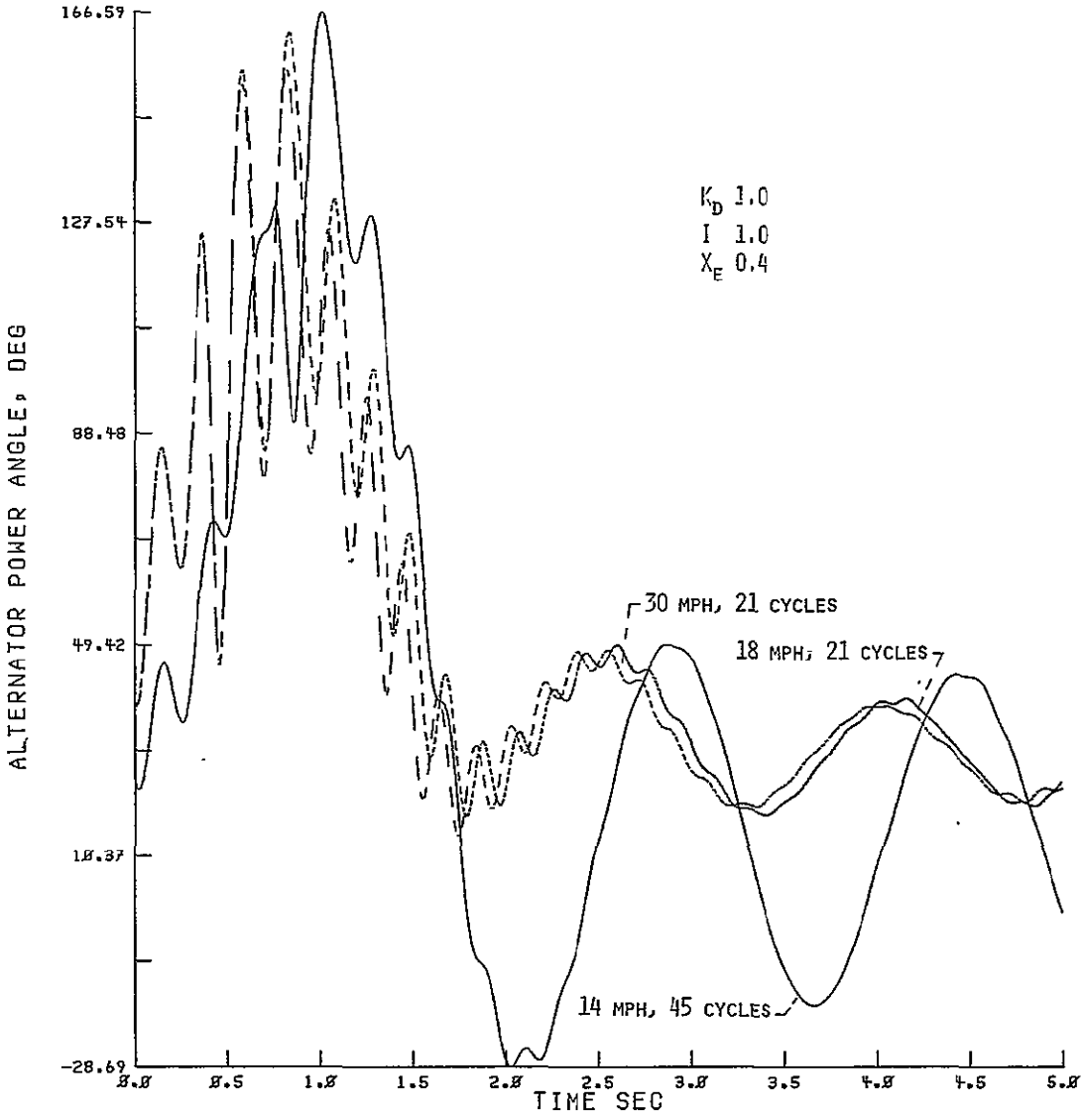

FIGURE 4.14. - SWING CURVES FOR "SOFT" TIE-LINE AT SELECTED WIND SPEEDS.

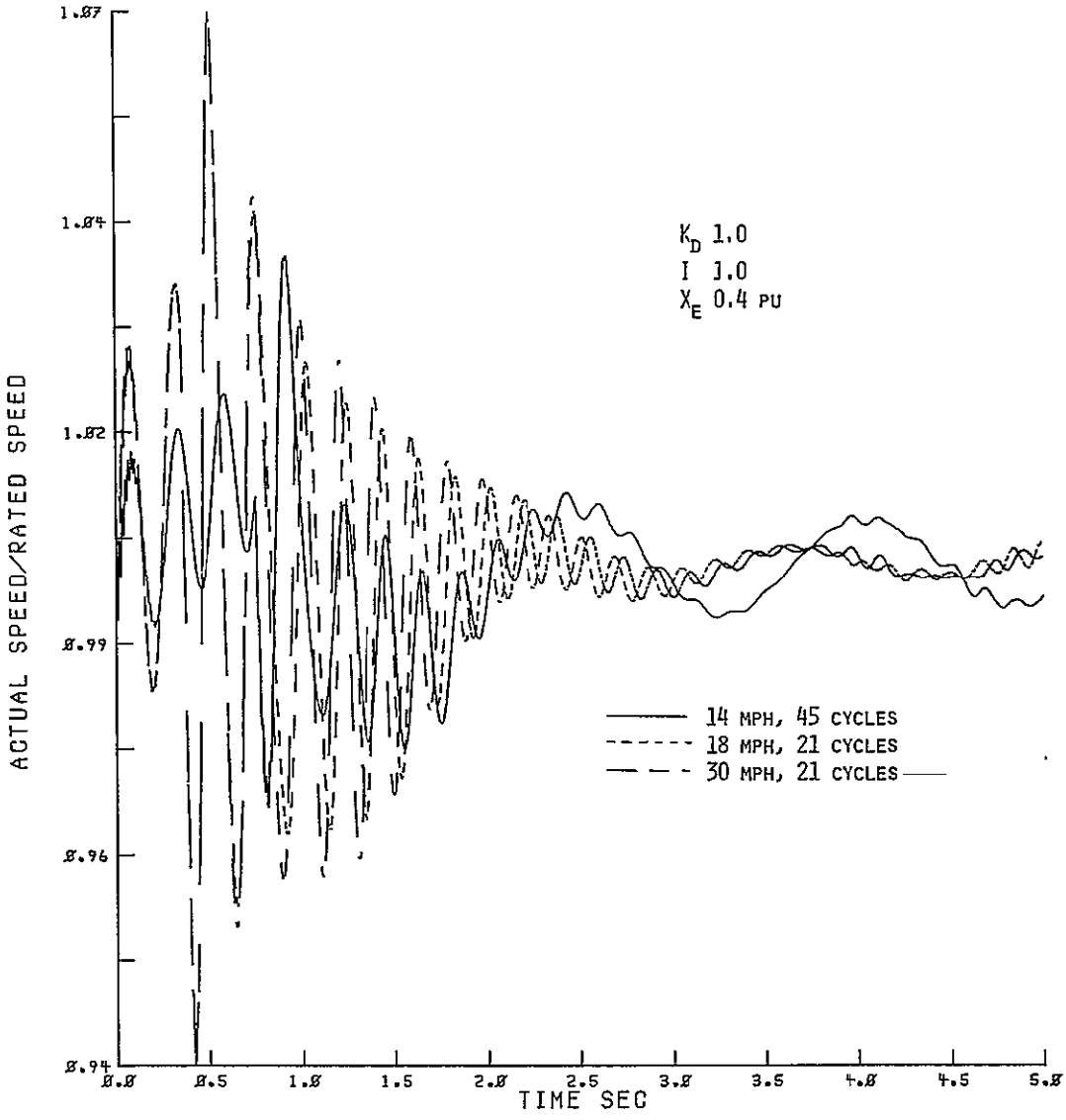

FIGURE 4.15. - ROTOR SPEED CURVES FOR "SOFT" TIE-LINE AT SELECTED WIND SPEEDS.

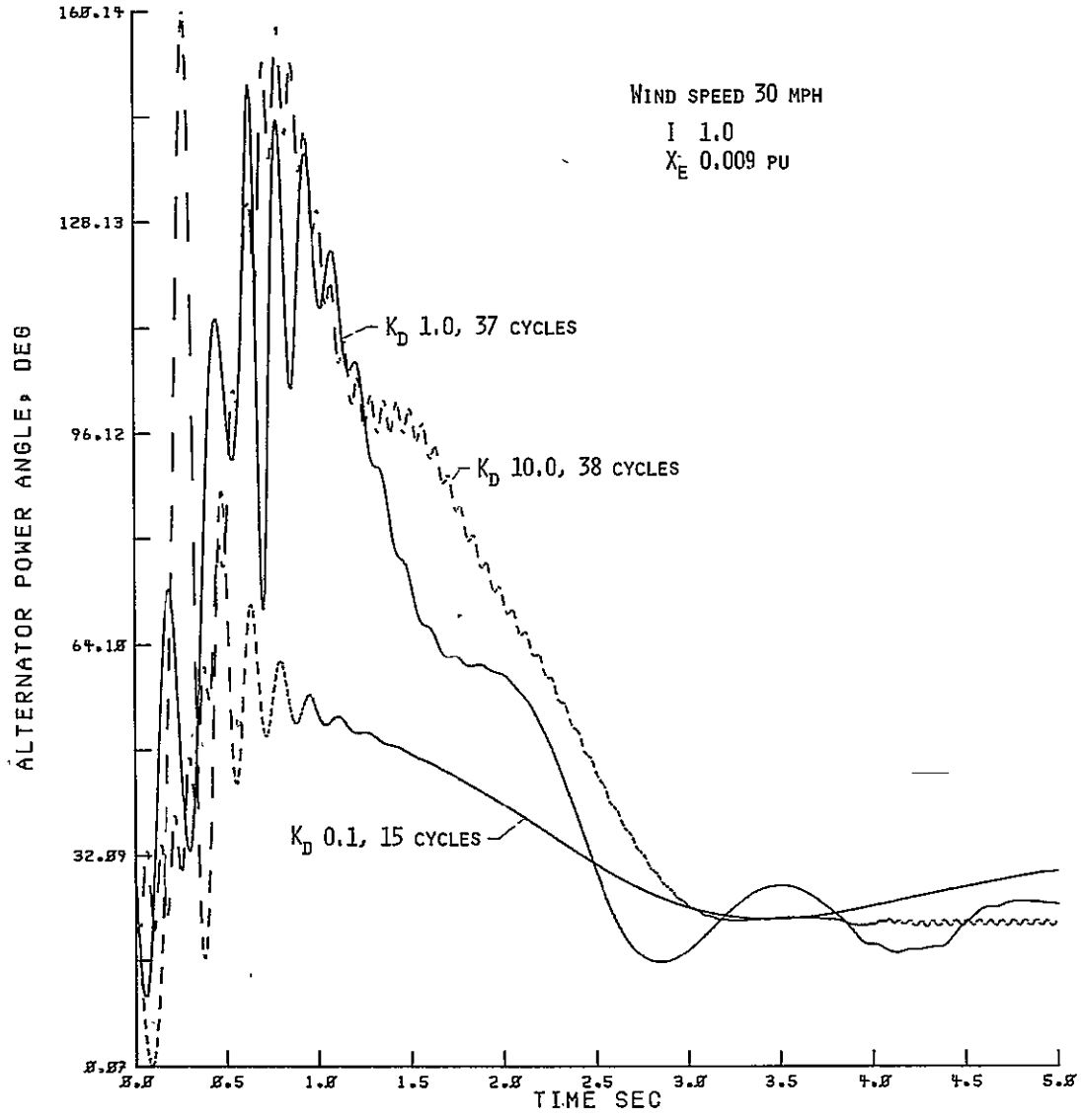

FIGURE 4.16. - SWING CURVES FOR "STIFF" TIE-LINE WITH SELECTED DRIVE TRAIN STIFFNESSES.

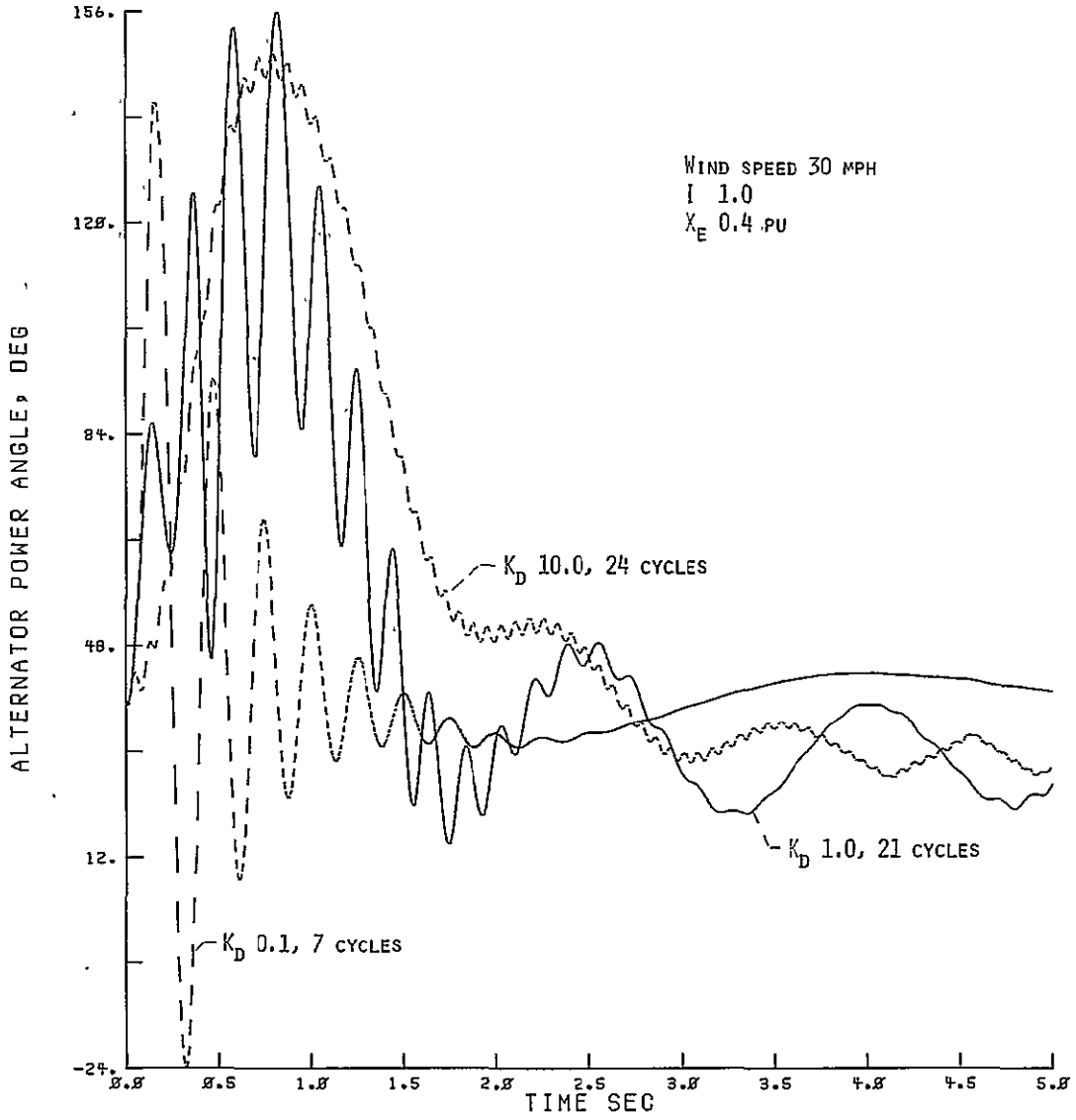

FIGURE 4.17. - SWING CURVES FOR "SOFT" TIE-LINE WITH SELECTED DRIVE TRAIN STIFFNESSES.

the same severe three phase, zero impedance, short circuit that causes the large swings for the stiffer systems, produces in the soft systems a transient whose frequency components are damped in one-third the time as the frequency components of the stiffer systems.

The "decoupling" that results from the soft transmission also has the effect of reducing the maximum clearing time over 60 percent. The large turbine rotary inertia is not as closely coupled as in the stiffer systems, and as a consequence of the reduced inertia the rotor accelerates faster. Synchronism is lost more quickly. This effect can be noted from a comparison of figures 4.18 and 4.19.

4.9 Effect of Tie-Line Reactance

The appreciable increase of the reactance between the fault and the alternator terminals from $x_e = 0.009$ pu to $x_e = 0.4$ pu reduces the maximum clearing time by almost 50 percent for otherwise corresponding circuit conditions. For the 18 pairs of corresponding conditions tabulated in Table 4.6 the average of the ratios of clearing time for $x_e = 0.4$ to clearing time for $x_e = 0.009$ is 0.56. This reduction is in accord with the reduced synchronous torque of the alternator. The equation for the synchronous torque is given by

$$T_{sync} = \frac{e'_q e_2}{x'_d + x_e} \cos \delta + \frac{e_2^2 (x'_d - x_q)}{(x'_d + x_e)(x_q + x_e)} \cos 2\delta \qquad (4.2)$$

The effect of increasing the reactance x_e is to reduce the torque coefficient T_{sync}. The torque coefficient is effectively the stiffness K_A of the spring indicated in figure 2.2. Reducing the stiffness of the system enables the rotor to accelerate more rapidly, and

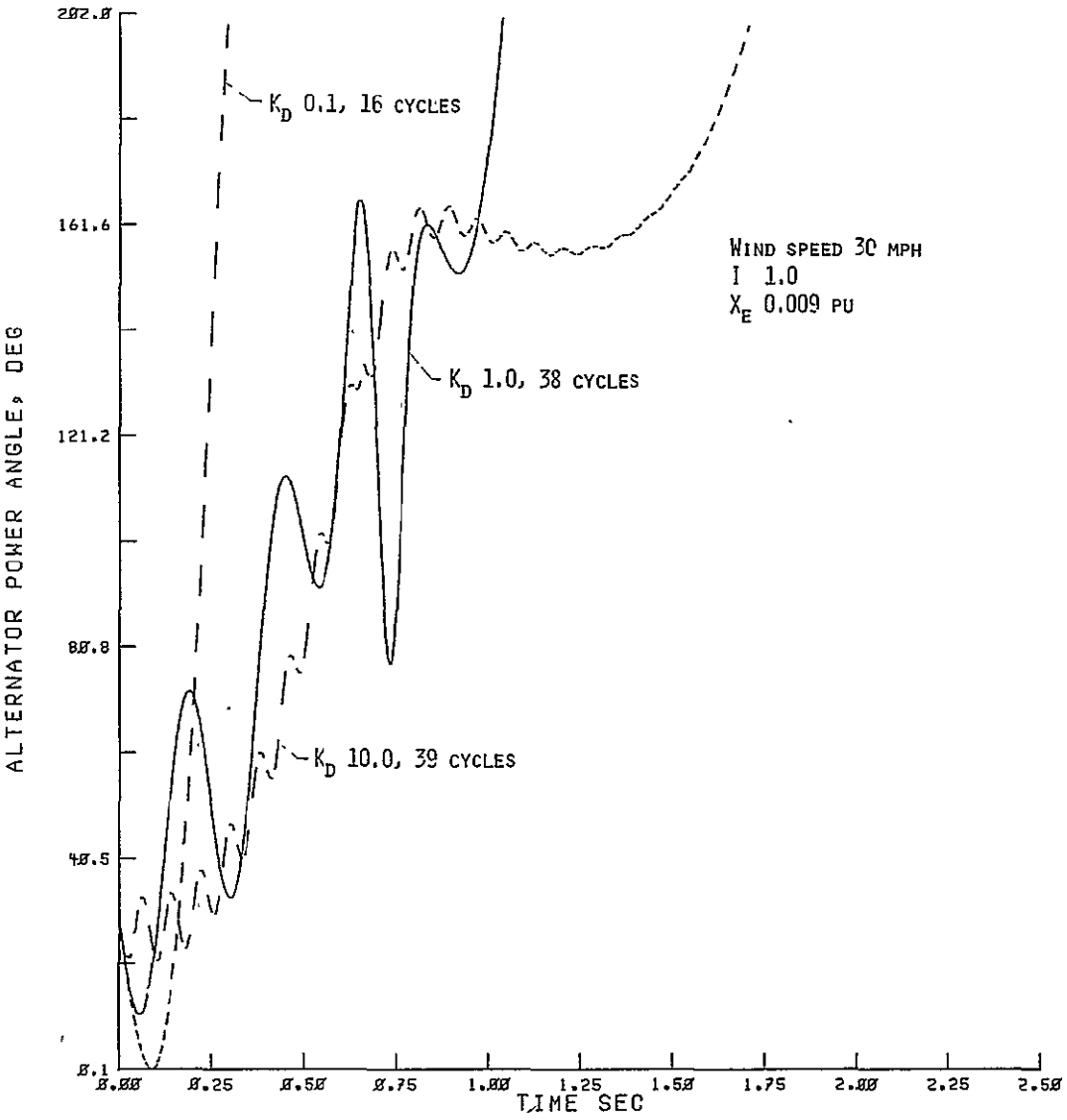

FIGURE 4.18. - SWING CURVES FOR "STIFF" TIE-LINE WITH SELECTED DRIVE TRAIN STIFFNESSES SHOWING LOSS OF SYNCHRONISM.

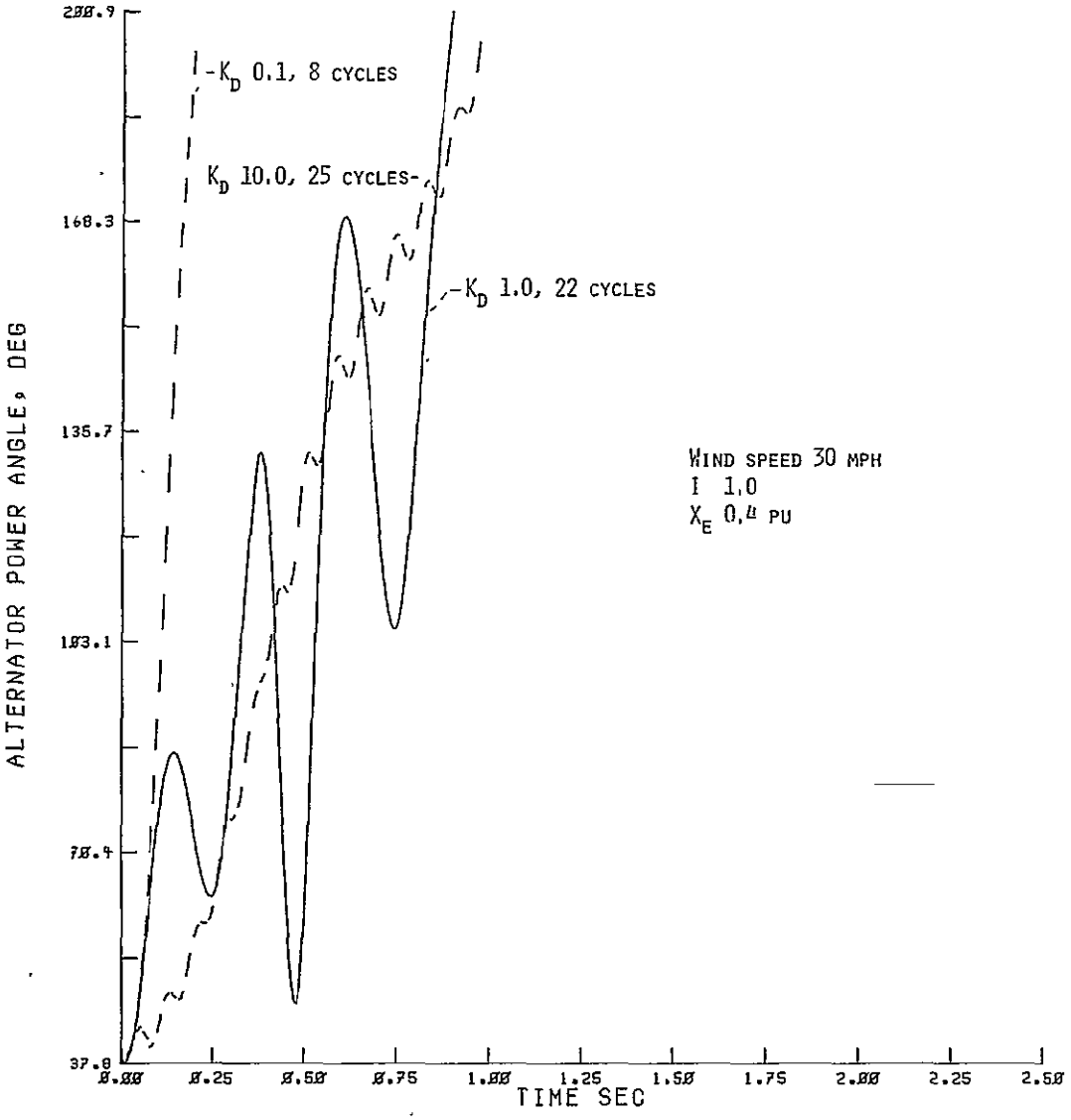

FIGURE 4.19. - SWING CURVES FOR "SOFT" TIE-LINE WITH SELECTED DRIVE TRAIN STIFFNESSES SHOWING LOSS OF SYNCHRONISM.

TABLE 4.6

EFFECT OF TIE-LINE REACTANCE ON MAXIMUM CLEARING TIME

x_e	Drive train relative stiffness	Relative rotary inertia	Number of 60 Hz cycles in maximum short at given wind speeds			Clearing time ratio for x_e increase		
			14 mph	18 mph	30 mph	14 mph	18 mph	30 mph (wind speed*)
0.4	0.1	1.0	15	7	7	0.60	0.47	0.47
.009	.1	1.0	25	15	15			
0.4	1.0	1.0	45	21	21	0.67	0.57	0.57
.009	1.0	1.0	67	37	37			
0.4	10.0	1.0	44	23	24	0.66	0.60	0.63
.009	10.0	1.0	67	38	38			
0.4	0.1	0.5	11	5	5	0.61	0.42	0.42
.009	.1	.5	18	12	12			
0.4	1.0	0.5	33	15	16	0.59	0.54	0.55
.009	1.0	.5	56	28	29			
0.4	10.0	0.5	32	17	18	0.60	0.59	0.60
.009	10.0	.5	53	29	30			
						Mean ratio = 0.56		

*Wind speed	Corresponding load
14 mph = 6.2 m/s	0.4 pu, 0.8 PF
18 mph = 8.0 m/s	0.8 pu, 0.8 PF
30 mph = 13.4 m/s	0.8 pu, 0.8 PF

consequently the maximum clearing time for the fault is reduced.

The reduction of the alternator "stiffness" is indicated also in Table 4.2 by the reduced frequencies for the $x_e = 0.4$ cases. This reduction is in accordance with equation (2.12) which relates the mode frequencies to the drive train and alternator stiffness factors.

The additional line reactance has reduced the transient stability of the power system so that for a given steady state load the system becomes unstable for a shorter fault duration. This behavior of the system is displayed in figures 4.20 and 4.21.

Increasing the tie-line reactance x_e also reduces the damping power that is produced by the fault excitation. This reduction is consistent with the analytical expression for damping power (eq. (2.9)).

The changes in maximum clearing time and in the damping of the transient following a short circuit to two systems with different external reactances are depicted in figures 4.22 to 4.27. For a given steady state load the system becomes unstable for a shorter fault duration as figures 4.20 and 4.21 show.

4.10 Effect of Neglecting "Transformer Voltages"

As implied in Section 2.2.2 the classical assumptions for calculating the transient response of one synchronous alternator when faulted with a three-phase short neglect the so-called transformer voltages ($d\lambda_d/dt$, $d\lambda_q/dt$) on the basis of the assumption that they are small in comparison to the so-called speed voltages ($\omega\lambda_d$, $\omega\lambda_q$). This assumption was not made during the previous simulations.

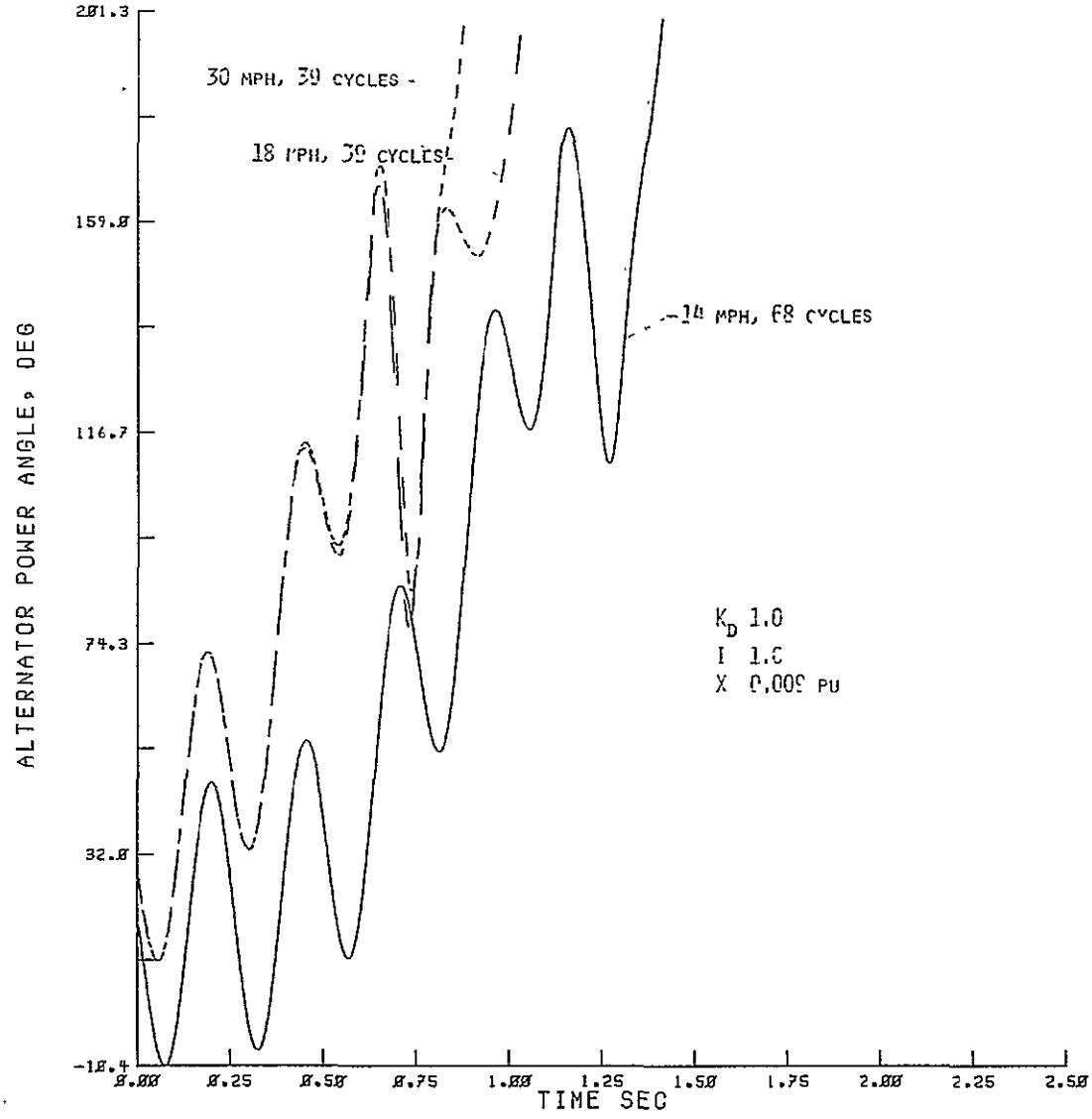

FIGURE 4.20. - SWING CURVES FOR "STIFF" TIE-LINE AT SELECTED WIND SPEEDS SHOWING LOSS OF SYNCHRONISM.

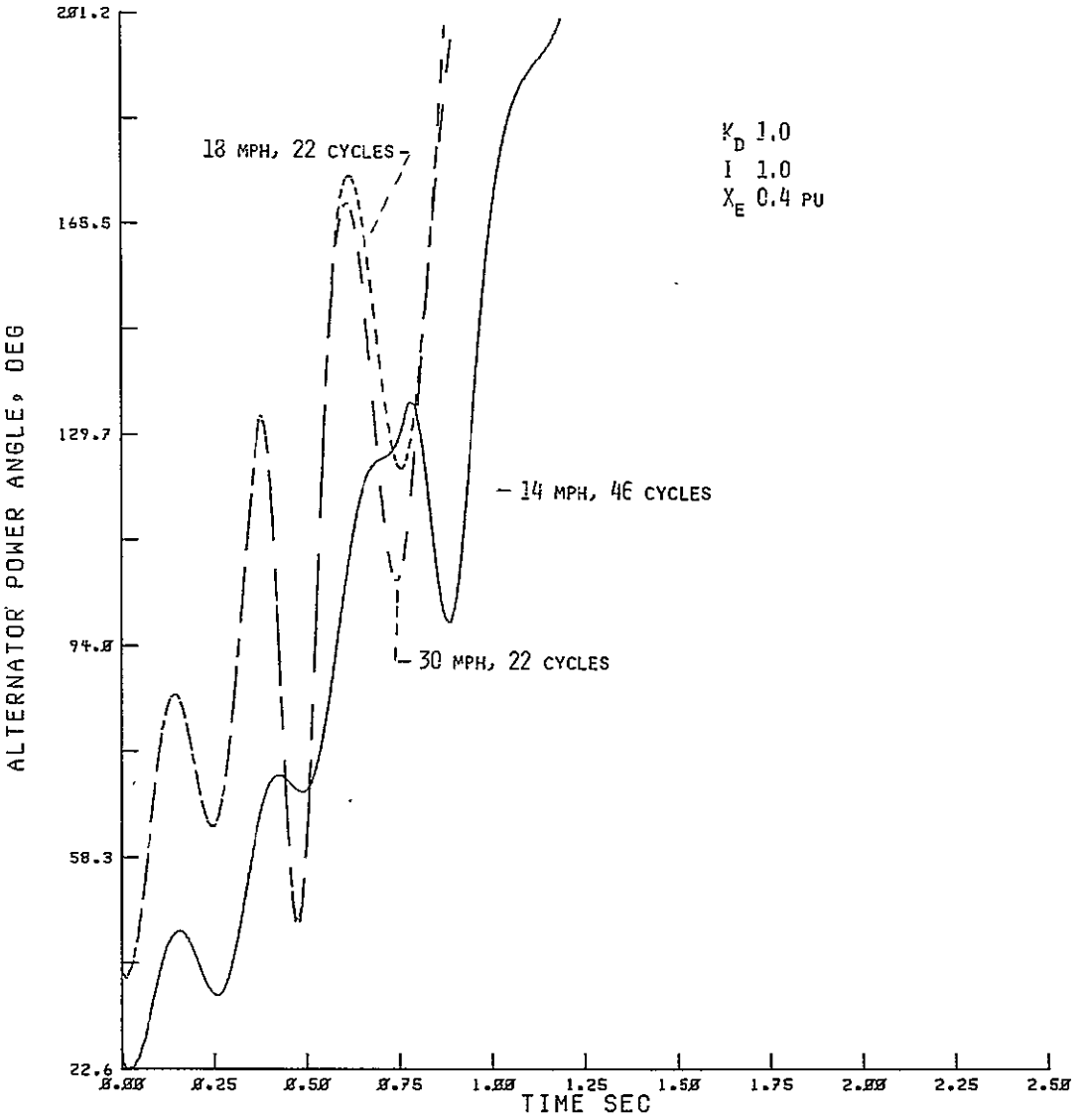

FIGURE 4.21. - SWING CURVES FOR "SOFT" TIE-LINE AT SELECTED WIND SPEEDS SHOWING LOSS OF SYNCHRONISM.

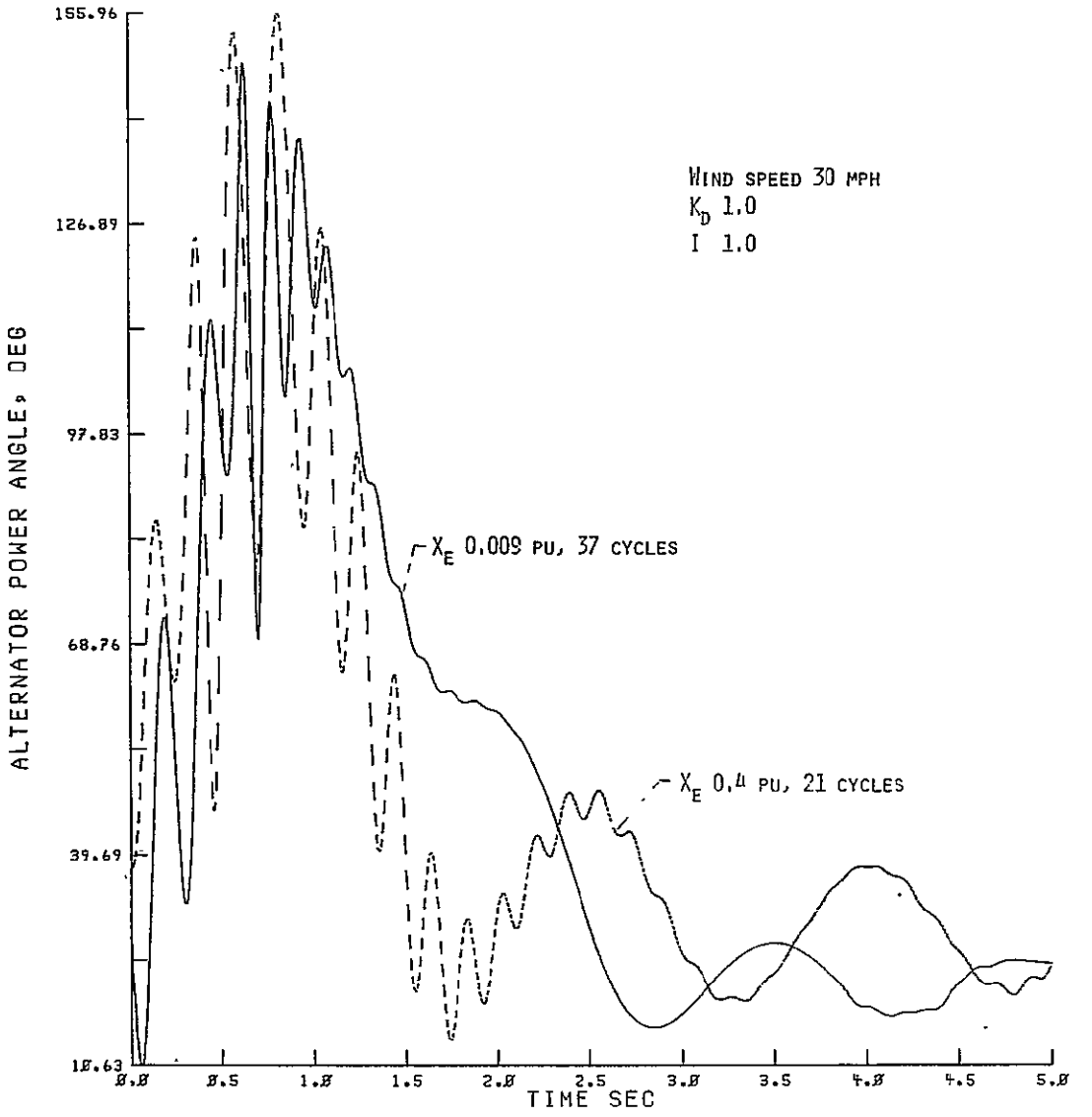

FIGURE 4.22. - COMPARISON OF SWING CURVES OF BASELINE MODEL WITH SELECTED TIE-LINE REACTANCES.

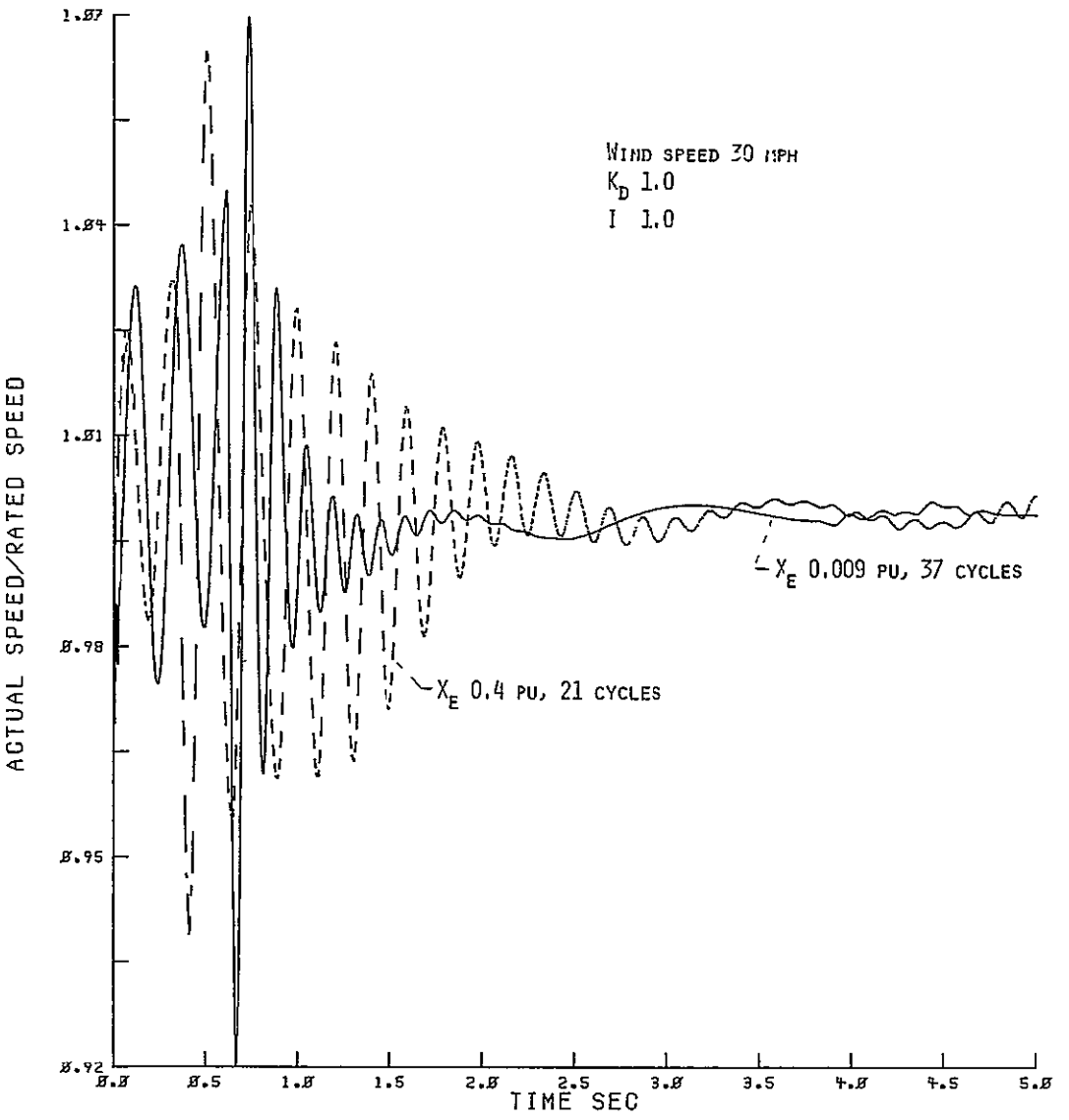

FIGURE 4.23. - COMPARISON OF ROTOR SPEED CURVES OF BASELINE MODEL WITH SELECTED TIE-LINE REACTANCES.

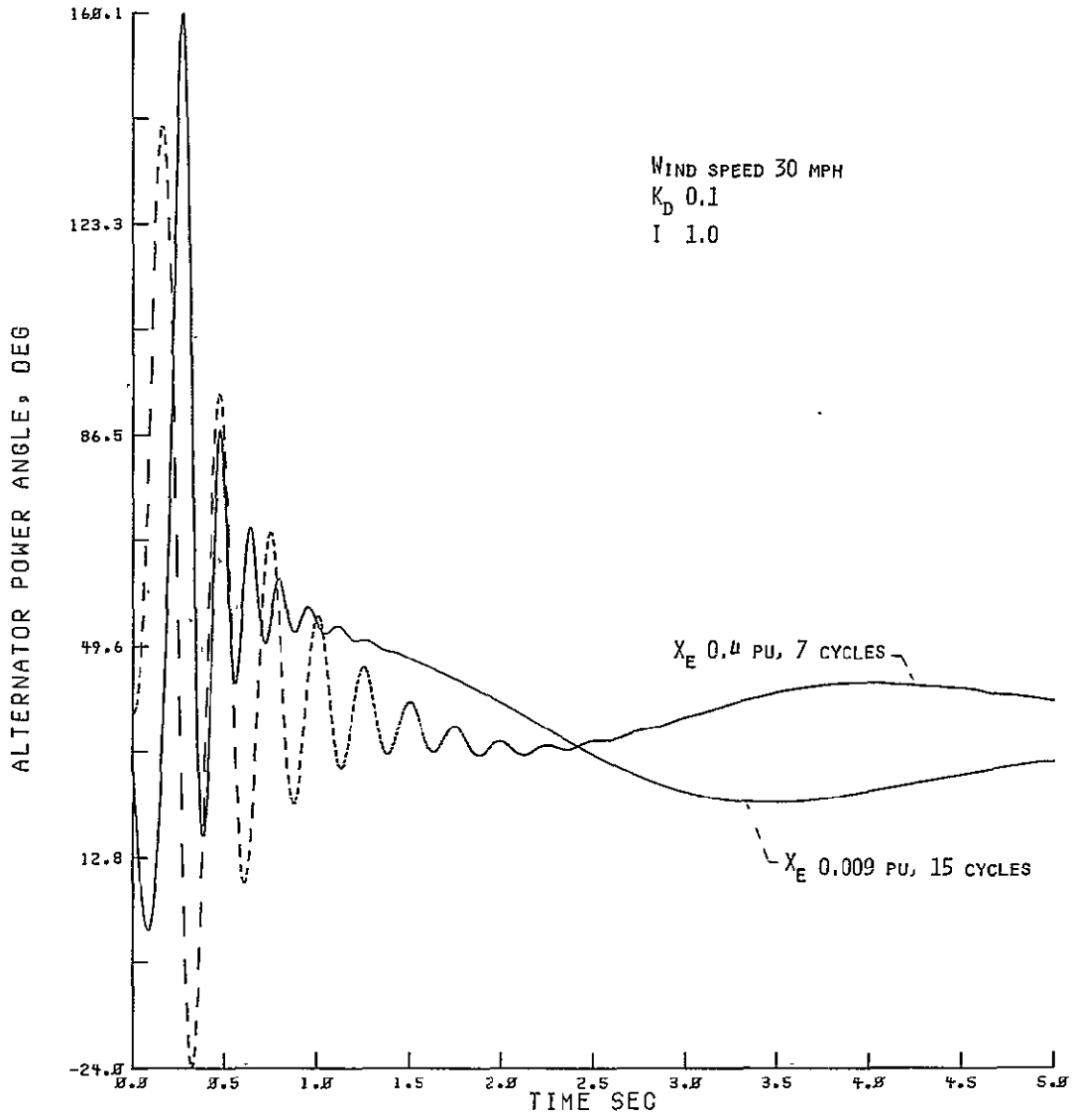

FIGURE 4.24. - COMPARISON OF SWING CURVES OF "SOFT" DRIVE TRAIN MODEL WITH SELECTED TIE-LINE REACTANCES.

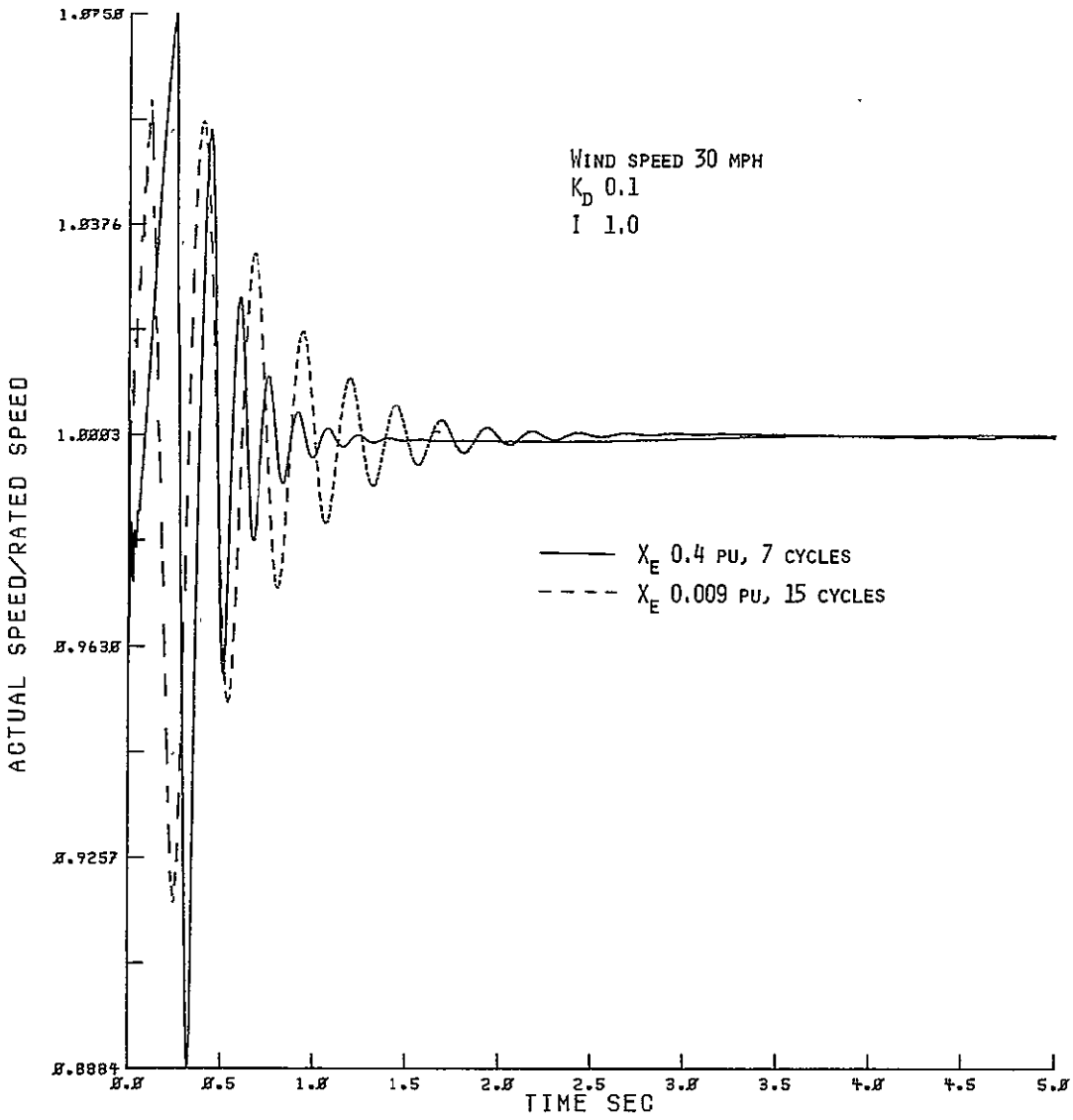

FIGURE 4.25. - COMPARISON OF ROTOR SPEED CURVES OF "SOFT" DRIVE TRAIN MODEL WITH SELECTED TIE-LINE REACTANCES.

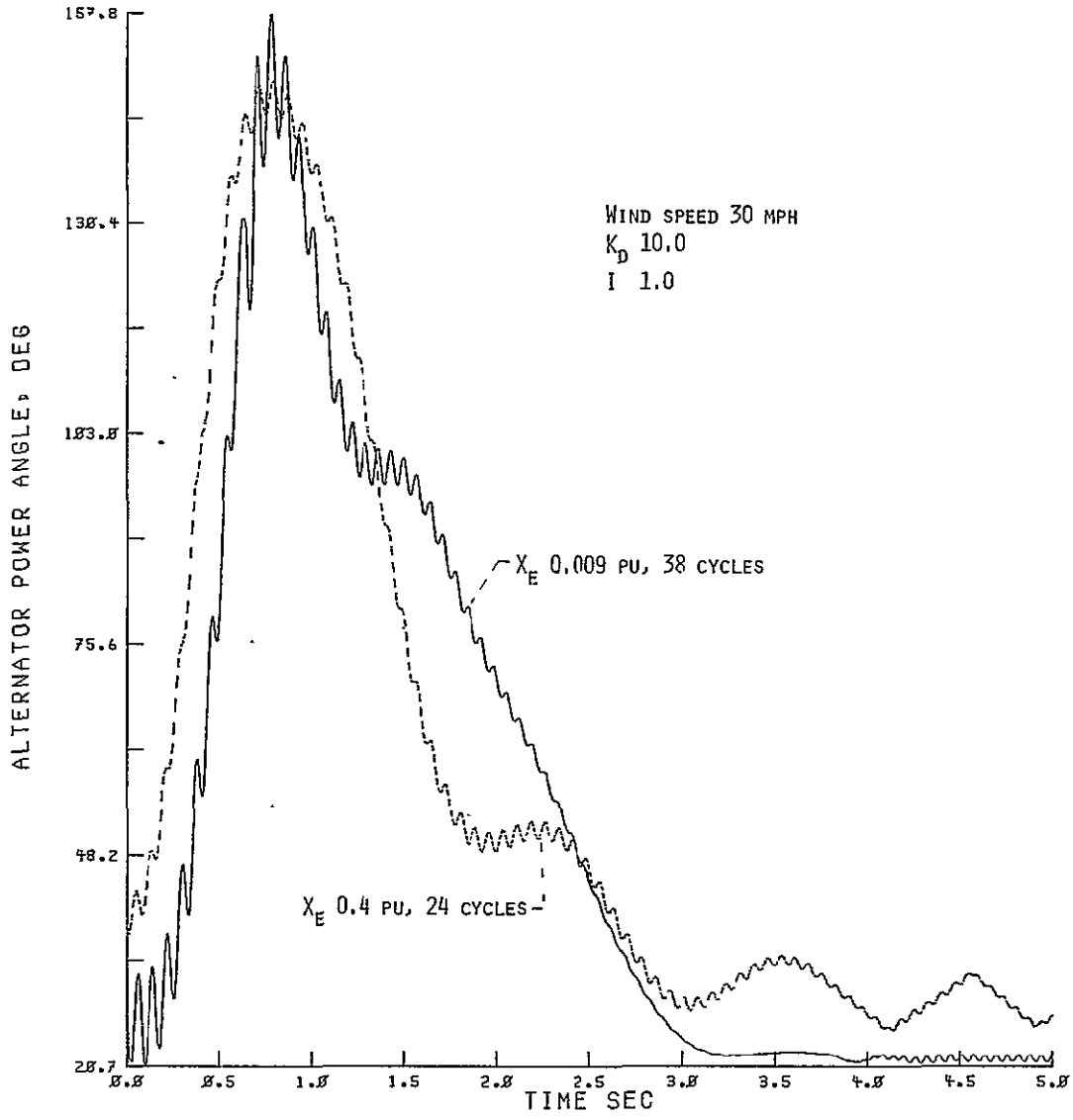

FIGURE 4.26. - COMPARISON OF SWING CURVES OF "SOFT" DRIVE TRAIN MODEL WITH SELECTED TIE-LINE REACTANCES.

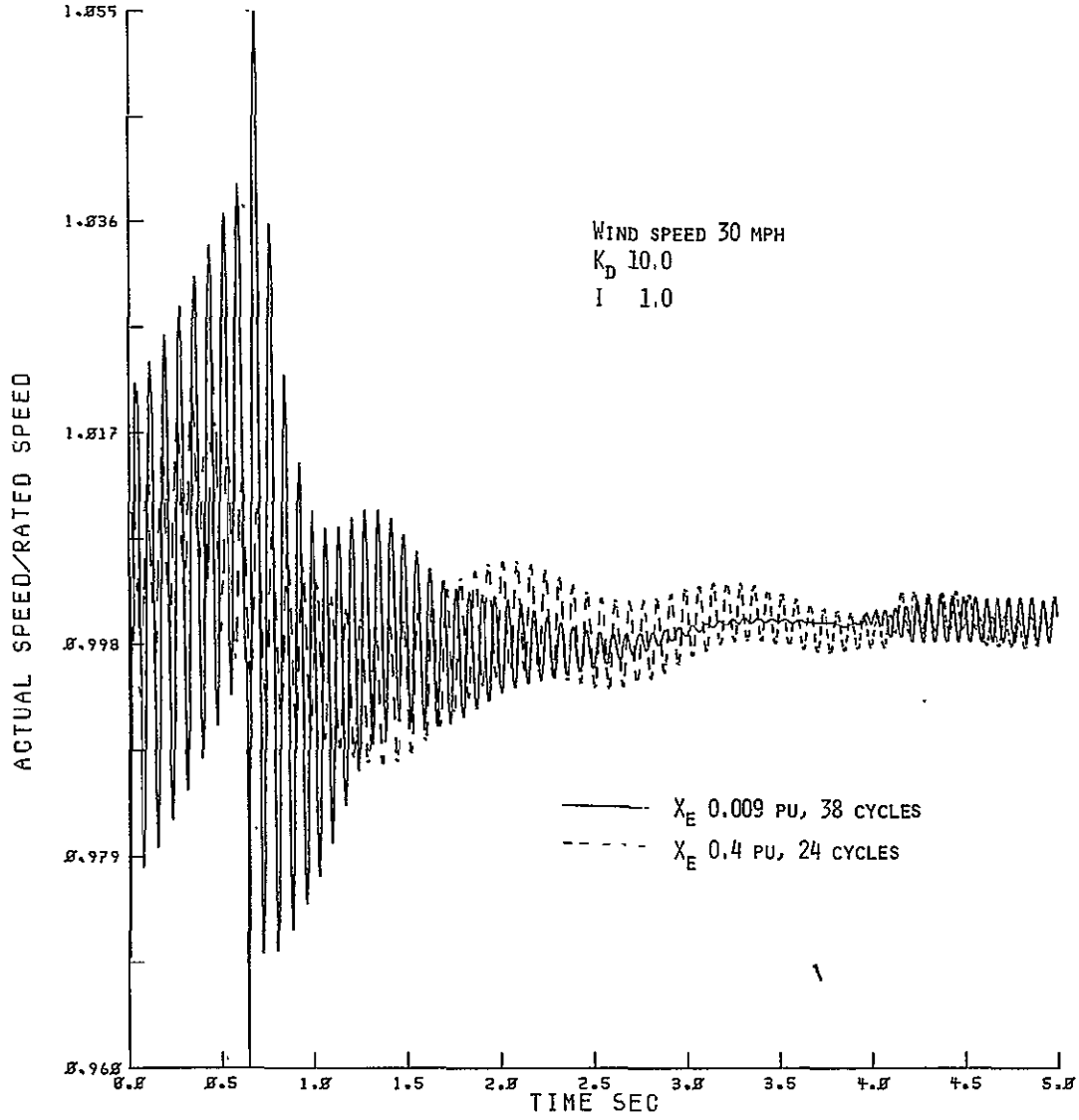

FIGURE 4.27. - COMPARISON OF ROTOR SPEED CURVES OF "STIFF" DRIVE TRAIN MODEL WITH SELECTED TIE-LINE REACTANCES.

In order to compare the transient response with and without the simplifying assumption, the research computer program was modified to assume the transformer voltages are negligible. When this assumption is made, the alternator equations (3.7) and (3.8) are modified to equation (4.3) and (4.4).

$$i_d = - \frac{r_a(v_d - e''_d) + x''_q(v_q - e''_q)}{x''_d x''_q + r_a^2} \tag{4.3}$$

$$i_q = \frac{x''_d(v_d - e''_d) - r_a(v_q - e''_q)}{x''_d x''_q + r_a^2} \tag{4.4}$$

The results of including this simplifying assumption are illustrated in figures 4.28 to 4.34.

Neglect of the transformer voltages produces a transient response very similar to the original response produced with the complete alternator model. The frequency content appears to be the same. The maximum amplitude is increased slightly, and the maximum clearing time is reduced slightly. Figures 4.28 to 4.31 show the transient traces of the power angle for the application of a 34 cycle three-phase short circuit fault in each model. The 34 cycle fault is the maximum clearing time for the model neglecting transformer voltages.

As a consequence of including the transformer voltages in the model the simulation does not indicate loss of synchronism for faults that cause loss of synchronism in the simpler model. The simplified model provides more conservative results.

The relative values of transformer and speed voltages for the example studied are shown in figures 4.30 and 4.31.

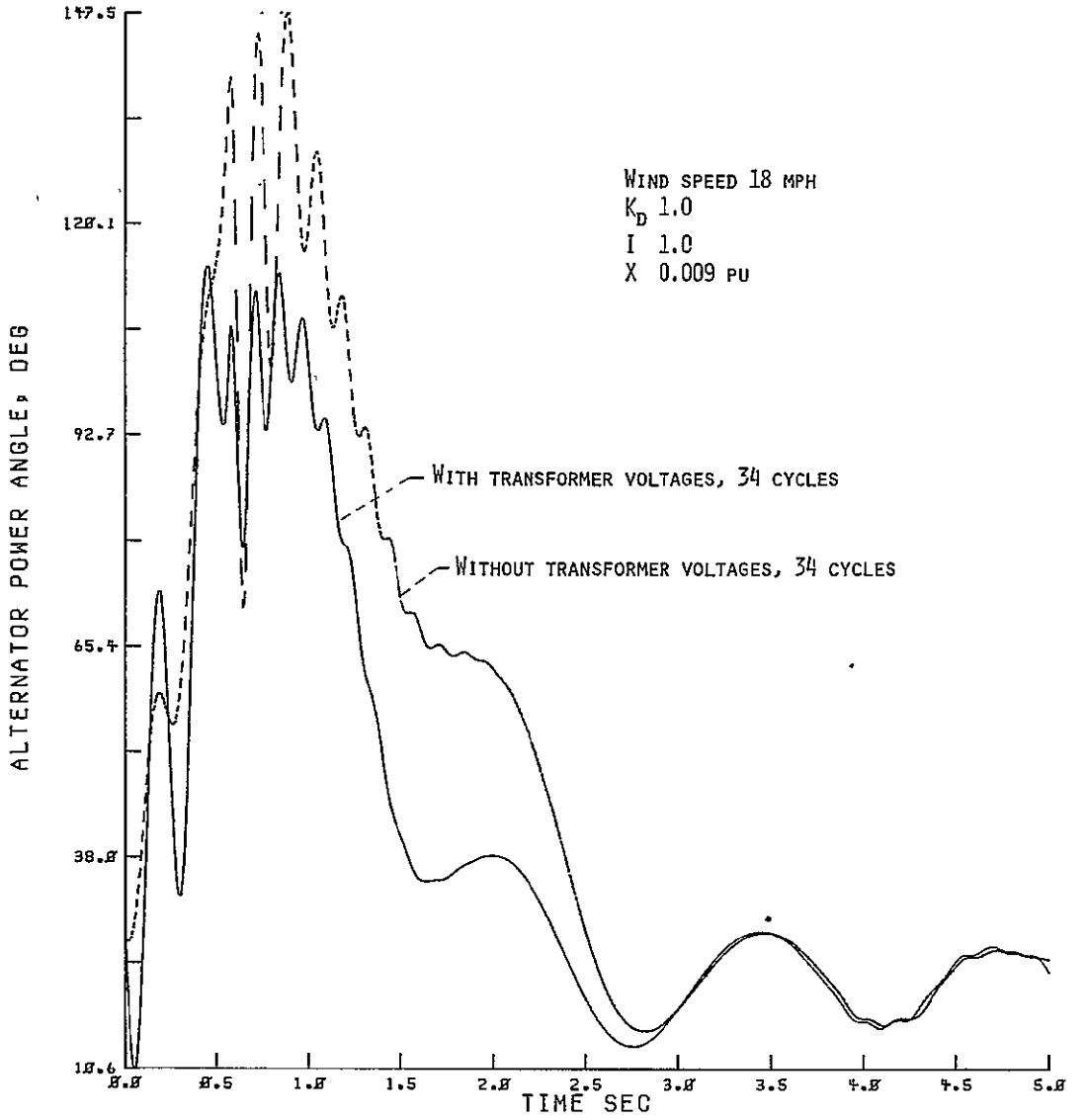

FIGURE 4.28. - COMPARISON OF SWING CURVES OF BASELINE MODEL WITH AND WITHOUT TRANSFORMER VOLTAGES IN MODEL (SAME CLEARING TIMES).

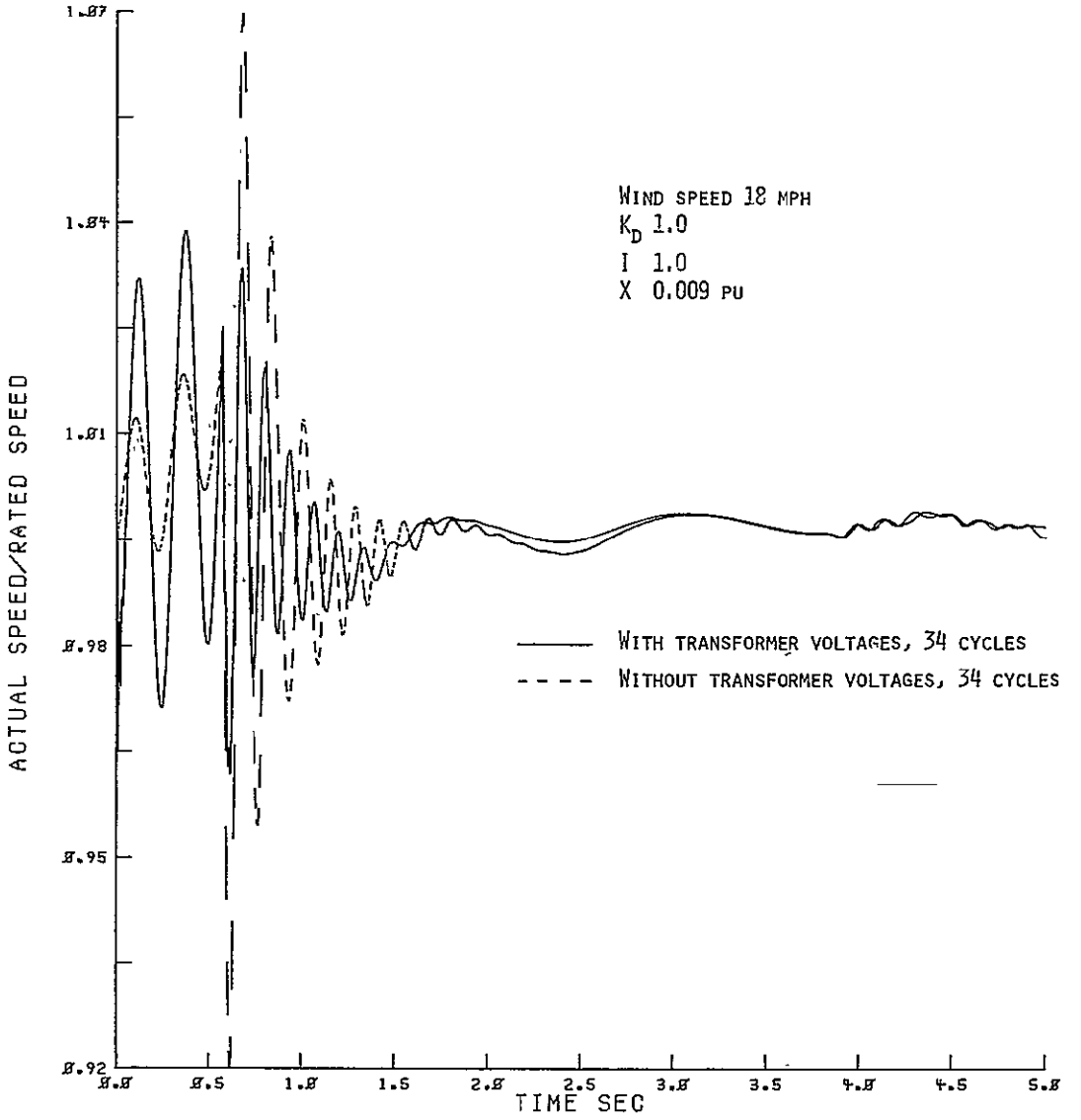

FIGURE 4.29. - COMPARISON OF ROTOR SPEED CURVES OF BASELINE MODEL WITH AND WITHOUT TRANSFORMER VOLTAGES IN MODEL (SAME CLEARING TIMES).

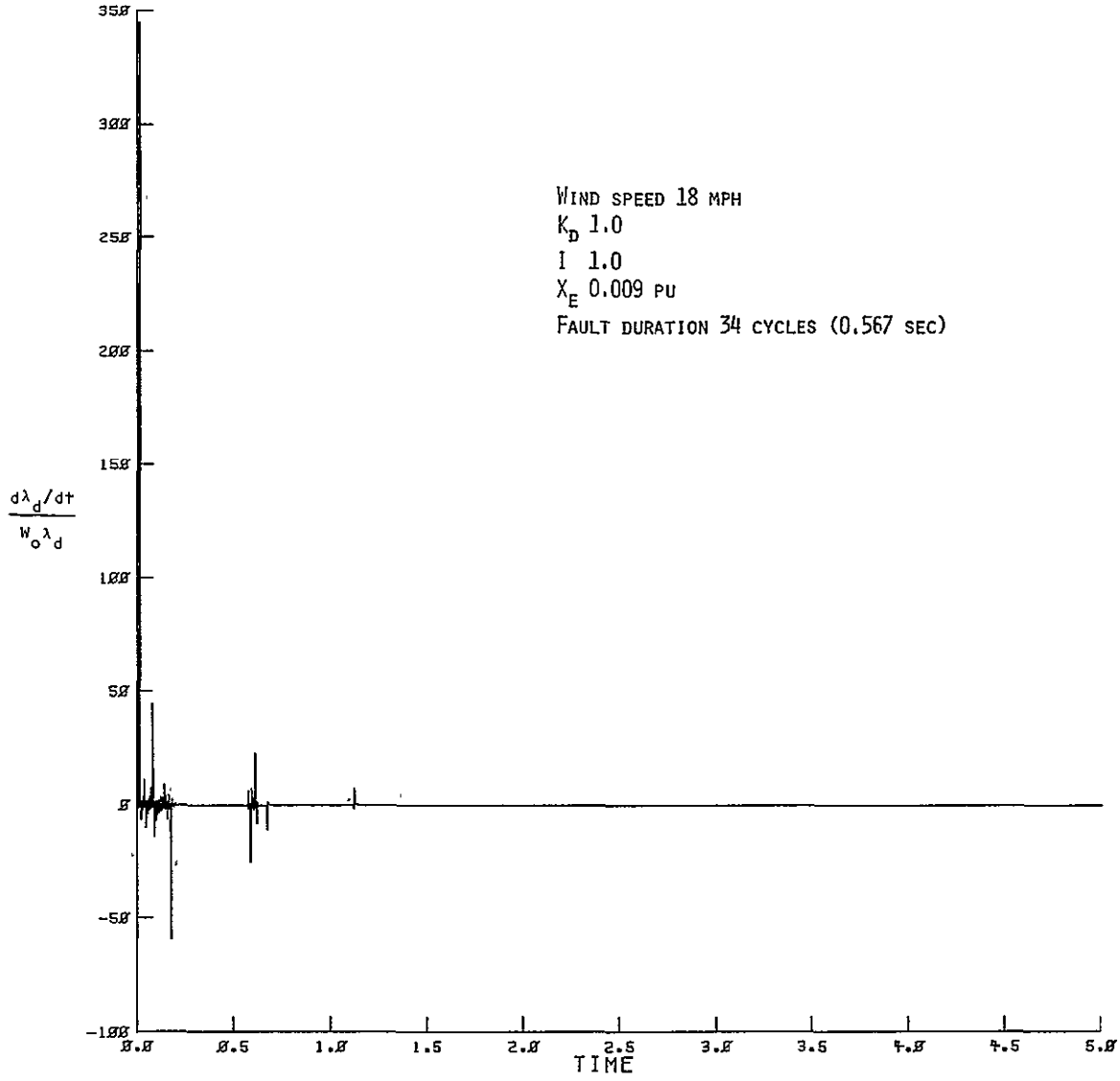

FIGURE 4.30. - RATIO OF DIRECT AXIS TRANSFORMER VOLTAGE TO SPEED VOLTAGE FOR BASELINE MODEL.

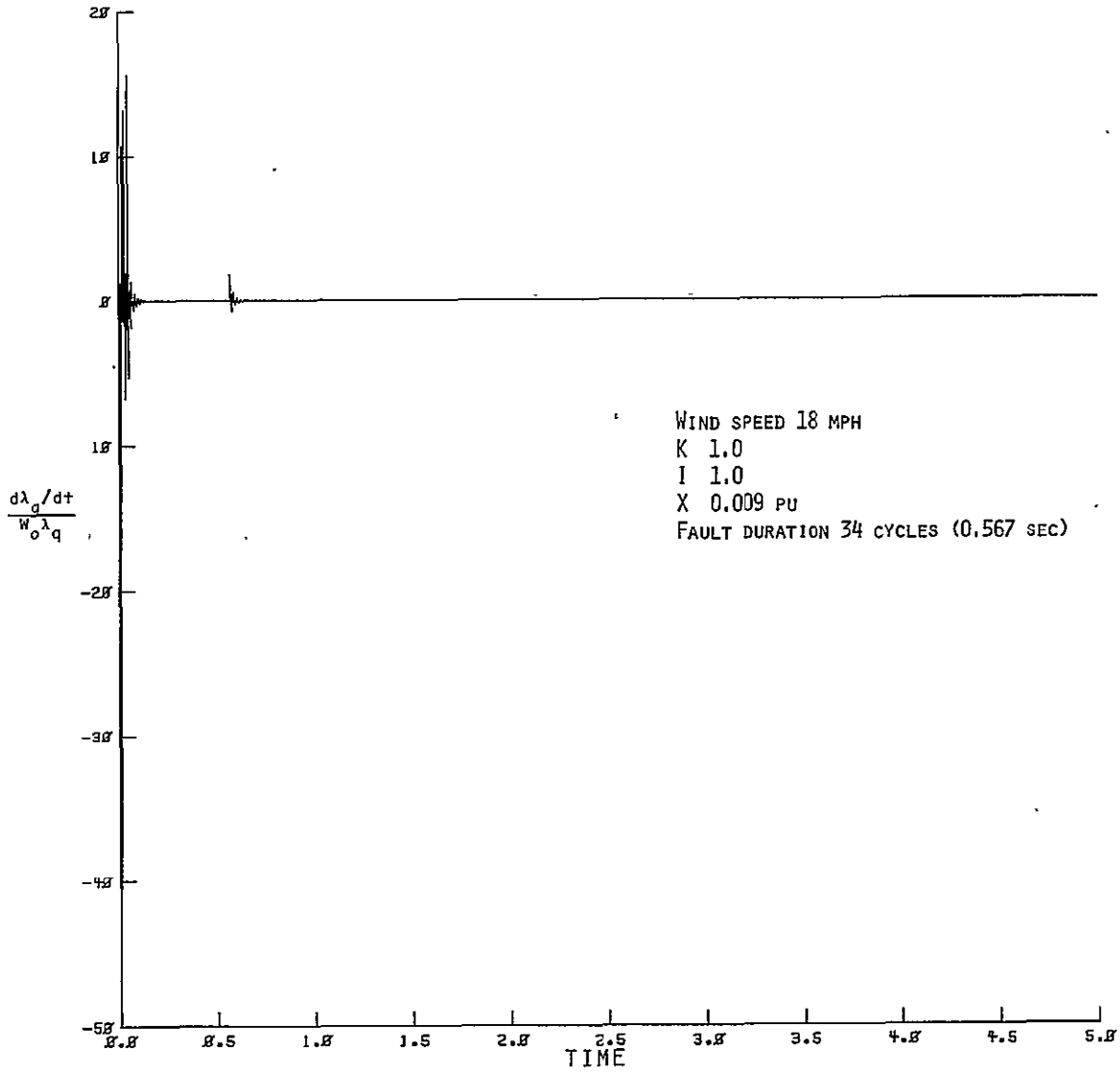

FIGURE 4.31. - RATIO OF QUADRATURE TRANSFORMER VOLTAGE TO SPEED VOLTAGE FOR BASELINE MODEL.

C-2

A comparison of the swing curves for the baseline model with and without transformer voltages is shown in figure 4.32. These are swing curves for the critical clearing times for each model. The loss of synchronism with and without transformer voltages in the model are shown in figures 4.33 and 4.34 for the shortest duration fault causing loss of synchronism.

4.11 Summary

The maximum clearing time for a synchronous alternator of a horizontal axis turbine generator subjected to a three-phase, zero impedance short circuit was determined for a selected set of operating conditions and system parameters, namely power load, tie-line reactance, drive train stiffness, and rotary inertia. The clearing time determination was made by simulating a three-phase short circuit at the infinite bus terminals of the power system.

The maximum swing curve was obtained for each selected operating condition without including tower shadow and wind shear excitation effects. Although these two effects are significant to the system performance of the wind turbine generator, they do not substantially affect the fault transient studied.

The typical maximum swing curve produced by the fault application and removal is a positive swing of the alternator power angle of 1 to 3 seconds duration. The two principal drive train modes of oscillation frequencies appear prominently in the transient.

The effects upon the transient of the rotary inertia, the steady state power load at the time of the fault occurrence, the drive train stiffness, and the tie-line reactance were observed and quantified.

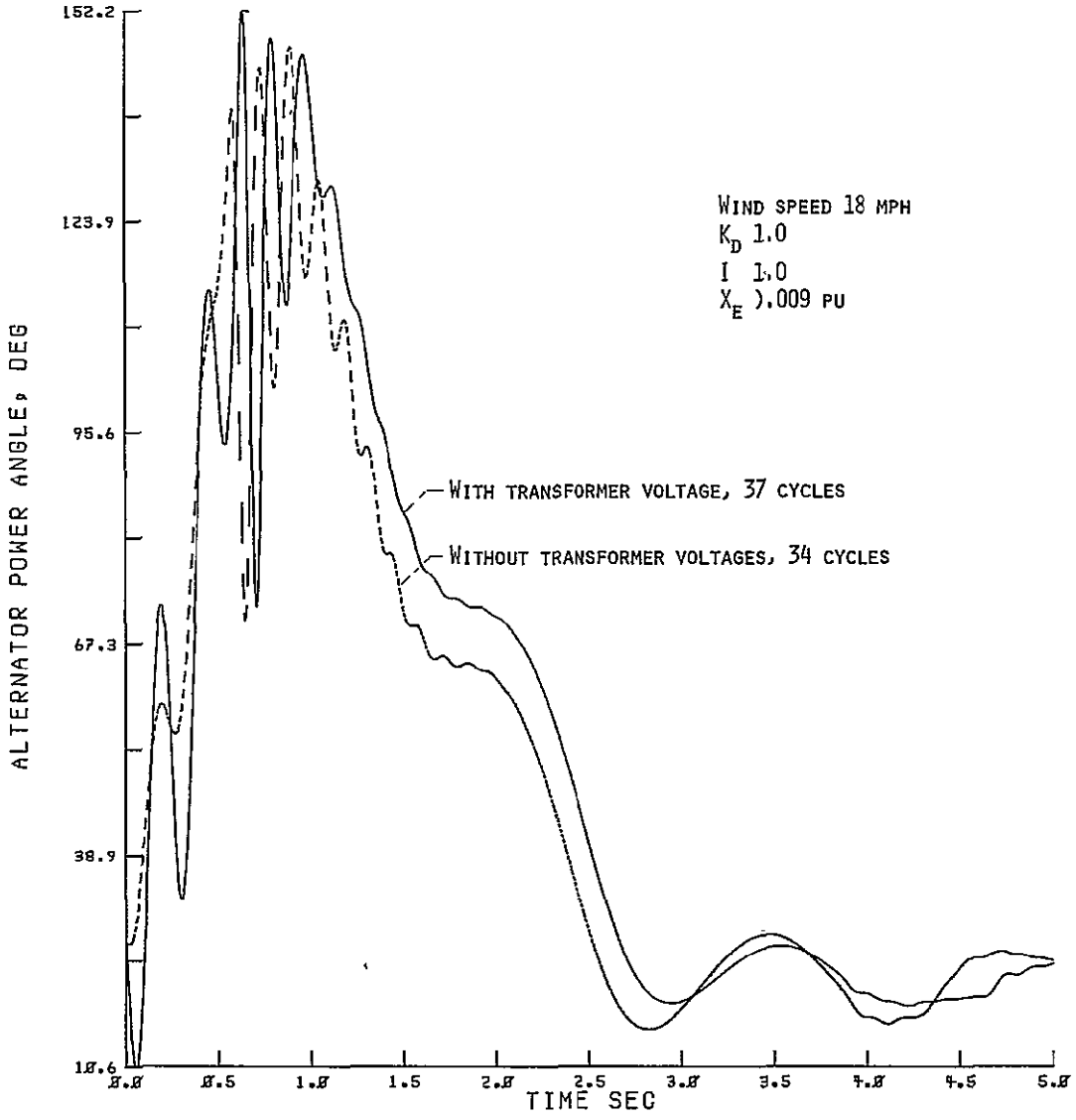

FIGURE 4.32. - COMPARISON OF SWING CURVES FOR BASELINE MODEL WITH AND WITHOUT TRANSFORMER VOLTAGES (CRITICAL CLEARING TIMES).

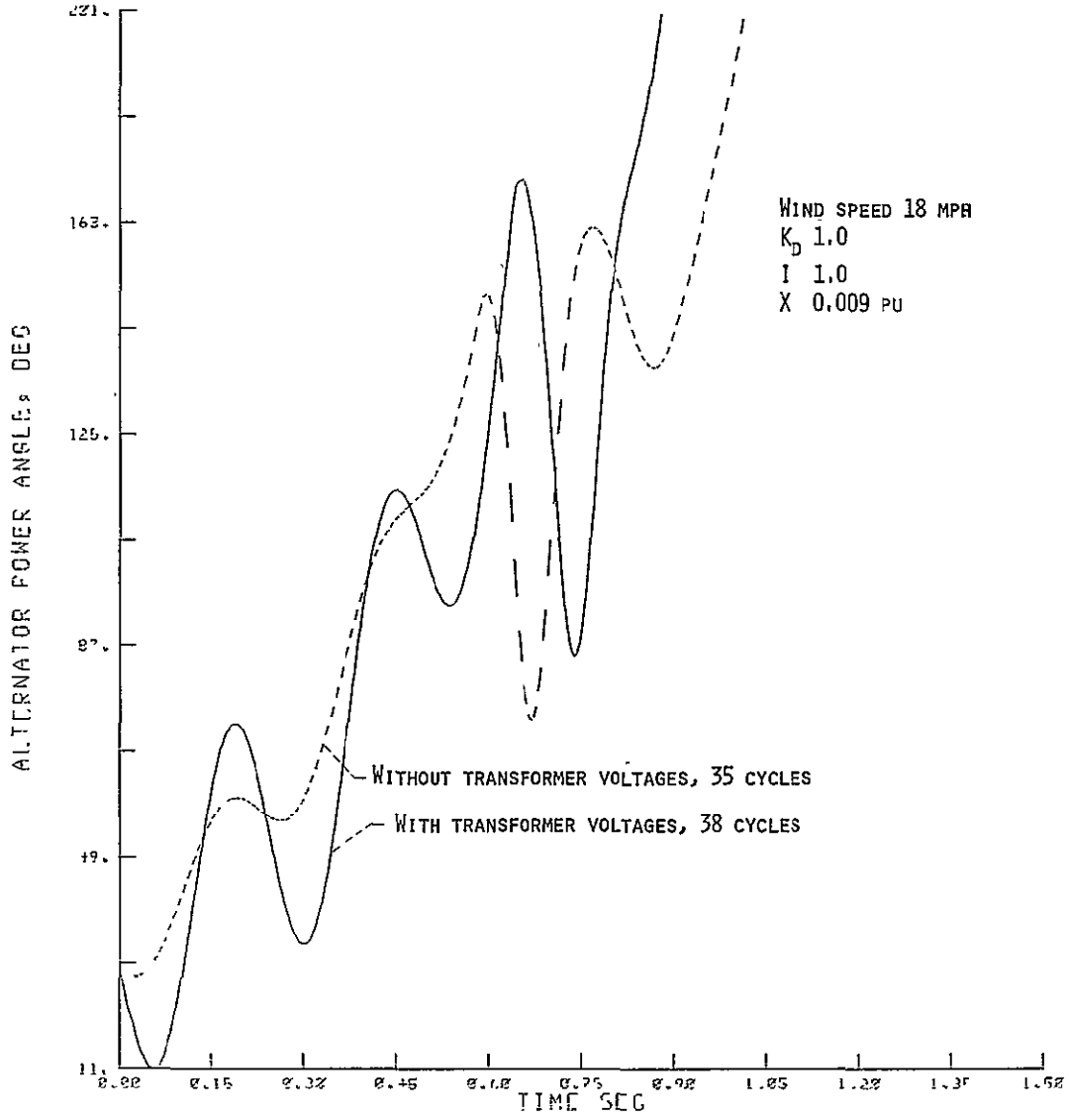

FIGURE 4.33. - COMPARISON OF SWING CURVES FOR BASELINE MODEL WITH AND WITHOUT TRANSFORMER VOLTAGES SHOWING LOSS OF SYNCHRONISM.

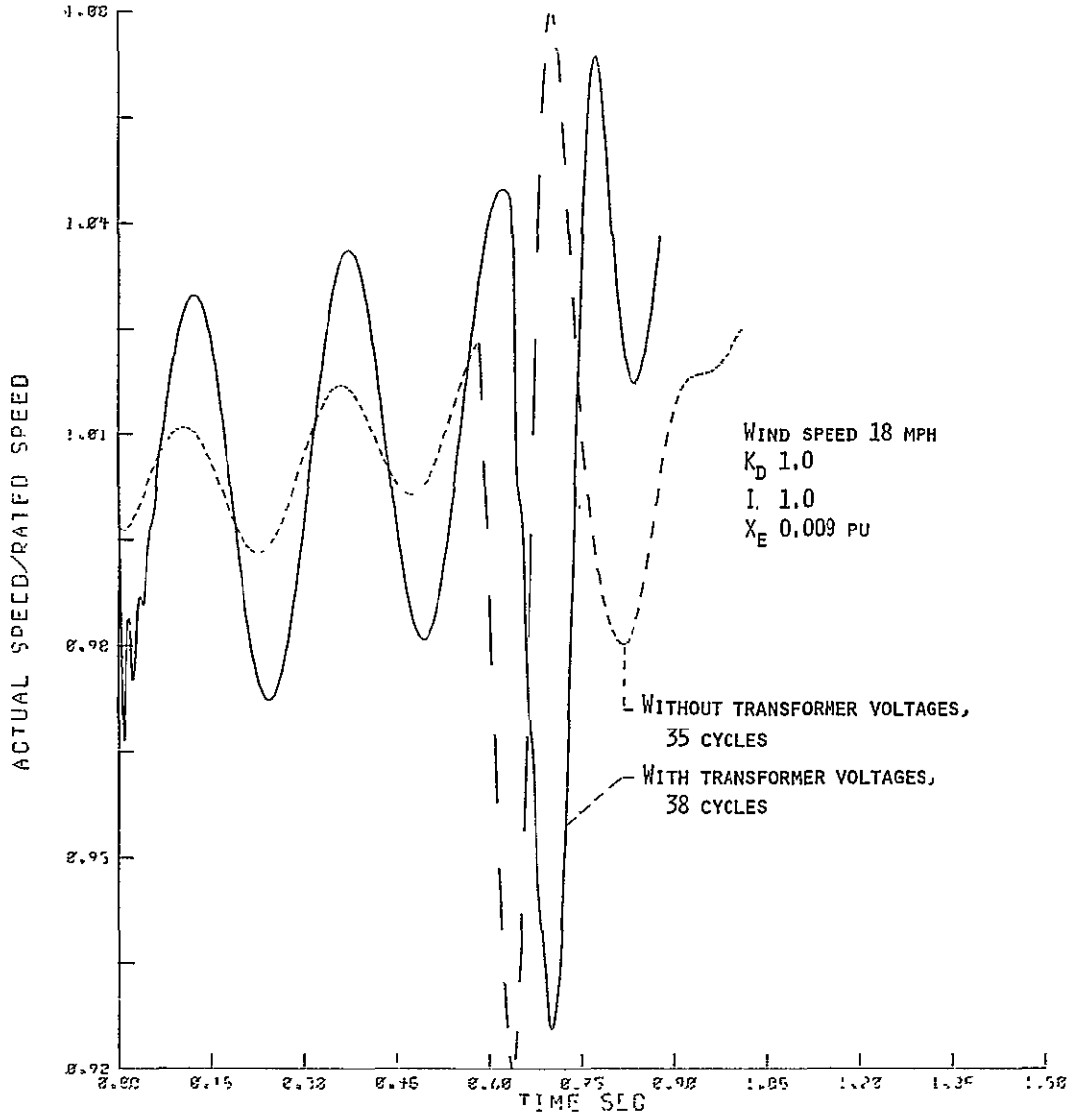

FIGURE 4.34. - COMPARISON OF ROTOR SPEED CURVES FOR BASELINE MODEL WITH AND WITHOUT TRANSFORMER VOLTAGES SHOWING LOSS OF SYNCHRONISM.

Increased inertia prolongs the maximum clearing time; clearing time is inversely proportional to power load; reduced drive train stiffness tends to "decouple" the alternator and turbine; increased tie-line reactance reduces maximum clearing time.

Chapter V

CONCLUSIONS AND RECOMMENDATIONS

The transient stability of a wind turbine generator - in particular the response of that system to a short circuit fault - was investigated in this study. The scope of the problem was limited to a single wind generator tied by one transmission line to an infinite bus. The 100 kW DOE/NASA wind turbine generator at Plum Brook, Ohio, was used as the baseline system for simulation on a digital computer.

5.1 Conclusions

There are two facets to the results obtained in this research: one aspect is the validity of the results - how well do they reflect the theory; the other aspect is the magnitude of the results - what is the significance of the maximum clearing times calculated.

5.1.1 Confirmation of analysis. - The relationships observed in the performance of the model and listed here indicate that the results of the simulation support the analysis that precedes them.

1. Tower shadow and wind shear which produce a twice per turbine revolution oscillation of the alternator power angle and thus a power oscillation have little or negligible effect on the transient resulting from a three-phase fault.

2. The maximum clearing time for the wind turbine alternator subjected to a three-phase short varies directly as the square root of the mass moment of inertia of the system.

3. The maximum clearing time increases as reactance between the alternator and the infinite bus is reduced.

4. Maximum clearing time increases with decreasing power load.

5. The maximum clearing time depends on the electrical load rather than the wind speed. When the load is doubled, the clearing time is halved; when the wind speed is almost doubled while the load remains constant, the clearing time is unchanged.

6. As the drive train stiffness decreases so that there is less coupling between the turbine and the alternator, the maximum clearing time decreases. The relatively large inertia of the turbine becomes less effective in prolonging the clearing time as the coupling decreases.

The transient characteristics enumerated are in agreement with the power system theory discussed in Section 2 of this dissertation and with the phenomena observed in conventional alternating voltage power systems. Accordingly, the simulation model used in this research is valid for studying the transient phenomena of a wind turbine generator following a three-phase short circuit fault.

5.1.2 Significance of results. - Simulation of the wind turbine generator tied to an infinite bus yields maximum clearing times for a three-phase, zero impedance short circuit that range from 67 cycles (1.12 sec) to 37 cycles (0.62 sec) as the power load ranges from 0.8 to 0.4 pu at 0.8 power factor on a "stiff" line. On a "soft" line the maximum clearing times range from 45 cycles (0.75 sec) to

21 cycles (0.35 sec) for the same load range. These times are relatively long clearing times for the average power circuit response to a three-phase, zero impedance fault.

Comparison of simulation results using a model which assumes that the "transformer voltages" are negligible with simulation results using a model including "transformer voltages" indicates the validity of assuming that the "transformer voltages" are negligible for the type of transient study performed for this research.

In order to provide a comparison between the wind turbine generator and conventional power equipment the function plotted in figure 5.1 is included. The figure is extracted from the General Electric Company publication "Electric Utility Systems and Practices" (28). It is represented in that publication as characteristic of a "typical system." The data is presented in this discussion to illustrate the limitation of the time scale of the switching time to 1 second. To provide 0.8 pu load stability the switching time for the "typical" circuit must be less than 0.1 second. This limitation is considerably less than the 0.75 second limitation of the wind turbine generator on a "soft" line.

The significance of the relatively long clearing time available with the wind turbine generator is that the system does not impose a requirement for extremely fast relays and circuit breakers on its circuits in order to maintain transient stability.

5.2 Recommendations for Additional Research

The simulation and determinations of fault transients developed in this study lead logically to the consideration of wind turbine

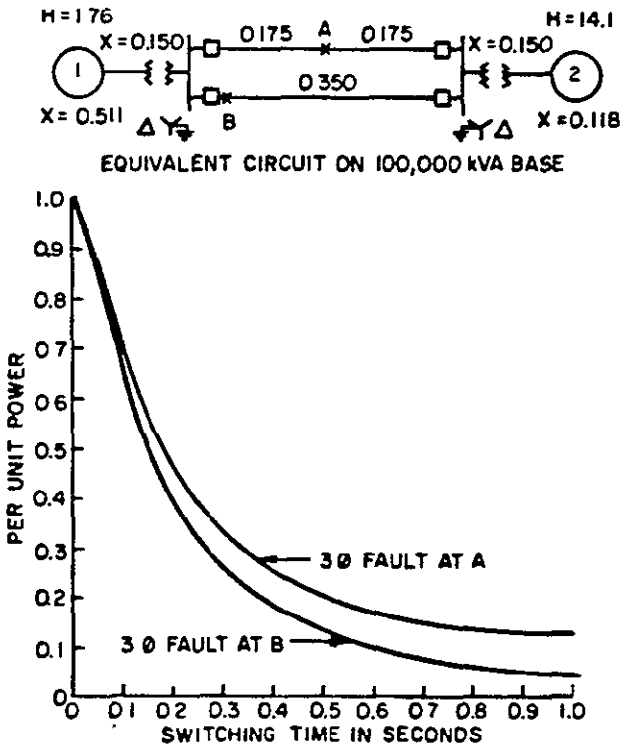

Figure 5.1-Effect of switching time on maximum power for a three-phase fault

generator performance in a network. Among the problems which can profitably be studied with the application of the simulation and information generated in this study are the following:

1. The two machine problem wherein both power generators have the same or similar capacity.

2. Transient stability of a wind turbine generator tied to a bus by more than one transmission line.

3. The effect of the excitation system on the stability of the wind power system.

4. Transient stability for types of faults other than three-phase short circuits.

5. The effect of stability of a cluster of several wind turbine generators tied together electrically.

The directions that further investigations in this field can take are as numerous as those which conventional power systems studies take. As the first studies are accomplished, how much of standard power system technology applies directly to wind turbine power systems should become progressively more evident.

APPENDIX A

SYMBOLS

Alternator Constants

$L_{ff}, L_{\ell\ell d}, L_{\ell\ell q}$	self inductance of field and damper circuits in direct and quadrature axes
$M_{af}, M_{a\ell d}, M_{a\ell q}$	Maximum mutual inductance between armature circuit and field or damper circuits in direct and quadrature axes
r_a	stator resistance in direct and quadrature axes circuits
x_d, x_q	synchronous reactance in direct and quadrature axes circuits
x'_d, x'_q	transient reactance in direct and quadrature axes circuits
x''_d, x''_q	subtransient reactance in direct and quadrature axes circuits
T'_{do}	direct axis transient open circuit time constant
T''_{do}	direct axis subtransient open circuit time constant
T'_d	direct axis transient short circuit time constant
T''_d	direct axis subtransient short circuit time constant
T''_{qo}	quadrature axis subtransient open circuit time constant

Alternator Voltages and Flux

v_d, v_q bus voltage in direct and quadrature axes circuits

v_{td}, v_{tq} stator voltages in direct and quadrature axes circuits

v_t stator voltage

i_d, i_q stator currents in direct and quadrature axes circuits

i_a stator current

λ_d, λ_q stator flux linkages in direct and quadrature axes circuits

λ_f field flux linkage

$\lambda_{\ell\ell d}, \lambda_{\ell\ell q}$ flux linkage in direct and quadrature axes

$$e_d = -\omega_o M_{a\ell q} i_{\ell\ell q}$$

$$e_d'' = -\omega_o \frac{M_{a\ell q}}{L_{\ell\ell q}} \lambda_{\ell\ell q}$$

$$e_{q1} = \omega_o M_{af} i_f$$

$$e_{q2} = \omega_o M_{\ell d} i_{\ell\ell d}$$

$$e_q' = \omega_o \frac{M_{af}}{L_{ff}} \lambda_f$$

$$e_q'' = \omega_o \frac{M_{a\ell d}}{L_{\ell\ell d}} \lambda_{\ell\ell d}$$

System Variables And Constants

B_1, B_2 drive train damping factors

h height above ground

h_{ref} height above ground at which wind speed = $V_{w_{ref}}$

H inertia constant

I	mass moment of inertia
I_1, I_2	mass moment of inertia of low speed and high speed components of drive train, respectively
k	wind shear surface roughness coefficient
KVA_{base}	alternator kVA rating
K_A	spring constant equivalent of alternator synchronous torque
K_d	equivalent stiffness of composite drive train spring
K_I	gain constant of controller
K_{PF}	excitation gain factor for power factor control
K_v	partial derivative of turbine torque with respect to wind speed
K_β	partial derivative of turbine torque with respect to blade pitch
K_Ω	partial derivative of turbine torque with respect to rotational speed
N	gear ratio between high and low speed shafts
p	alternator instantaneous output power
PF	power factor
poles	number of poles of alternator
P_o	electrical power output of alternator
P_d	damping power output of alternator
$P(\delta)$	synchronous power output of alternator
s	slip of alternator; or Laplace operator
t	time
T	accelerating torque
T_e	electromagnetic torque

T_{in}	turbine torque
T_{sh}	shaft torque to alternator
T_{sync}	synchronous torque
u	control variable
V_b	infinite bus voltage
V_{ref}	voltage regulator reference voltage
$V_{R_{nom}}$	nominal regulator voltage
V_w	wind speed
$V_{w_{ref}}$	wind speed at reference height h_{ref}
x	state variable
x_e	external or tie-line reactance
β_{nom}	reference blade pitch
β_i	state variables of controller and pitch servo
δ	alternator rotor angle
ζ_s	pitch servo damping factor
θ_1, θ_2	position angle of low speed and high speed components of drive train model
τ_e	time constant of exciter
ω	angular frequency of alternator
ω_s	natural frequency of pitch servo
ω_o	angular frequency of infinite bus
Ω_A	angular frequency of alternator shaft
Ω_o	angular frequency of turbine

APPENDIX B

BASELINE MODEL OF WIND TURBINE GENERATOR

The baseline wind turbine generator system for the analytical model of this research is the DOE/NASA 100 kW wind turbine generator at the Plumbrook Station of the Lewis Research Center. This power generator is referred to as the Mod-0 system. The system is a prototype of the first half dozen large wind turbine systems which will be erected in the next several years. Although improved designs are expected to evolve as each system is tested, the general configuration and composition of these systems are not expected to change radically. On the basis of that expectation the Mod-0 system was esteemed to be a satisfactory model on which to base this stability study. A schematic diagram of the Mod-0 wind turbine generator drive train assembly is shown in figure B.1.

System Description

Configuration

The Mod-0 machine is a horizontal axis wind turbine generator system mounted on top of a 30.5 meter truss tower. (General specifications of the system are listed in Table B-1.) The turbine (rotor) blades are downwind of the tower, an arrangement that is selected to provide safety from a blade striking the tower, and which is also more stable with respect to yawing motions. However,

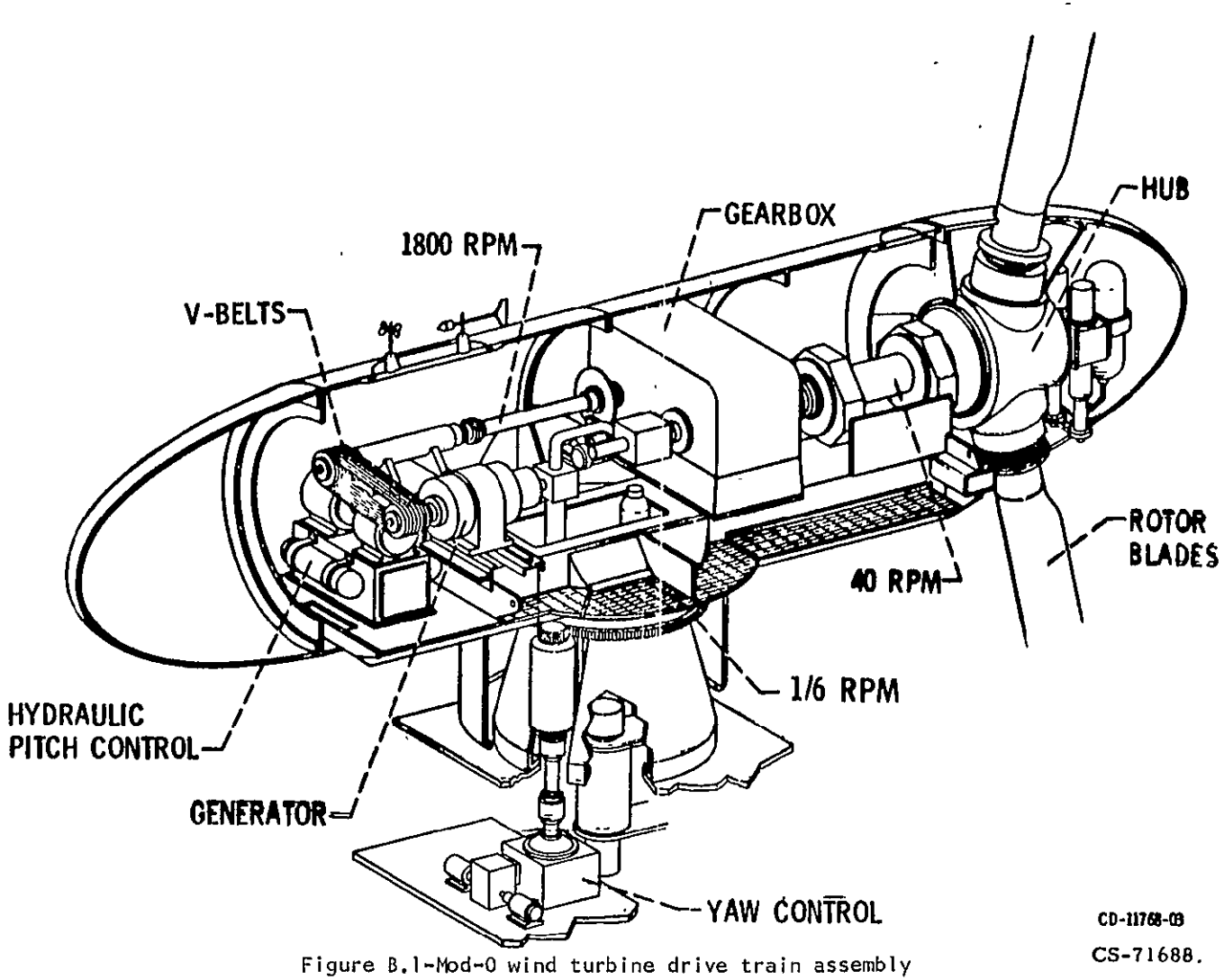

Figure 8.1-Mod-0 wind turbine drive train assembly

Table B-1 - General Specifications for the Mod-0 100 kW Wind Turbine Generator

Configuration	Horizontal axis, two-bladed downwind turbine
Power Output	100 kW in 8.05 m/s wind
Cut-in Wind Speed	4.47 m/s
Cut-out Wind Speed	17.88 m/s
Turbine Speed	40 r/min
Yaw Rate	1/6 r/min
Tower Height	30.48 m
Tower Weight	19,958 kg
Blade Length	19.05 m
Blade Weight	907.2 kg
Airfoil	NACA 23,000, .34 deg nonlinear twist
Coning Angle	7 deg
Hub	Fixed type
Generator	Synchronous, 125 kVA, 480 v
Weight of Components on Tower	18,140 kg

with this configuration the rotor blades are subject to tower shadow effect whereby the wind forces on a blade are abruptly and substantially reduced as the blade passes behind the tower.

Rotor Blades

The rotor has two all-metal blades, each 19.0 meters long and each weighing 907 kg. The blades are designed to produce 133 kW of power at 8.05 m/s wind speed when rotating at 40 r/min.

Hub

The hub connects the blades to the low speed shaft. The hub also houses the mechanical gears, linkages, and actuators required for changing the pitch of the blades to compensate for changing wind and load conditions. Wind loads and centrifugal loads are absorbed by the hub and transmitted to the low speed shaft. The hub is a fixed hub; that is, the hub is bolted rigidly onto the main low speed shaft with the blades fixed to the hub allowing only the pitch change degree of freedom.

Pitch Change Mechanism

The pitch change mechanism consists of a hydraulic pump, a pressure control valve, an actuator, and a gear for connecting a linear motion of the actuator to a rotational motion (pitch) for the blades. The actuator is a rack and pinion that turns a master gear which in turn rotates the blades by means of a bevel gear mounted on the roots of each blade. The hydraulic pump is mounted separately on the bed plate structure and the hydraulic fluid is brought into the low spee shaft through rotating seals, thence to the pitch change components rotating at the other end of the shaft.

Bed Plate

The rotor, transmission train, alternator, and all shafts and bearings are mounted on a bed plate. The bed plate is supported on a large gear bearing assembly which is capable of rotating (yawing) the entire machine on top of the tower.

Yaw Control

The yaw control is a dual control to increase structural stiffness between the tower and the rotating bed plate. Each pinion gear is driven by an electric motor. The yaw rate is 1/6 r/min. The control is designed to follow slow directional changes of the wind rather than sudden changes. The entire structure atop the tower is enclosed in a fiberglass housing for protection from the environment.

Transmission Train

The hub transmits the high torque at low speed to the gear box via a low speed shaft. Out of the gear box a high speed shaft transmits the low torque at high speed, through a hydraulic slip coupling, to the alternator by means of a V-belt connection.

The gear box is a standard triple reduction design, but is used in a step up ratio rather than the more conventional step down ratio for which the gear box was originally designed. The gear box ratio is 45:1.

Alternator

The alternator is an 1800 r/min synchronous machine, three phase, y-connected, and self-cooled with a directly connected brushless exciter and regulator. The machine is rated at 125 kVA, 0.8 power factor, 480 volts, 60 Hertz.

Tower

The tower upon which the entire wind turbine generator is placed is 30.5 meters tall, constructed of steel, and is a pinned truss

design. It rests on a concrete foundation. The tower is designed to withstand high wind and thrust loads, both steady and cyclic.

Controls

The wind turbine generator system develops a net power of 100 kW at wind speeds of 8.05 m/s and greater. Between 4.47 m/s and 8.05 m/s the rotor blade pitch is fixed and the net power is a function of the wind speed. At wind speeds greater than 8.05 m/s the net power generated is limited to 100 kW by rotating the variable pitch blades toward feather, spilling the excess energy in the wind. At wind speeds of 17.88 m/s or greater, the turbine blades are completely feathered, shutting down the system.

APPENDIX C

DETERMINATION OF STEADY STATE INITIAL CONDITIONS

Alternator

The phasor diagram representing the initial conditions of the synchronous generator prior to a fault is shown in figure C.1. Given

(1) Infinite bus voltage, V_B

(2) Alternator power, P,

(3) Power factor, cos θ,

such that $P = V_t I_a \cos\theta$, determine ϕ.

$$\tan\theta = \frac{AC}{0A} = \frac{AB + BC}{0A} = \frac{V_B \sin\phi + I_a x_e}{V_B \cos\phi}$$

$$P = V_t I_a \cos\theta = V_B I_a \cos\phi$$

$$\tan\theta = \frac{V_B \sin\phi + x_e P / V_B \cos\phi}{V_B \cos\phi}$$

$$\frac{\sin\theta}{\cos\theta} = \frac{V_B^2 \sin\phi \cos\phi + x_e P}{V^2 \cos^2\phi}$$

$$\sin\theta \cos^2\phi = \sin\phi \cos\phi \cos\theta + \frac{x_e P \cos\theta}{V_B^2}$$

$$2 \sin\theta \cos^2\phi = 2 \sin\phi \cos\phi \cos\theta + \frac{2 x_e P \cos\theta}{V_B^2}$$

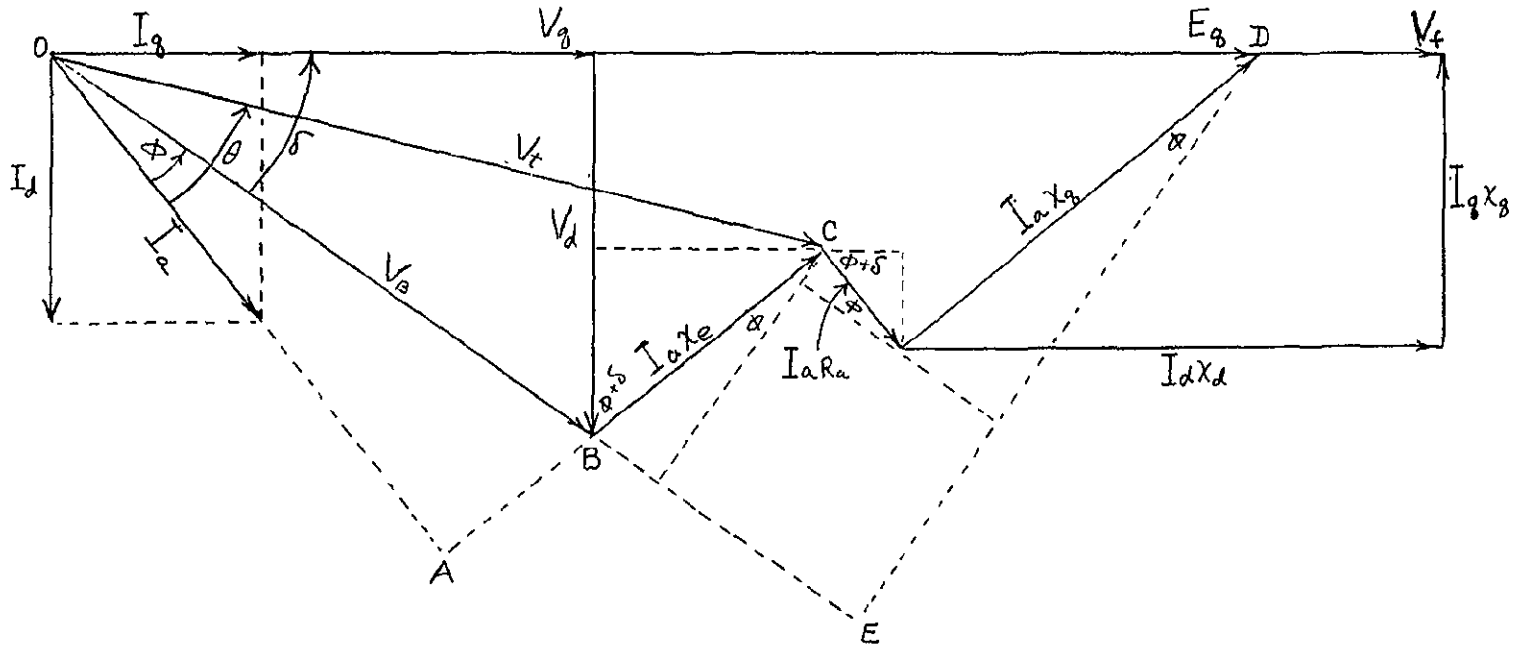

FIGURE C.1- PHASOR DIAGRAM USED TO CALCULATE INITIAL CONDITIONS

$$\sin\theta(2\cos^2\phi) = (2\sin\phi\cos\phi)\cos\theta + \frac{2x_eP\cos\theta}{V_B^2}$$

$$\sin\theta(1+\cos 2\phi) = \sin 2\phi\cos\theta + \frac{2x_eP\cos\theta}{V_B^2}$$

$$\sin\theta\cos 2\phi - \sin 2\phi\cos\theta = \frac{2x_eP\cos\theta}{V_B^2} - \sin\theta$$

$$\sin(\theta - 2\phi) = \frac{2x_eP\cos\theta}{V_B^2} - \sin\theta$$

$$\theta - 2\phi = \sin^{-1}\left(\frac{2x_eP\cos\theta}{V_B^2} - \sin\theta\right)$$

$$\phi = \frac{1}{2}\left[\theta + \sin^{-1}\left(\sin\theta - \frac{2x_eP\cos\theta}{V_B^2}\right)\right] \qquad (C.1)$$

(a)
$$I_a = \frac{P}{V_B\cos\phi} \qquad (C.2)$$

(b)
$$V_t = \frac{V_B\cos\phi}{\cos\theta} \qquad (C.3)$$

$$\delta = \tan^{-1}\frac{DE}{0E}$$

$$DE = I_ax_q\cos\phi + I_ax_e\cos\phi - I_aR_a\sin\phi$$

$$0E = V_B + I_ax_e\sin\phi + I_aR_a\cos\phi + I_ax_q\sin\phi$$

(c) $$\delta = \tan^{-1}\left\{\frac{\left[(x_q + x_e)\cos\phi - R_a \sin\phi\right]I_a}{V_B + \left[(x_q + x_e)\sin\phi + R_a\cos\phi\right]I_a}\right\} \qquad (C.4)$$

$$V_f = V_B \cos\delta + I_a x_e \sin(\phi + \delta) + I_a R_a \cos(\phi + \delta) + I_d x_d$$

Since

$$I_d x_d = \left[I_a \sin(\phi + \delta)\right]x_d$$

(d) $$V_f = V_B \cos\delta + I_a\left[(x_d + x_e)\sin(\phi + \delta) + R_a\cos(\phi + \delta)\right] \qquad (C.5)$$

(e) $$I_d = I_a \sin(\phi + \delta) \qquad (C.6)$$

(f) $$I_q = I_a \cos(\phi + \delta) \qquad (C.7)$$

At steady state the derivatives of equations (3.12), (3.13), and (3.14) are zero, so that

(g) $$E_d = 0 \qquad (C.8)$$

(h) $$E_{q2} = 0 \qquad (C.9)$$

(i) $$E_{q1} = V_f \qquad (C.10)$$

(j) $$\Lambda_d = E_q'' - I_a x_a'' \qquad (3.5)$$

(k) $$\Lambda_q = -E_d'' - I_q x_q'' \qquad (3.6)$$

Simultaneous solution of equations (3.5), (3.6), (3.9), (3.10), and (3.11) give

(ℓ) $$E_d'' = (x_q - x_q'')I_q \qquad (C.11)$$

(m) $$E_q' = -(x_d - x_d')I_d + V_f \qquad (C.12)$$

(n) $$E_q'' = -(x_d - x_d'')I_d + V_f \qquad (C.13)$$

(o) $$T_e = E_d''I_d + E_q''I_q - I_dI_q(x_d'' - x_q'') \tag{3.15}$$

Drive Train

The initial conditions for a steady state condition of the drive train with a constant input torque is given by the relationships shown in figure 3.4.

$$\theta_2 = \frac{2}{\text{poles}} \cdot \frac{\delta}{N} \tag{C.14}$$

$$\theta_1 = \frac{T_{in} - \beta_i\Omega_o}{K_D} + \theta_2 \tag{C.15}$$

Turbine

The correct value of β_{nom} (fig. 3.8) for the given wind speed and nominal turbine speed will produce the torque required for the power output desired and system losses. This value is determined from the turbine torque program (Section 3.1) and can be tabulated for operating conditions of interest. For the appropriate value of β_{nom} other initial conditions of the controller are zero.

APPENDIX D

LINEARIZED SIMULATION MODEL

The complete set of 26 nonlinear differential equations which comprise the simulation model have been linearized for small perturbations, and the incremental equations are listed. The block diagram for the system is shown in figure D.1.

The torque developed by the turbine is expressed as

$$\Delta T_{in} = \frac{\partial T}{\partial V_w} \Delta V_w + \frac{\partial T}{\partial \dot{\theta}_1} \Delta \dot{\theta}_1 + \frac{\partial T}{\partial \beta} \Delta \beta_1 = K_v V_w + K_\Omega \dot{\theta}_1 + K_\beta \beta_i$$

$$\lambda_d = \frac{R_a^2}{Q} e_q'' - \frac{R_a x_d''}{Q} e_d'' + C_1 x_d'' \delta$$

$$\lambda_q = - \frac{R_a x_q''}{Q} e_q'' - \frac{R_a^2}{Q} e_d'' - C_2 x_q'' \delta$$

$$e_d = - \frac{R_a (x_q - x_q'')}{Q} e_q'' + \frac{\left(R_a^2 + x_d'' x_q\right)}{Q} e_d'' - C_2 (x_q - x_q'') \delta$$

$$e_{q1} = C_3 e_q' - C_4 e_q''$$

$$e_{q2} = - C_e e_q' + C_3 \frac{\left(R_a^2 + x_d' x_q''\right)}{Q} e_q'' + C_3 \frac{R_a (x_d' - x_d'')}{Q} e_d''$$

$$- C_1 C_3 (x_d' - x_d'') \delta$$

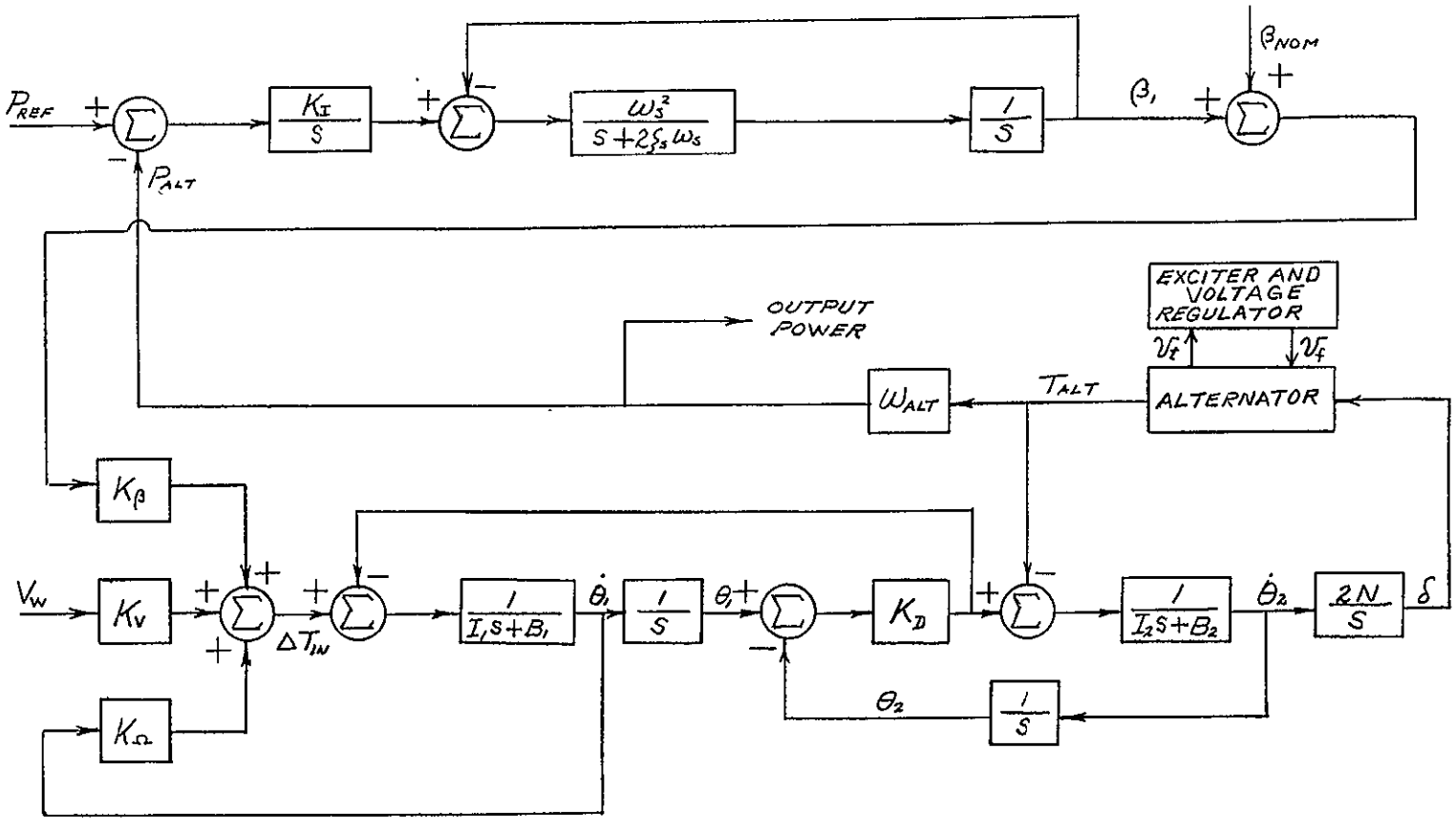

Figure D.1-Linearized simulation model block diagram

$$i_d = \frac{x_q''}{Q}\, e_q'' + \frac{R_a}{Q}\, e_d'' - C_1\delta$$

$$i_q = \frac{R_a}{Q}\, e_q'' - \frac{x_d''}{Q}\, e_d'' + C_2\delta$$

$$v_{td} = -\frac{R_a x_e}{Q}\, e_q'' + \frac{x_a'' x_e}{Q}\, e_d'' + (V_B \cos\delta_o - C_2 x_e)\delta$$

$$v_{tq} = \frac{x_q x_e}{Q}\, e_q'' + \frac{R_a x_e}{Q}\, e_d'' - (V_B \sin\delta_o + C_1 x_e)\delta$$

$$v_t = \frac{x_e}{t_{to}Q}(-R_a v_{tdo} + x_q'' v_{tqo})e_q'' + \frac{x_e}{v_{to}Q}(x_d'' v_{tdo} + R_a v_{tqo})e_d''$$

$$+ \frac{1}{v_{to}}\left[V_B(v_{tdo}\cos\delta_o - v_{tqo}\sin\delta_o) - x_e(C_2 v_{tdo} + C\, v_{tqo})\right]\delta$$

$$Te = \left(I_{qo} + \frac{Gx_q''}{Q} + \frac{HR_a}{Q}\right)e_q'' + \left(I_{do} + \frac{GR_a}{Q} - \frac{Hx_d''}{Q}\right)e_d'' - (C_1 G - C_2 H)\delta$$

$$\dot{e}_q' = -\frac{C_3}{T_{do}'}\, e_q' + \frac{C_4}{T_{do}'}\, e_q'' + \frac{V_F}{T_{do}'}$$

$$\dot{e}_q'' = \frac{1}{T_{do}''}\, e_q' - \frac{\left(R_a^2 + x_d' x_q''\right)}{T_{do}'' Q}\, e_q'' - \frac{R_a(x_d' - x_d'')}{T_{do}'' Q}\, e_d'' + C_1 \frac{(x_d' - x_d'')}{T_{do}''}\,\delta$$

$$\dot{e}_d'' = \frac{R_a(x_q - x_q'')}{T_{qo}'' Q}\, e_q'' - \frac{\left(R_a^2 + x_d'' x_q\right)}{T_{qo}'' Q}\, e_d'' - C_2 \frac{(x_q - x_q'')}{T_{qo}''}\,\delta$$

$$\ddot{\theta}_1 = -\frac{B_1}{I_1}\,\dot{\theta}_1 - \frac{K_D}{I_1}\,\theta_1 + \frac{K_D}{I_1}\,\theta_2 + \frac{T_{in}}{I_1}$$

$$\dot{\theta}_1 = \dot{\theta}_1$$

$$\ddot{\theta}_2 = -\frac{W}{I_2}\left(I_{qo} + \frac{Gx_q''}{Q} + \frac{HR_a}{Q}\right)e_q'' - \frac{W}{I_2}\left(I_{do} + \frac{GR_a}{Q} - \frac{Hx_d''}{Q}\right)e_d''$$

$$+ \frac{K_D}{I_2}\theta_1 - \frac{B_2}{I_2}\dot{\theta}_2 - \frac{K_D}{I_2}\theta_2 + \frac{W}{I_2}(C_1G - C_2H)\delta$$

$$\dot{\theta}_2 = \dot{\theta}_2$$

$$\dot{\beta}_1 = \beta_2$$

$$\dot{\beta}_2 = -\omega_s\beta_1 - 2\zeta_s\omega_s\beta_2 + \omega_s^2\beta_3$$

$$\dot{\beta}_3 = -K_I p(KVA_{base})$$

$$p = \frac{(x_q''V_{do} + R_aV_{qo})}{Q}e_q'' + \frac{(R_aV_{do} - x_d''V_{qo})}{Q}e_d''$$

$$+ \left[V_B(I_{do}\cos\delta_o - I_{qo}\sin\delta_o) + (C_1V_{do} - C_2V_{qo})\right]\delta$$

$$i_a = \frac{(I_{do}x_q'' + I_{qo}R_a)}{I_{ao}Q}e_q'' + \frac{(I_{do}R_a - I_{qo}x_d'')}{I_{ao}Q}e_d'' - \frac{(C_1I_{do} - C_2I_{qo})}{I_a}\delta$$

$$\dot{v}_e = F_1e_q'' + F_2e_d'' + F_3v_e + F_4\delta$$

$$\dot{v}_f = v_e$$

$$\dot{\delta} = 2N\dot{\theta}_2$$

where

$$Q = R_a^2 + x_d''x_q''$$

$$C_1 = \frac{V_B(R_a\cos\delta_o - x_d''\sin\delta_o)}{Q}$$

$$C_2 = \frac{V_B(x_d'' \cos \delta_o + R_a \sin \delta_o)}{Q}$$

$$C_3 = \frac{x_d - x_d''}{x_d' - x_d''}$$

$$C_4 = \frac{x_d - x_d'}{x_d' - x_d''}$$

$$W = T_{base}(\text{lb-ft})$$

$$F_1 = \frac{\mu}{\tau_e}\left[\frac{K_{PF}}{v_{to}} \cdot \frac{(x_q''V_{do} + R_aV_{qo})}{Q} - (PF)K_{PF}\frac{(I_{do}x_q'' + I_{qo}R_a)}{I_{ao}Q} - x_e\left(\frac{P_oK_{PF}}{v_{to}^2} + 1\right)\left(\frac{-R_aV_{tdo} + x_q''V_{tqo}}{v_{to}Q}\right)\right]$$

$$F_2 = \frac{\mu}{\tau_e}\left[\frac{K_{PF}}{v_{to}} \cdot \frac{(R_aV_{do} - x_d'V_{qo})}{Q} - (PF)K_{PF}\frac{(I_{do}R_a - I_{qo}x_d')}{I_{ao}Q} - x_e\left(\frac{P_oK_{PF}}{V_{to}^2} + 1\right)\left(\frac{x_d'V_{tdo} + R_aV_{tqo}}{V_{to}Q}\right)\right]$$

$$F_3 = -\frac{1}{\tau_e}$$

$$F_4 = \frac{\mu}{\tau_e}\left\{\frac{K_{PF}}{V_{to}}\left[V_B(I_{do}\cos\delta_o - I_{qo}\sin\delta_o) - (C_1V_{do} - C_2V_{qo})\right] + (PF)K_{PF}\frac{(C_1I_{do} - C_2I_{qo})}{I_{ao}} - \left(\frac{P_oK_{PF}}{V_{to}^2} + 1\right)\left[\frac{V_B(V_{tao}\cos\delta_o - V_{tqo}\sin\delta_o) - x_e(C_2V_{tdo} + C_1V_{tqo})}{V_{to}}\right]\right\}$$

$$G = E_{do}'' - I_{qo}(x_d'' - x_q'')$$

$$H = E''_{qo} - I_{do}(x'_d - x''_q)$$

The system equations are expressed in state space form

$$\dot{x} = Ax + B_u$$

$$z = C_y$$

Matrices A and C are given on the following pages

$$B = \left[0,0,0,\frac{1}{I_1},0,\ldots\ldots\ldots 0\right]^T$$

The closed loop state equation is

$$\dot{x} = \left(A + BK\left[\frac{I}{C}\right]\right)x$$

where I is the identity matrix and

$$K = \left[0,0,0,K_\Omega,0,0,0,K_\beta,0,\ldots\ldots\ldots 0\right]$$

The vectors x, u, and z are given by

$$x = \left[e'_q, e''_q, e''_d, \dot{\theta}_1, \theta_1, \dot{\theta}_2, \theta_2, \beta_1, \beta_2, \beta_3, v_e, v_f, \delta\right]$$

$$u = T_{in}$$

$$z = \left[\lambda_d, \lambda_q, e_d, e_{q1}, e_{q2}, i_d, i_q, v_{td}, v_{tq}, v_t, T_e\right]$$

Matrix dimensions are x(13,1), z(11,1), u(1), A(13,13), B(13,1), C(11,13), K(1,24), and I(13,13).

e_q'	e_q''	e_d	$\dot{\theta}_1$	θ_1	$\dot{\theta}_2$	θ_2	β_1	β_2	β_3	v_e	v_f	δ
$-\frac{C_3}{T_{do}'}$	$\frac{C_4}{T_{do}'}$										$\frac{1}{T_{do}'}$	
$\frac{1}{T_{do}''}$	$-\frac{\left(R_a^2 + x_d'x_q''\right)}{T_{do}''Q}$	$-\frac{R_a(x_d' - x_d'')}{T_{do}''Q}$										$\frac{C_1(x_d' - x_d'')}{T_{do}''}$
	$\frac{R_a(x_q - x_q'')}{T_{qo}''Q}$	$-\frac{R_a^2 + x_d''x_q}{T_{qo}''Q}$										$-\frac{C_2(x_q - x_q'')}{T_{qo}''}$
			$-\frac{B_1}{I_1}$	$-\frac{K_D}{I_1}$		$\frac{K_D}{I_1}$						
			1									
$-\frac{W}{I_2}\left(I_{qo} + \frac{Gx_q''}{Q} + \frac{HR_a}{Q}\right)$	$-\frac{W}{I_2}\left(I_{do} + \frac{GR_a}{Q} - \frac{Hx_d''}{Q}\right)$			$\frac{K_D}{I_2}$	$-\frac{B_2}{I_2}$	$-\frac{K_D}{I_2}$						$\frac{W}{I_2}(C_1G - C_2H)$
					1							
							1					
							$-\omega_s$	$-2\zeta_s\omega_s$	ω_s^2			
$-\frac{K_IK_{VA}(x_q''V_{do} + R_aV_{qo})}{Q}$	$-\frac{K_IK_{VA}(R_aV_{do} - x_d''V_{qo})}{Q}$											$K_IK_{VA}\left[\overline{V_B}(I_{do}\cos\delta_o - I_{qo}\sin\delta_o) - (C_1V_{do} - C_2V_{qo})\right]$
F_1	F_2								F_3			F_4
									1			
					2N							

MATRIX A (13x13)

e_q'	e_q''	e_d''	δ
	$\frac{R_a^2}{Q}$	$-\frac{R_a x_d''}{Q}$	$C_1 x_d''$
	$-\frac{R_a x_q''}{Q}$	$-\frac{R_a^2}{Q}$	$-C_2 x_q''$
	$-\frac{R_a(x_q - x_q'')}{Q}$	$\frac{R_a^2 + x_d'' x_q}{Q}$	$-C_2(x_q - x_q'')$
C_3	$-C_4$		
$-C_3$	$\frac{C_3(R_a^2 + x_d' x_q'')}{Q}$	$\frac{C_3 R_a(x_d' - x_d'')}{Q}$	$-C_1 C_3(x_d' - x_d'')$
	$\frac{x_q''}{Q}$	$\frac{R_a}{Q}$	$-C_1$
	$\frac{R_a}{Q}$	$-\frac{x_d''}{Q}$	C_2
	$-\frac{R_a x_e}{Q}$	$\frac{x_d'' x_e}{Q}$	$(V_B \cos \delta_o - C_2 x_e)$
	$\frac{x_q x_e}{Q}$	$\frac{R_a x_e}{Q}$	$-(V_B \sin \delta_o + C_1 x_e)$
	$\frac{x_e}{V_{to} Q}(-R_a V_{tdo} + x_q'' V_{tqo})$	$\frac{x_e}{V_{to} Q}(x_d'' V_{tdo} + R_a V_{tqo})$	$\frac{1}{V_{to}}\left[V_B(V_{tdo} \cos \delta_o - V_{tqo} \sin \delta_o) - x_e(C_2 V_{tdo} + C_1 V_{tqo})\right]$
	$\left(I_{qo} + \frac{G x_q''}{Q} + \frac{H R_a}{Q}\right)$	$\left(I + \frac{G R_a}{Q} - \frac{H x_d''}{Q}\right)$	$-(C_1 G - C_2 H)$

MATRIX C (11x13)

APPENDIX E

SYSTEM CONSTANTS

Alternator Constants

Base kVA = 125 kVA

Base Voltage = 480 Volts

Base Frequency = 60 Hertz

Base Ohms = 1.843 ohms per phase wye

r_a = 0.018 pu

x_d = 2.21 pu

x'_d = 0.165 pu

x''_d = 0.128 pu

x_q = 1.064 pu

x''_q = 0.193 pu

T'_{do} = 1.942 sec

T''_{do} = 0.011 sec

T'_d = 0.145 sec

T''_d = 0.008 sec

T''_{qo} = 0.062 sec

T''_q = 0.011 sec

Other Constants

$B_1 = B_2 = 1{,}186 \cdot P_o$ N-m/rad/sec where P_o is per unit output power

h = 30.48 m

h_{ref} = 9.14 m

k = 0.22

K_I = $6 \cdot 10^{-7}$ rad/kw-sec

K_{PF} = 0.2

N = 45

poles = 4

v_b = 1.0 pu

ζ_s = 1.0

τ_o = 0.05 sec

ω_o = 377 rad/sec

ω_s = 9.4 rad/sec

Ω_A = 1,800 r/min

Ω_o = 4.189 rad/sec

APPENDIX F

SIMULATION PROGRAM LISTING

```
*     THREE-PHASE SHORT CIRCUIT

FIXED ACTUAL,COUNT,EVERY,TOTAL,COUNTR,COUNTB,COUNTW

FUNCTION BETIC1 = (14.366,1.0),(18.,0.2439),(30.,-10.9878)                    X=0.009
FUNCTION BETIC2 = (14.361,1.0),(18.,0.1847),(30.,-10.9733)                    X=C.4


*XXXXXXXXXXXXXXXXXXXXXXXXXXXXXXXXXXXXXXXXXXXXXXXXXXXXXXXXXXXXXXXXXXXXXXXXXXXX
*                                                                           X
*                                  INITIAL                                  X
INITIAL                                                                     X
*XXXXXXXXXXXXXXXXXXXXXXXXXXXXXXXXXXXXXXXXXXXXXXXXXXXXXXXXXXXXXXXXXXXXXXXXXXXX

NOSORT

*     TOTAL IS THE NUMBER OF TIMES THAT THE DYNAMIC PORTION OF THE
*           PROGRAM CYCLES.
*     COUNT IS THE MAXIMUM NUMBER OF CYCLES OF THE DYNAMIC PORTION OF THE
*           PROGRAM ALLOWED WITHOUT A TRQTUR CALCULATION.
*     KOUNTB,KOUNTR,KOUNTW ARE THE NUMBER OF CYCLES FOR WHICH THE CHANGE
*           IN BETA,RPMROT,OR WNDVEL IN ONE CYCLE OF THE DYNAMIC PORTION
*           OF THE PROGRAM IS GREATER THAN BETALL,RPMALL, OR WNDALL,
*           RESPECTIVELY, CAUSING A NEW CALCULATION OF TRQTUR.

      ACTUAL = 0
      BETALL = 0.005
      COUNTR = 0
      COUNTB = 0
      COUNTW = 0
      EVERY  = 20
      COUNT  = EVERY-1
      KOUNTR = 0.0
      KOUNTB = 0.0
      KOUNTW = 0.0
      RPMALL = 0.005
      TOTAL  = 0
      TRQSET = 0.0
      TRQSUB = 0.0
      WNDALL = 0.04

SORT

*     ALPHA IS ANGULAR WIDTH OF TOWER SHADOW.
      ALPHA  = 30.

      BLDRAD = 62.5
      DAMPR1 = 875.*PWRPU
      DAMPR2 = DAMPR1
      DAMPS  = 1.0
      G3     = 6.0E-07
      INERT1 = 95023.
      INERT2 = 6073.
      INITAN = ICANGL*TORAD
```

```
0005500       KSTIFF = 3630572.
0005600       KVABAS = 125.
0005700       NN     = 45.0
0005800       OBETA  = BETNOM
0005900       OMEGAS = 2.*1.5*PI
0006000       OMERAT = 1.
0006100       OMEGA0 = 2.*PI*60.
0006200       ORPMRO = RPMNOM
0006300       OWNDV1 = WNDNOM
0006400       OWNDV2 = WNDNOM
0006500       PASSHA = 0.0
0006600       PF     = 0.8
0006700       PI     = 3.14159265
0006800       POLES  = 4.
0006900       PSI1   = 0.0
0007000       PSI2   = ALPHA
0007100       PSI3   = 180.
0007200       PSI4   = ALPHA+180.
0007300       PWRLOD = KVABAS*PWRPU
0007400       PWRNOM = 100.
0007500       PWRREF = PWRNOM
0007600       RADNOM = RPMNOM/TORPM
0007700       RPMNOM = 40.0
0007800       RUN    = 1.
0007900       SRVLIM = 2.*PI/NN
0008000       SYNSPD = 1800.
0008100       BETLIM = 1.0
0008200       TODEG  = 180./PI
0008300       TORAD  = PI/180.
0008400       TORPM  = 30./PI
0008500       TRQNOM = PWRNOM*WTOFPS*1000./(RADNOM*0.8)
0008600       TRQTUR =  (PWRPU+LA*IA*RA)*TRQNOM+DAMPR1*ICT1D+DAMPR2*ICT2D
0008700       WTOFPS = 0.7378
0008800
0008900
0009000 *     BLOCK1 = 0.0  SETS GUSAMP TO ZERO.
0009100       BLOCK1 = 0.0
0009200
0009300 *     BLOCK2 = 1.0 APPLIES SHORT TO LINE
0009400       BLOCK2 = 0.0
0009500
0009600 *     CLTIME IS THE TIME THAT SHORT CLEARS AND LINE IS OPENED.
0009700       CLTIME = 100.
0009800
0009900 *     CYCLES IS DURATION OF SHORT IN 60 HERTZ CYCLES.
0010000       CYCLES = 36.
0010100
0010200 *     DURATN IS THE DURATION OF THE SHORT.
0010300       DURATN = CYCLES/60.
0010400
0010500 *     EFLENG = 0.0 ELIMINATES WIND SHEAR.  USE 0.75 IF WIND SHEAR IS INCLUDED.
0010600       EFLENG = 0.0
0010700
0010800 *     REDUCT = 0.0 ELIMINATES TOWER SHADOW.
```

```
0010900       REDUCT = 0.0
0011000
0011100 *     SHASRT IS THE TIME FOR START OF TOWER SHADOW.
0011200       SHASRT = 0.0
0011300
0011400 *     SHORTM IS THE TIME AT WHICH THE SHORT IS APPLIED.
0011500       SHORTM = 7.40
0011600
0011700 *     WNDNOM IS WIND SPEED AT ZROTOR
0011800       WNDNOM = 18.
0011900
0012000 *     WNDTIM IS THE TIME THAT GUST STARTS.
0012100       WNDTIM = 1000.
0012200
0012300 *_____________________ALTERNATOR CHARACTERISTICS_____________________
0012400
0012500       RA     = 0.018
0012600       TD0P   = 1.94212
0012700       TD0PP  = 0.01096
0012800       TQ0PP  = 0.06230
0012900       X      = 0.008625
0013000 *     X      = 0.4
0013100       XD     = 2.21+X
0013200       XDP    = 0.165+X
0013300       XDPP   = 0.128+X
0013400       XQ     = 1.064+X
0013500       XQPP   = 0.193+X
0013600       X1TERM = 1./X2TERM
0013700       X2TERM = (XD-XDPP)/(XDP-XDPP)
0013800
0013900 *_____________________VOLTAGE REGULATOR CONSTANTS_____________________
0014000
0014100       KVREF  = 0.2
0014200       MUE    = 15.0
0014300       T1     = 0.05
0014400       VFRLIM = 3.5875
0014500
0014600 *_____________________________GUST MODEL_____________________________
0014700
0014800       GUSPER = 1.0
0014900       ZREF   = 30.
0015000       ZROTOR = 100.
0015100       ZZERO  = 0.220*3.281
0015200       GUSTK  = 3./2.*WNDNOM/ALOG(ZROTOR/ZZERO)
0015300       GUSAMP = (GUSTK*SQRT(1.-EXP(-WNDNOM*1.467*GUSPER/...          BLOCK1
0015400                (1.48*ZROTOF))))*BLOCK1
0015500       WNDREF = WNDNOM*(ZREF/ZROTOR)**0.220
0015600
0015700 *_____________________________INITIAL CONDITIONS_____________________________
0015800
0015900 *     ICANGL IS AZIMUTH ANGLE OF BLADE 1 AT SYNC.
0016000       ICANGL = 0.0
0016100       ICDELT = DELTA0*TORAD/((POLES/2.)*NN)
0016200       ICEDPP = EDPP*(-TQ0PP)
```

```
0016300        ICEFD   = VF
0016400        ICEQP   = EQP
0016500        ICEQPP  = EQPP*(-TD0PP/X1TERM)
0016600        ICLD    = (EQPP-ID*XDPP)/OMEGA0
0016700        ICLQ    = -(EDPP+IQ*XQPP)/OMEGA0
0016800        ICPWR   = 0.0
0016900        ICS     = 0.0
0017000        ICSRVR  = 0.0
0017100        ICT1    = (DAMPR1*RADNOM+(PWRPU+IA*IA*RA)*TRQNOM)/KSTIPP+ICT2
0017200        ICT1D   = RADNOM
0017300        ICT2    = (2./POLES)*(DELTAR/NN)
0017400        ICT2D   = ICT1D
0017500
0017600 PROCED PWRPU = PWR(WNDNOM)
0017700        IF(WNDNOM.LT.18.) GO TO 1
0017800        PWRPU = 0.8
0017900        GO TO 2
0018000 1      PWRPU = 0.4
0018100 2      CONTINUE
0018200 ENDPRO
0018300
0018400        VB      = 1.0
0018500        PHI     = ARCOS(PF)
0018600        CP      = COS(PHI)
0018700        BETAX   = 0.5*(PHI+ARSIN(SIN(PHI)-2.*PWRPU*X*CP/(VB*VB)))
0018800        CT      = COS(BETAX)
0018900        IA      = PWRPU/(VB*CT)
0019000        ARG1    = (XQ*CT-RA*ST)*IA
0019100        ST      = SIN(BETAX)
0019200        ARG2    = VB+(XQ*ST+RA*CT)*IA
0019300        ARG     = ARG1/ARG2
0019400        DELTAR  = ATAN(ARG)
0019500        DELTA0  = DELTAR*TODEG
0019600        CD      = COS(DELTAR)
0019700        CDT     = COS(DELTAR+BETAX)
0019800        SDT     = SIN(DELTAR+BETAX)
0019900        VF      = VB*CD+RA*IA*CDT+XD*IA*SDT
0020000        ID      = IA*SDT
0020100        IQ      = IA*CDT
0020200        EQPP    = -(XD-XDPP)*ID+VF
0020300        EDPP    = (XQ-XQPP)*IQ
0020400        EQP     = -(XD-XDP)*ID+VF
0020500        VD      = VB*SIN(DELTAR)
0020600        VQ      = VB*CD
0020700        VTD     = VD-X*IQ
0020800        VTQ     = VQ+X*ID
0020900        VT      = SQRT(VTD*VTD+VTQ*VTQ)
0021000
0021100
0021200 PROCED BETNOM = TH1OR2(WNDNOM,X)
0021300        IF(X.EQ.0.4) GO TO 50
0021400        BETNOM = AFGEN(BETIC1,WNDNOM)
0021500        GO TO 51
0021600 50     BETNOM = AFGEN(BETIC2,WNDNOM)
```

```
0021700 51     CONTINUE
0021800 ENDPRO
0021900
0022000       VFO    = VF
0022100       VNOM   = VT
0022200       VRZ    = 0.0
0022300       VTDEL  = 0.0
0022400
0022500 *_____________________________________DEBUG_____________________________________
0022600
0022700 NOSORT
0022800 1000  CONTINUE
0022900       CALL DEBUG(1,0.0)
0023000
0023100 *XXXXXXXXXXXXXXXXXXXXXXXXXXXXXXXXXXXXXXXXXXXXXXXXXXXXXXXXXXXXXXXXXXXXXXXXXXXXXXX
0023200 *                                                                              X
0023300 *                                    DYNAMIC                                   X
0023400 DYNAMIC                                                                        X
0023500 *XXXXXXXXXXXXXXXXXXXXXXXXXXXXXXXXXXXXXXXXXXXXXXXXXXXXXXXXXXXXXXXXXXXXXXXXXXXXXXX
0023600
0023700
0023800 *_____________________________DRIVE TRAIN_____________________________
0023900
0024000       TH1    = INTGRL(ICT1,OMEGA1)
0024100       OMEGA1 = INTGRL(ICT1D,TH1DD)
0024200       RPMROT = OMEGA1*TORPM
0024300       TRQTPU = TRQTUR/TRQNOM
0024400       TH1DD  = (TRQTUR-KSTIFF*(TH1-TH2)-DAMPR1*OMEGA1)/INERT1
0024500       TH2    = INTGRL(ICT2,OMEGA2)
0024600       OMEGA2 = INTGRL(ICT2D,TH2DD)
0024700       SPEED  = ALTRPM/SYNSPD
0024800       ALTRPM = OMEGA2*TORPM*NN
0024900       TH2DD  = (KSTIFF*(TH1-TH2)-DAMPR2*OMEGA2-TRQLOD)/INERT2
0025000       RADDPS = OMEGA2-RADNOM
0025100       RPMERR = RADDPS*TORPM
0025200       OMEGAR = OMEGA0+(POLES/2.)*RADDPS*NN
0025300       DELTAR = (POLES/2.)*NN*INTGRL(ICDELT,RADDPS)
0025400       DELTAD = DELTAR*TODEG
0025500       ABDELT = ABS(DELTAD)
0025600
0025700 *_____________________CONTROLLER AND SERVO_____________________
0025800
0025900       PWRERR = PWRREF-PWRLOD
0026000       SERVIN = G3*INTGRL(ICPWR,PWRERR)
0026100       SRVERR = OMEGAS*OMEGAS*(SERVIN-SERVOT)-2.*DAMPS*OMEGAS*LIMIN
0026200       LIMIN  = INTGRL(ICSRVR,SRVERR)
0026300       ANGIN  = LIMIN*TODEG
0026400       LIMOUT = LIMIT(-SRVLIM,SRVLIM,LIMIN)
0026500       ANGOUT = LIMOUT*TODEG
0026600       SERVOT = INTGRL(ICS,LIMOUT)
0026700       BETA1  = SERVOT
0026800       BETERR = BETA1*TODEG
0026900       BETOUT = BETERR+BETNOM
0027000
```

```
0027100 *_____________________________BETA LIMIT_____________________________
0027200
0027300 PROCED BETA  = THET(BETOUT,BETLIM)
0027400        BETA  = BETOUT
0027500        IF(BETA.LE.BETLIM) GO TO 40
0027600        BETA  = BETLIM
0027700 40     CONTINUE
0027800 ENDPRO
0027900
0028000 *_____________________TURBINE TORQUE DEVELOPED_____________________
0028100
0028200 PROCED TRQTUR,TRQTU1,TRQTU2,ACTUAL,COUNT,TOTAL,KOUNTB,KOUNTR,KOUNTW,...
0028300        COUNTB,COUNTR,COUNTW = TRQ(WNDVE1,WNDVE2,RPMROT,BETA,EVERY,...
0028400        OBETA,ORPMRO,OWNDV1,OWNDV2,BETALL,RPMALL,WNDALL,TRQSUB)
0028500        TOTAL  = TOTAL+1
0028600        COUNT  = COUNT+1
0028700        TRQSET = 0.0
0028800        IF(COUNT.EQ.EVERY) GO TO 14
0028900        BETABS = ABS(BETA-OBETA)
0029000        RPMABS = ABS(RPMROT-ORPMRO)
0029100        WNDAB1 = ABS(WNDVE1-OWNDV1)
0029200        WNDAB2 = ABS(WNDVE2-OWNDV2)
0029300        IF(BETABS.LE.BETALL) GO TO 11
0029400        COUNTB = COUNTB+1
0029500        KOUNTB = COUNTB
0029600        TRQSET = 1.0
0029700 11     IF(RPMABS.LE.RPMALL) GO TO 12
0029800        COUNTR = COUNTR+1
0029900        KOUNTR = COUNTR
0030000        TRQSET = 1.0
0030100 12     IF(WNDAB1.LE.WNDALL) GO TO 13
0030200        IF(WNDAB2.LE.WNDALL) GO TO 13
0030300        COUNTW = COUNTW+1
0030400        KOUNTW = COUNTW
0030500        TRQSET = 1.0
0030600 13     IF(TRQSET.EQ.1.0) GO TO 14
0030700        TRQTUR = TRQSUB
0030800        GO TO 15
0030900 14     TRQ1,THR1,BET1 = TORKZ(WNDVE1,RPMROT,BETA)
0031000        TRQTU1 = 0.5*TRQ1
0031100        TRQ2,THR2,BET2 = TORKZ(WNDVE2,RPMROT,BETA)
0031200        TRQTU2 = 0.5*TRQ2
0031300        TRQTUR = TRQTU1+TRQTU2
0031400        ACTUAL = ACTUAL+1
0031500        TRQSUB = TRQTUR
0031600        COUNT  = 0
0031700 15     OBETA  = BETA
0031800        ORPMRO = RPMROT
0031900        OWNDV1 = WNDVE1
0032000        OWNDV2 = WNDVE2
0032100 16     CONTINUE
0032200 ENDPRO
0032300
0032400 *_____________________________TOWER SHADOW_____________________________
```

```
0032500
0032600 PROCED REMAIN,SHADO1,SHADO2,GAMDEG = SHADO(RPMROT,PASSHA,SHASRT)
0032700        SHADO1 = 0.0
0032800        SHADO2 = 0.0
0032900        PSIRAD = INITAN+(1.0/TORPM)*INTGRL(0.0,RPMROT)
0033000        PSIDEG = PSIRAD*TODEG
0033100        REMAIN = AMOD(PSIDEG,360.)
0033200        ANGLE  = REMAIN
0033300        IF((REMAIN.GE.PSI1).AND.(REMAIN.LE.PSI2)) ANGLE = PSI1
0033400        IF((REMAIN.GE.PSI3).AND.(REMAIN.LT.210.)) ANGLE = PSI3
0033500        GAMDEG = (180./PSI2)*(REMAIN-ANGLE)
0033600        IF(PASSHA.EQ.1.0) GO TO 22
0033700        IF((ABS(GAMDEG).LE.0.001).AND.(TIME.GE.SHASRT).AND....
0033800           (REDUCT.NE.0.0)) GO TO 22
0033900        GO TO 21
0034000 22     PASSHA = 1.0
0034100        GAMRAD = GAMDEG*TORAD
0034200        IF(ANGLE.EQ.PSI3) GO TO 20
0034300        SHADO1 = REDUCT*SIN(GAMRAD)
0034400        GO TO 21
0034500 20     SHADO2 = REDUCT*SIN(GAMRAD)
0034600 21     CONTINUE
0034700 ENDPRO
0034800
0034900       SHADOW = SHADO1+SHADO2
0035000
0035100 *_____________________VOLTAGE REGULATOR_____________________
0035200
0035300       VF     = AMIN1(VF0+VFDEL,VFRLIM)
0035400       VTDEL  = (VNOM-VT)-KVRPP*(PF*IA-(VTD*ID+VTQ*IQ)/VT)
0035500       ZINTER = REALPL(0.0,T1,VTDEL)
0035600       VRZ    = MUE*ZINTER
0035700       VFDEL  = INTGRL(0.0,VRZ)
0035800
0035900 *_____________________ALTERNATOR EQUATIONS_____________________
0036000
0036100 PROCED OMERAT = ORATIO(BLOCK2,OMEGA0,SHORTM,OMEGAR)                  BLOCK2
0036200        IF(BLOCK2.EQ.1.0) GO TO 70                                    BLOCK2
0036300 71     OMERAT = 1.0
0036400        GO TO 72
0036500 70     IF(TIME.LT.SHORTM) GO TO 71
0036600        OMERAT = OMEGAP/OMEGA0
0036700 72     CONTINUE
0036800 ENDPRO
0036900
0037000 PROCED VD,VQ  = VOLTS(DELTAR,OMERAT,SHORTM,DURATN,CLTIME,EDPP,EQPP)
0037100        IF((TIME.GE.CLTIME).AND.(TIME.LT.(SHORTM+DURATN))) GO TO 30
0037200        SWITCH = 1.-BLOCK2*(STEP(SHORTM)-STEP(SHORTM+DURATN))         BLOCK2
0037300        VD     = SIN(DELTAR)*SWITCH
0037400        VQ     = COS(DELTAR)*SWITCH
0037500        GO TO 31
0037600 30     VD     = EDPP*OMERAT
0037700        VQ     = EQPP*OMERAT
0037800 31     CONTINUE
```

```
0037900 ENDPRO
0038000
0038100       VTD    = VD-X*IQ
0038200       VTQ    = VQ+X*ID
0038300       VT     = SQRT(VTD*VTD+VTQ*VTQ)
0038400
0038500 PROCED PFLOAD = LOADPF(VT,VTD,VTQ,IA,ID,IQ)
0038600        IF((VT*IA).EQ.0.0) GO TO 80
0038700        PFLOAD = (VTD*ID+VTQ*IQ)/(VT*IA)
0038800        GO TO 81
0038900 80     PFLOAD = 0.0
0039000 81     CONTINUE
0039100 ENDPRO
0039200
0039300       TERMLD = (VD+RA*ID-(ED+XQ*IQ)*OMERAT)
0039400       TERMLQ = (VQ+RA*IQ+(XD*ID-EQ1-EQ2)*OMERAT)
0039500       LAMDAD = OMEGA0*INTGRL(ICLD,TERMLD)
0039600       LAMDAQ = OMEGA0*INTGRL(ICLQ,TERMLQ)
0039700       LMDDOT = DERIV(0.0,LAMDAD)
0039800       LMQDOT = DERIV(0.0,LAMDAQ)
0039900       RATIOD = LMDDOT/(OMEGA0*LAMDAD)
0040000       RATIOQ = LMQDOT/(OMEGA0*LAMDAQ)
0040100       EDPP   = (-1./TQ0PP)*INTGRL(ICEDPP,ED)
0040200       EQPP   = (-X1TERM/TD0PP)*INTGRL(ICEQPP,EQ2)
0040300       TERM1  = (VF-EQ1)/TD0P
0040400       EQP    = INTGRL(ICEQP,TERM1)
0040500       ID     = (EQPP-LAMDAD)/XDPP
0040600       EQ1    = EQP*X2TERM-EQPP*(XD-XDP)/(XDP-XDPP)
0040700       EQ2    = (((XDP-XDPP)*LAMDAD+XDPP*EQP-XDP*EQPP)*X2TERM/(-XDPP))
0040800       IQ     = (EDPP+LAMDAQ)/(-XQPP)
0040900       ED     = ((LAMDAQ*(XQ-XQPP)+EDPP*XQ)/XQPP)
0041000       IA     = SQRT(ID*ID+IQ*IQ)
0041100       TALTPU = EQPP*IQ+EDPP*ID-ID*IQ*(XDPP-XQPP)
0041200       TRQALT = TALTPU*TRQNOM/NN
0041300       TRQLOD = TRQALT*NN
0041400       PWRPU  = VD*ID+VQ*IQ
0041500       PWRLOD = KVABAS*PWRPU
0041600       TORQIN = TRQTUR-DAMPR1*OMEGA1-DAMPR2*OMEGA2
0041700       PWRIN  = TORQIN*OMEGA2/(1000.*WTOFPS)
0041800
0041900 *_____________________________TORQUE LOSS_____________________________
0042000
0042100       TRQLOS = DAMPR1*(OMEGA1+OMEGA2)+INERT1*TH1DD+INERT2*TH2DD...
0042200              +INERT2*TH2DD
0042300
0042400 *_____________________________WIND SPEED_____________________________
0042500
0042600       ZBLAD1 = ZROTOR+BLDRAD*EFLENG*COS((REMAIN-ALPHA/2.)*TORAD)
0042700       ZBLAD2 = ZROTOR-BLDRAD*EFLENG*COS((REMAIN-ALPHA/2.)*TORAD)
0042800       WNDNO1 = WNDREF*(ZBLAD1/ZREF)**0.220
0042900       WNDNO2 = WNDREF*(ZBLAD2/ZREF)**0.220
0043000       WNDVE1 = (WNDNO1+GUST)*(1.-SHAD01)
0043100       WNDVE2 = (WNDNO2+GUST)*(1.-SHAD02)
0043200       WNDAVE = 0.5*(WNDVE1+WNDVE2)
```

```
0043300       GUST   = GUSAMP*(1.-COS(2.*PI*(TIME-WNDTIM)/GUSPER))...
0043400                *(STEP(WNDTIM)-STEP(WNDTIM+GUSPER))
0043500       PERCNT = 100.*GUST/WNDNOM
0043600
0043700 PROCED ILINE = LINEI(ID,IQ,OMEGAR,TIME)
0043800        IF(TIME.LT.(SHORTM-0.5)) GO TO 90
0043900        ILINE = ID*COS(OMEGAR*TIME)-IQ*SIN(OMEGAR*TIME)
0044000 90     CONTINUE
0044100 ENDPRO
0044200
0044300 *XXXXXXXXXXXXXXXXXXXXXXXXXXXXXXXXXXXXXXXXXXXXXXXXXXXXXXXXXXXXXXXXXXXXXXXXXXXXXXXXXXXXXXX
0044400 *                                                                                          X
0044500 *                          TERMINAL                                                        X
0044600 TERMINAL                                                                                   X
0044700 *XXXXXXXXXXXXXXXXXXXXXXXXXXXXXXXXXXXXXXXXXXXXXXXXXXXXXXXXXXXXXXXXXXXXXXXXXXXXXXXXXXXXXXX
0044800
0044900       WRITE(3,200) DELTAD,TIME,CYCLES
0045000       WRITE(6,200) DELTAD,TIME,CYCLES
0045100 200   FORMAT(///5X,'DELTAD=',F7.2,5X,'TIME=',F7.3,5X,'CYCLES=',F4.0///)
0045200       WRITE(06,100)EVERY,TOTAL,ACTUAL,G3,PWRPU,KSTIPF,WNDNOM,RUN,RA,...
0045300        DELTA0,X,BETNOM,EFLENG,BLOCK1,BLOCK2,REDUCT,DAMPR1,CYCLES
0045400 100   FORMAT(1H0,7HEVERY =,I3,8X,7HTOTAL =,I6,8X,7HACTUAL=,I6,
0045500      $       8X,7HG3    =,F10.7,2X,7HPOWER =,F4.1,7X,7HKSTIPF=,F10.0//
0045600      $       1X,7HWNDNOM=,F7.3,4X,7HRUN   =,F6.0,8X,7HRA    =,F5.3,9X,
0045700      $       7HDELTA0=,F8.3,4X,7HX     =,F6.3,5X,7HBETNOM=,F11.6//
0045800      $       1X,7HEFLENG=,F5.2,6X,7HBLOCK1=,F4.1,10X,7HBLOCK2=,F4.1,
0045900      $       10X,7HREDUCT=,F4.2,8X,7HDAMPR1=,F5.0,6X,7HCYCLES=,F4.0)
0046000
0046100 METHOD RKSFX
0046200
0046300 RANGE DELTAD,SPEED,KOUNTB,KOUNTR,KOUNTW
0046400
0046500 PRTPLT DELTAD (SPEED,TRQTUR,PWRPU )
0046600
0046700 PREPARE DELTAD,SPEED,PWRPU,TRQTPU,SHADOW,WNDVE1
0046800
0046900 FINISH ABDELT = 200.
0047000
0047100 TIMER FINTIM = 2.0, OUTDEL = 0.002, DELT = 0.002
0047200
0047300 END
0047400 STOP
0047500 ENDJOB
```

REFERENCES

1. Putnam, Palmer Cosslett: Power From The Wind. D. Van Nostrand Company, Inc., 1948.

2. Golding, E. W.; and Stodhart, A. H.: The Use of Wind Power in Denmark. Tech. Rep. No. C/T 112, British Electrical and Allied Industries Research Association, 1954.

3. Power From Windmills. British Engineering, Sept. 1955, pp. 2-4.

4. Note sur le Performance des Aerogenerateurs Neyrpic de Diametre 35 m et 21.2 m. (Report on the Performance of Neyrpic Wind Generators 35 m and 21.2 m in Diameter.) Electricite de France (Cheton), Oct. 1963.

5. Hutter, U.: A Wind Turbine With a 34-m Rotor Diameter. Dtsch Luft-Raumfahrt, Mitt., no. 8, 1968, pp. 404-411.

6. Kimbark, Edward Wilson: Power System Stability. Volume I, Elements of Stability Calculations. John Wiley & Sons, Inc., 1948.

7. Burke, B. L.; and Meroney, R. N.: Energy From the Wind: Annotated Bibliography. Colorado State University, 1975.

8. Technology Application Center: Wind Energy Utilization: A Bibliography With Abstracts. (TAC-W-75-700, Univ. New Mexico.) NASA-CR-147342 and NASA-CR-145816, 1975.

9. Hwang, H. H.; and Gilbert, Leonard J.: Synchronization of the the ERDA-NASA 100 kW Wind Turbine Generator With Large Utility Networks. NASA TM X-73613, 1977.

10. Hwang, H. H.; and Gilbert, Leonard J.: Synchronization of Wind Turbine Generators Against an Infinite Bus Under Gusting Wind Conditions. IEEE Paper F 77 675-2, July 1977.

11. Johnson, Craig C.; and Smith, Richard T.: Dynamics of Wind Generators on Electric Utility Networks. IEEE Trans. Aerosp. Electron. Syst., vol. AES-12, no. 4, July 1976, pp. 483-493.

12. Pantalone, David Kelly: Effects of Large Interconnected Wind Generators on the Electric Power System. Ph.D. Dissertation, Iowa State Univ., 1977.

13. Hwang, H. H.; Mozeico, H. V.; and Guo, Tenhuei: Employing Static Excitation Control and Tie Line Reactance to Stabilize Wind Turbine Generators. (University of Hawaii, NASA Contract NAS3-3132.) NASA-CR-135344, 1978.

14. Clarke, Edith: Circuit Analysis of A-C Power Systems. Volume II. John Wiley & Sons, Inc.; Chapman and Hall (London), 1950.

15. Concordia, Charles: Synchronous Machines, Theory and Performance. John Wiley & Sons, Inc.; Chapman and Hall (London), 1951.

16. Kimbark, Edward Wilson: Power System Stability. Volume III, Synchronous Machines. John Wiley & Sons, Inc., 1956.

17. Park, R. H.: Two-Reaction Theory of Synchronous Machines, Part I. AIEE Trans., vol. 48, July 1929, pp. 716-727. Part II, AIEE Trans., vol. 52, June 1933, pp. 352-354.

18. Dahl, O. G. C.: Electric Power Circuits: Theory and Applications. Vol. II, Power System Stability. McGraw-Hill Book Co., Inc., 1938.

19. Savino, Joseph M.; and Wagner, Lee H.: Wind Tunnel Measurements of the Tower Shadow on Models of the ERDA/NASA 100-kW Wind Turbine Tower. NASA TM X-73548, 1976.

20. Davenport, Alan Garnett: The Application of Statistical Concepts to the Wind Loading of Structures. Proc. Inst. Civ. Eng., vol. 20, Aug. 1961, pp. 449-472.

21. System Dynamics of Multi-Unit Wind Energy Conversion System Applications. 77SDS4249, General Electric Co., Sep. 1977.

22. Anderson, P. M.; and Fouad, A. A.: Power System Control and Stability. Iowa State Univ. Press, 1977.

23. Concordia, Charles; and Schulz, Richard P.: Appropriate Component Representation for the Simulation of Power System Dynamics. IEEE Power Engineering Society Winter Meeting, IEEE, 1975, pp. 16-23.

24. Wilson, Robert E.; and Lissaman, Peter B. S.: Applied Aerodynamics of Wind Power Machines. Oregon State Univ., May 1974, (NSF/RA/N-74-113).

25. Olive, David W.: Digital Simulation of Synchronous Machine Transients. IEEE Trans. Power Appar. Syst., vol. PAS-87, no. 8, Aug. 1968, pp. 1669-1675.

26. Fitzgerald, Arthur E.; and Kingsley, Charles, Jr.: Electric Machinery. Second ed., McGraw-Hill Book Co., Inc., 1961.

27. System/360 Continuous System Modeling Program User's Manual. Fifth ed., International Business Machines Corp., 1972.

28. Electric Utility Systems and Practices. Third ed., General Electric Co., 1974.

1. Report No NASA TM-78902	2. Government Accession No.	3. Recipient's Catalog No
4 Title and Subtitle TRANSIENT RESPONSE TO THREE-PHASE FAULTS ON A WIND TURBINE GENERATOR		5. Report Date June 1978 6. Performing Organization Code
7. Author(s) Leonard J. Gilbert		8. Performing Organization Report No E-9638 10. Work Unit No
9. Performing Organization Name and Address National Aeronautics and Space Administration Lewis Research Center Cleveland, Ohio 44135		11. Contract or Grant No. 13. Type of Report and Period Covered Technical Memorandum
12. Sponsoring Agency Name and Address National Aeronautics and Space Administration Washington, D.C. 20546		14. Sponsoring Agency Code

15. Supplementary Notes
Thesis submitted in partial fulfillment of the requirements for the Degree of Doctor of Philosophy.

16 Abstract
As a consequence of the world energy supply problems large kilowatt and megawatt capacity wind turbine generators are being designed and built to take advantage of the energy in the wind. These apparatus are equipped with synchronous alternators for direct synchronization with utility networks. Because a wind turbine generator inherently has unique power system features - such as a large moment of inertia relative to its power capacity and a continuously varying input torque - its electrical behavior must be investigated either by testing or by analysis. The transient response of the system to electrical faults is one made of the system behavior that must be studied analytically rather than experimentally. In order to obtain a measure of its response to short circuits a large horizontal axis wind turbine generator is modeled and its performance is simulated on a digital computer. The baseline model for the simulation is the DOE/NASA 100 kW wind turbine generator located near Sandusky, Ohio. Simulation of short circuit faults on the synchronous alternator of a wind turbine generator, without resort to the classical assumptions generally made for that analysis, indicates that maximum clearing times for the system tied to an infinite bus are longer than the typical clearing times for equivalent capacity conventional machines. Also, maximum clearing times are independent of tower shadow and wind shear. Variation of circuit conditions produce the modifications in the transient response predicted by analysis. The model and simulation developed for this study of transient stability are applicable for more extensive investigations of power systems involving wind turbine generators, and will continue to be useful until the extent that standard power system technology applies directly to wind turbine power systems is fully determined.

17. Key Words (Suggested by Author(s)) Wind turbine generator Power system analysis Wind power system electrical faults	18. Distribution Statement Unclassified - unlimited STAR Category 44		
19. Security Classif. (of this report) Unclassified	20. Security Classif. (of this page) Unclassified	21. No. of Pages	22. Price*

* For sale by the National Technical Information Service, Springfield, Virginia 22161